Cal Poly Humboldt Schatz Energy Research Center

H. T. HARVEY & ASSOCIATES
Ecological Consultants
50 years of field notes, exploration, and excellence

Mooring Sensors for Environmental Awareness (MoorSEA)—Environmental Data Memo

Project #4806-01

Prepared for:

Schatz Energy Research Center,
California State Polytechnic Institute, Humboldt
1 Harpst Street
Arcata, CA 95521

Prepared by:

H. T. Harvey & Associates

and

Schatz Energy Research Center

August 2024, Revised May 2026

Executive Summary

The Mooring Sensors for Environmental Awareness Project (MoorSEA, hereafter referred to as 'the Project'), funded by the California Energy Commission and led by the Schatz Energy Research Center at Cal Poly Humboldt, is developing an innovative monitoring system to detect collisions and entanglements with mooring cables associated with floating offshore wind platforms in the Humboldt and Morro Bay Wind Energy Areas (WEAs). This technical memorandum provides the physiological and morphological traits of key marine species, the meteorological and oceanographic characteristics of the WEAs, and physical parameters of fishing gear to inform the Project's modeling and simulation efforts.

Of the potential marine megafauna species present in the WEAs, we recommend focusing on five cetaceans (humpback whale, blue whale, sperm whale, killer whale, and Pacific white-sided dolphin), two pinnipeds (California sea lion and northern elephant seal), and one sea turtle (leatherback sea turtle) for the MoorSEA modeling and simulation efforts. These eight key species were chosen due to their presence in both WEAs, their federal and/or state listing status, and/or their relatively higher risks of entanglement compared to other marine species. Behavioral (e.g., dive depth and force) and morphological information (body dimensions) relevant for sensor development and simulating potential interactions with mooring cables is provided for each key species. Derelict fishing gear has potential to wrap around mooring cables and create secondary entanglement hazards. Therefore, this report describes types of gear that were involved in documented entanglement events. Gear specifications, as well as details on the geographic range of the fishery with respect to the WEAs, are described. Lastly, the meteorological and oceanographic conditions (wind, waves, and currents) that will be used to simulate baseline conditions at the WEAs are provided. The meteorological ocean conditions considered were influenced by standards from the American Bureau of Shipping and the International Electrotechnical Commission's 61400 series. We also utilized site-specific data from the Pacific Northwest National Laboratories' Light Detection and Ranging (LiDAR) Buoy Program, which recently conducted year-long deployments at both WEAs.

Table of Contents

List of Tables

List of Figures

List of Preparers

Sharon Kramer, Principal, Senior Marine Ecologist, H. T. Harvey & Associates

Sophie Bernstein, Wildlife Ecologist, H. T. Harvey & Associates

Erica Escajeda, Marine Mammal Ecologist, H. T. Harvey & Associates

Jim Harvey, Senior Marine Mammal Ecologist, H. T. Harvey & Associates

Ben Pridonoff, Research Scientist, Schatz Energy Research Center

Greyson Adams, Senior Research Scientist, Schatz Energy Research Center

Eli Wallach, Senior Research Engineer, Schatz Energy Research Center

List of Acronyms

Acronym	Definition
ABS	American Bureau of Shipping
ALDFG	Abandoned, lost, or otherwise discarded fishing gear
BIA	Biologically important areas
BOEM	Bureau of Ocean Energy Management
CCS	California Current System
CFGC	California Fish and Game Code
CDFW	California Department of Fish and Wildlife
DLC	Design load case
DPS	Distinct population segment
ENP	Eastern North Pacific
ESA	Endangered Species Act
IEC	International Electrotechnical Commission
LiDAR	Light Detection and Ranging
met-ocean	Meteorological and oceanographic
MMPA	Marine Mammal Protection Act
MMS	Minerals Management Service
NMFS	National Marine Fisheries Service
NOAA	National Oceanic and Atmospheric Administration
OSW	Offshore wind
PNNL	Pacific Northwest National Laboratory
the Project	Mooring Sensors for Environmental Awareness Project
SAR	Stock assessment report
SST	Sea-surface temperature
USFWS	U.S. Fish and Wildlife Service
USGS	U.S. Geological Survey

Acronym	Definition
WEA	Wind Energy Area
WERC	U.S. Geological Survey Western Ecological Research Center

Section 1.0 Introduction

The mooring cables associated with floating offshore wind (FOSW) structures have the potential to create multiple hazards for marine life. First, the mooring lines themselves are a collision risk for marine life since they obstruct the marine environment, and they are an entanglement risk for larger marine life such as baleen whales (Maxwell et al. 2022). Direct entanglement in a mooring cable is referred to as primary entanglement, whereas entanglement with fishing gear or other marine debris wrapped around a mooring cable is referred to as secondary entanglement. Marine organisms already entangled in gear/debris may swim in close proximity to the mooring lines and become entangled, in which case the entanglement is considered a tertiary entanglement. All of these potential impacts are top priority environmental issues for FOSW stakeholders (Gorton and Harker-Kilmes 2020).

The Mooring Sensors for Environmental Awareness Project (the 'Project') funded by the California Energy Commission and led by the Schatz Energy Research Center at California State Polytechnic University, Humboldt, is developing, testing, and verifying an innovative monitoring system to detect collisions and entanglements with mooring cables associated with FOSW platforms. The Project addresses a critical need of the FOSW industry by integrating a sensor system within the mooring cables, and employing remotely operated vehicles (ROVs) to detect and verify entanglement hazards on mooring cables as well as entangled wildlife. The goal of the Project is to provide a cost-effective method for remotely monitoring mooring cables for entanglement risks at two California offshore wind energy areas (WEAs): the Humboldt WEA and the Morro Bay WEA (Figure 1).

The purpose of this document is to provide a high-level overview of the data collected on key marine species at risk of entanglement, the type of fishing gear that may ensnare on the mooring cables, and the meteorological and oceanographic (met-ocean) conditions present at the WEAs. All of these inputs will be utilized to develop and model 'baseline' environmental and operational conditions for the mooring simulation, and ultimately, the development of the detection algorithm. Together, these data will inform the modeling and simulation efforts for the Project as well as various entanglement scenarios, ultimately supporting avoidance and mitigation efforts.

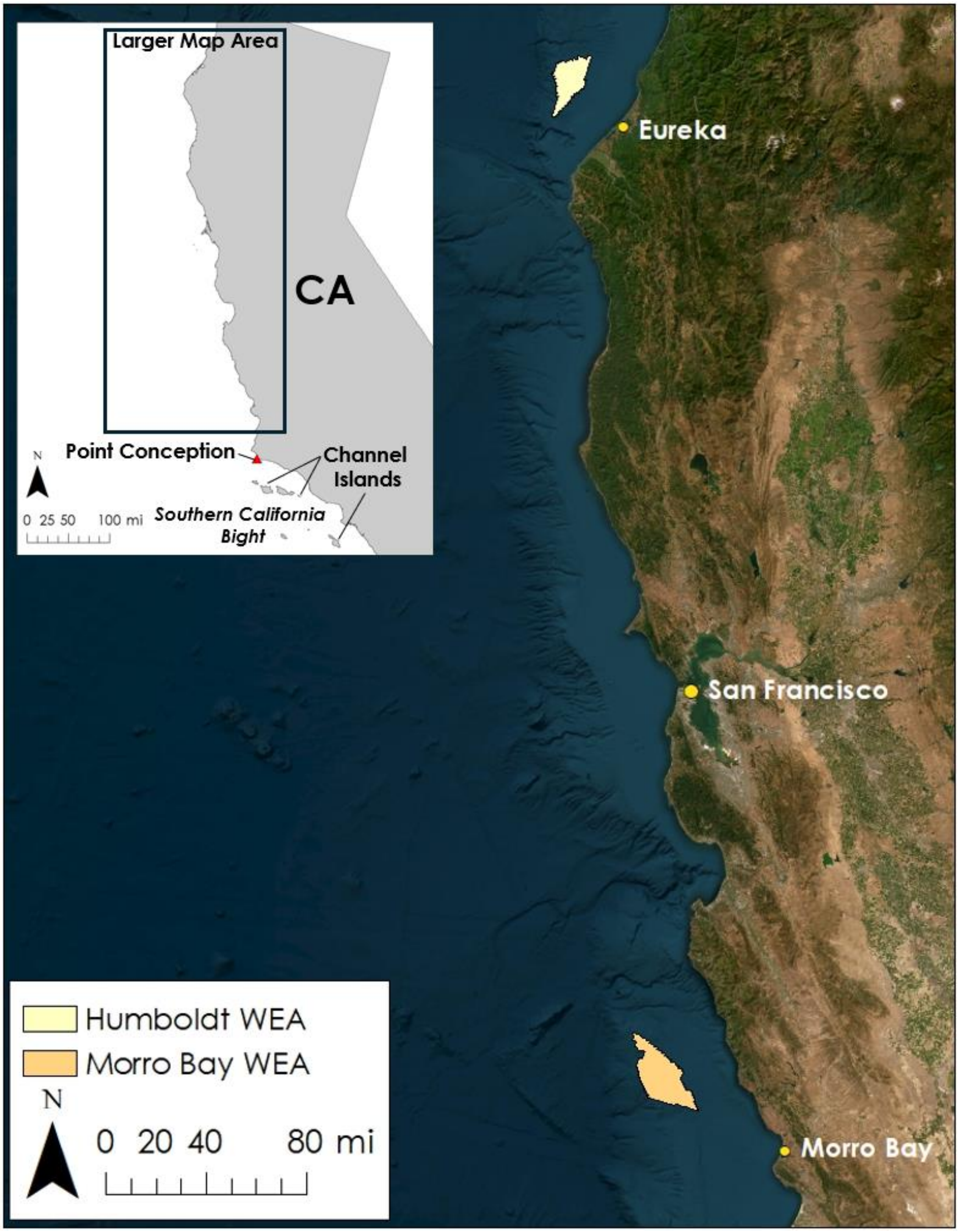

Figure 1. Map of the Humboldt and Morro Bay Wind Energy Areas (WEA)

Source: Background Imagery: Esri, Maxar, Earthstar Geographics, and the GIS User Community; WEA Shapefiles: BOEM; California State polygon: data.ca.gov. Map created by H.T. Harvey & Associates using ArcMap v. 10.7 (ESRI 2019).

Section 2.0 Marine Megafauna

The California Current System (CCS) is a biologically diverse and highly productive eastern boundary current ecosystem whose productivity is driven by the seasonal upwelling of nutrient-rich, subsurface waters (Rykaczewski and Checkley 2008, Checkley and Barth 2009). This upwelling system supports a rich community of marine species, including mysticetes (baleen whales), odontocetes (toothed whales, dolphins, and porpoises), pinnipeds (seals and sea lions), sea otters, and sea turtles. Both the Humboldt and Morro Bay WEAs are located within the CCS, therefore minimizing impacts to this rich ecosystem is a top priority for FOSW developers and wildlife managers alike.

In deciding which species to consider for the Project’s entanglement scenarios, we considered the marine megafauna’s degree of exposure in the two WEAs as well as their vulnerability to entanglement. The degree to which a species is exposed to entanglement stressors depends on the species’ spatial and temporal presence in the WEAs. We gathered information on marine mammal and sea turtle species that are found in the CCS and examined available data on species presence in the WEAs. Appendix A provides an overview of the marine mammal and sea turtle species that are found in the CCS, including when the species is observed in the CCS, whether the species is expected to occur in each WEA based on the most recent stock assessment report (SAR) from the National Marine Fisheries Service (NMFS) and habitat-based species density models (Becker et al. 2020), and their habitat preferences. Another important consideration is a species’ listing status under the federal Endangered Species Act (ESA) and California ESA (CESA) as well as any additional protection under federal or state statutes. Also included in Appendix A is an evaluation of each species’ vulnerability to entanglement as assessed by Southall et al. (2023) as well as whether the species has been documented in recent entanglement reports by NMFS.

Vulnerability to entanglement depends on the biology, behavior, and life history characteristics of a species. Based on their review of existing literature, Benjamins et al. (2014) concluded that the mooring cables associated with FOSW and other marine energy devices presented a 'modest risk' of primary entanglement for most species since the cables are large (e.g., 0.3 meters in diameter) and tend to be taut, which lowers the risk of entanglement. However, if derelict fishing gear attaches to the mooring cables, the risk of secondary entanglement increases. The risk of secondary entanglement, according to Benjamins et al. (2014), is influenced by four biological factors: body size, flexibility, ability to detect moorings, and feeding mode.

- **Body Size**—Mooring cables pose a low primary entanglement risk to small animals because the cables are thick (e.g., 0.3 meters in diameter). However, small animals may be at risk for secondary entanglement in derelict fishing gear or other debris ensnared around the mooring cables. Species with long appendages, such as humpback whales and sea turtles, may have a greater tendency to become entangled in fishing gear.
- **Flexibility**—Different marine megafauna have varying degrees to which they can flex their body while swimming. More flexible animals may be better suited to avoid entanglement upon exposure than animals with more rigid bodies.
- **Ability to Detect Moorings**—Marine megafauna species have different physiological mechanisms (e.g., sensory systems such as echolocation in toothed whales, or vibrissae/whiskers in pinnipeds) that allow them to detect objects in their vicinity. Species able to detect mooring cables, debris, and fishing gear are better able to avoid hazards, and thus are less susceptible to entanglement than species that rely on vision alone for advance warning of obstacles in their path (e.g., baleen whales and sea turtles).
- **Feeding Mode**—Foraging is an important risk factor that leads to entanglement since many entanglements occur when a line or net becomes wrapped around an animal's mouth and/or extremities while it is feeding.

Given the Project's timeline and resources, it was not feasible to model every marine megafauna species found in the CCS for the entanglement simulations, therefore we selected eight key species for the model effort: humpback whales (*Megaptera novaeangliae*), blue whales (*Balaenoptera musculus*), sperm whales (*Physeter macrocephalus*), killer whales (*Orcinus* spp.), Pacific white-sided dolphins (*Lagenorhynchus obliquidens*), California sea lions (*Zalophus californianus*), northern elephant seals (*Mirounga angustirostris*), and leatherback sea turtles (*Dermochelys coriacea*). The eight species were selected based on: (1) their taxonomic group, with at least one representative species chosen for each group (i.e., mysticetes, odontocetes, pinnipeds, and sea turtles); (2) their potential for occurring in each WEA; (3) their regulatory status (with preference given to listed species); and (4) their entanglement vulnerability. The criteria are described in more detail below in addition to a discussion of each key species and the factors that contribute to their entanglement exposure and vulnerability. The section concludes with useful behavioral and morphological information for each key species for the modeling components of the Project as well as a description of how force factors, a useful model input, were calculated.

2.1 Identifying Key Species

2.1.1 Potential Presence

A species' potential for occurrence within the WEAs was determined using expert input, published observations from previous aerial and vessel-based surveys (Table 1), species distribution maps from recent NMFS SAR, and habitat-based species density models (Becker et al. 2020). Observations were collated from multiple sources, including vessel-based surveys from the California Cooperative Oceanic Fisheries Investigations (CalCOFI), Bureau of Ocean Management (BOEM), National Oceanic and Atmospheric Administration (NOAA) Southwest Fisheries Science Center (SWFSC), the U.S. Geological Survey (USGS) Western Ecological Research Center (WERC), and aerial surveys from WERC and the U.S. Department of the Interior Minerals Management Service (MMS, now BOEM; Table 1). These surveys collectively cover both WEAs and include data from 1980 through 2018. All eight key species are regularly observed in or near both WEAs. Abundance and seasonality of each species' presence in the WEAs were not considered since there are no reliable, site-specific abundance estimates for the WEAs.

Table 1. Reviewed Aerial and Vessel-based Surveys with Observations near the Wind Energy Areas

Dataset Name	Source	Website	Observations within 20 km of Morro Bay WEA	Observations within 20 km of Humboldt WEA
MMS High Altitude Aerial Survey 1980–1983	MMS	https://seamap.env.duke.edu/dataset/50	Y	Y
MMS Low Altitude Aerial Survey 1980–1983	MMS	https://seamap.env.duke.edu/dataset/41	Y	Y
At-Sea Aerial Survey Species Observations in Southern California, 1999–2002	USGS	https://www.sciencebase.gov/catalog/item/57c761bfe4b0f2f0cebed538	Y	N
BOEM PaCSEA Aerial Surveys 2011–2012	BOEM	https://www.boem.gov/2014-003/	N	Y
CalCurCEAS 2014	NOAA SWFSC	https://seamap.env.duke.edu/dataset/2130	Y	N
CAMMS 1991	NOAA SWFSC	https://seamap.env.duke.edu/dataset/207	N	Y
Delphinus 2009	NOAA SWFSC	https://seamap.env.duke.edu/dataset/1069	Y	N

Dataset Name	Source	Website	Observations within 20 km of Morro Bay WEA	Observations within 20 km of Humboldt WEA
CSCAPE 2005	NOAA SWFSC	https://seamap.env.duke.edu/dataset/1057	Y	N
ORCAWALE 1996	NOAA SWFSC	https://seamap.env.duke.edu/dataset/219	Y	N
ORCAWALE 2001	NOAA SWFSC	https://seamap.env.duke.edu/dataset/1047	Y	Y
ORCAWALE 2008	NOAA SWFSC	https://seamap.env.duke.edu/dataset/1065	Y	N
CCES 2018	NOAA SWFSC	https://seamap.env.duke.edu/dataset/2147	Y	Y
CalCOFI – marine mammal sightings 2005–2015	California Current Ecosystem LTER	https://oceaninformatics.ucsd.edu/datazoo/catalogs/ccelter/datasets/262	Y	N
NMFS Rockfish Recruitment Survey	NMFS	https://portal.edirepository.org/nis/mapbrowse?scope=knb-lter-cce&identifier=255&revision=3	Y	Y

Dataset Name	Source	Website	Observations within 20 km of Morro Bay WEA	Observations within 20 km of Humboldt WEA
Cascadia Research Blue Whale Photo IDs	Cascadia Research Collective	https://seamap.env.duke.edu/dataset/99	Y	N

Notes: The name of each dataset is provided along with the source (i.e., agency conducting the survey), website for accessing the survey data, and whether the dataset contained observations within 20-km of the Morro Bay (MB) or Humboldt (H) Wind Energy Area (WEA): Yes [Y], No [N]. Note that the 20-km buffer was arbitrarily chosen.

Other Acronyms: WEA = wind energy area; MMS = Minerals Management Service (now Bureau of Ocean Energy Management [BOEM]); NOAA SWFSC = National Oceanic and Atmospheric Administration Southwest Fisheries Science Center; CalCurCEAS = California Current Cetacean & Ecosystem Assessment Survey; CSCAPE = Collaborative Survey of Cetacean Abundance and the Pelagic Ecosystem; ORCAWALE = Oregon, California and Washington Line-Transect Experiment; CCES = California Current Ecosystem Survey; USGS = U.S. Geological Survey; CalCOFI = California Cooperative Oceanic Fisheries Investigations; LTER = Long Term Ecosystem Report; PaCSEA = Pacific Continental Shelf Environmental Assessment.

2.1.2 Regulatory Status

The next selection criterion for the key species was regulatory status. All marine mammals are protected under the Marine Mammal Protection Act (MMPA), therefore species with additional protected status were prioritized for selection since these species may experience greater population-level impacts from entanglement-based mortality. Other protections include listing under the federal ESA and state-level CESA, and listing as a fully protected species under California law.

2.1.3 Entanglement Vulnerability

The second criterion we used in selecting the key species was vulnerability to entanglement. The risk of primary and secondary entanglement with FOSW structures is unknown, therefore entanglements with fishing gear or marine debris are the best available proxies for predicting entanglement risk for marine megafauna. All of the resources we consulted for assessing entanglement risk used fishing gear entanglements as a starting point for evaluating risk. We assessed the vulnerability of each species to entanglement using a variety of sources. First, we applied the entanglement vulnerability index developed by Southall et al. (2023) which was based on NMFS SARs, peer-reviewed publications, and entanglement reports from the U.S. West Coast from Point Conception, CA, northward to the U.S.–Canada border. The index has four levels of risk: high, moderate, low and zero entanglement potential. Odontocetes as a group received low entanglement risk scores, so this selection criterion was not as important as each species' regulatory status. For all other taxonomic groups, we selected species with moderate and high entanglement risk as candidates for the Project.

The next resource we consulted were NMFS entanglement reports as well as an analysis of large whale entanglements by Saez et al. (2021). The NMFS West Coast Region's Protected Resources Division oversees the Large Whale Entanglement Response Network, which works closely with the West Coast Marine Mammal Stranding Network, the U.S. Coast Guard, state agencies, among other responders to generate annual summaries of entanglements from California, Oregon, and

Washington (NOAA 2023a). These summaries include descriptions of the entangled species, the location of the entangled individual(s), and any identified gear involved in the entanglement. Saez et al. (2021) analyzed the complete historical record of large whale entanglements reported to NMFS for the U.S. West Coast from 1982 through 2017 in addition to pertinent information from neighboring countries. Pinnipeds were not covered in Saez et al. (2021) but NMFS does collect, verify, document, and respond to pinniped entanglements. A summary of pinniped entanglements is provided in an unpublished NMFS report, which was used to select the most at-risk pinniped species. Marine mammals and sea turtles that are routinely documented in entanglement reports were selected as a key species for the modeling/simulation efforts.

2.2 The Key Species

2.2.1 Mysticetes: Humpback & Blue Whales

Mysticetes, i.e., baleen whales, have been considered to have the greatest entanglement risk of all marine mammals due to their limited ability to detect obstacles in their path, their behavior and foraging habitats, and their morphology/large body size (Benjamins et al. 2014, Maxwell et al. 2022). Baleen whales rely on their vision and passive listening to survey their environment and consequently, are more susceptible to collision with and entanglement in the mooring cables. They also filter- and lunge-feed which makes them more vulnerable to entanglement since they swim through swarms/schools of prey with their mouths open, which exposes them to entanglement around their mouth (Knowlton and Kraus 2001, as cited in Benjamins et al. 2014; Johnson et al. 2005). Finally, since baleen whales are large, they could become entangled in the mooring cables themselves if the cables are not taut (Benjamins et al. 2014). That said, the risk of primary entanglement in the mooring cables is estimated to be low given the size of the cables (Maxwell et al. 2022).

Humpback whales are expected to occur in both WEAs during the summer and fall months, though they have been detected year-round in the coastal waters of California (Appendix A). They are also of regulatory concern because the two populations that occur off the coast of

California—the Mexico and Central America distinct population segment (DPS)—are listed as threatened and endangered under the ESA, respectively. The estimated risk of entanglement associated with FOSW is high (Southall et al. 2023) based on the species' high risk of entanglement in fishing gear (Benjamins et al. 2014) and the fact that they are the most frequently reported entangled baleen whale species along the U.S. West Coast (Saez et al. 2021). Humpback whales are especially susceptible to entanglement in part due to their physiology. They have long pectoral fins that are flexible, have a high aspect ratio (Woodward et al. 2006), and are covered in a line of bumps, or tubercles, which make them more prone to being snagged. The high susceptibility of humpback whales to entanglement is also due in part to their foraging behavior and behavior once trapped. Humpback whales are known to react violently to becoming entangled, which could make any entanglement worse since they are likely to thrash when entangled (J. Harvey pers. comm. 2024). While foraging, humpback whales dive down, rapidly change speed, and lunge for prey before returning to the surface (Goldbogen et al. 2008). When lunging, their mouths and throat pleats are fully extended to engulf large quantities of euphausiids and/or small schooling fishes. This feeding behavior exposes a humpback whale to entanglement around their mouth (Johnson et al. 2005, Benjamins et al. 2014). They also bubble net feed, a cooperative hunting strategy where multiple individuals blow bubbles to trap fish near the surface (Wiley et al. 2011, as cited in Saez et al. 2021). When feeding with this strategy, humpback whales side-roll and twist, loop and spiral extensively in the water column. Humpback whales are also known to roll when they encounter fishing lines and nets (Weinrich 1999), which can make the entanglement more severe.

Blue whales are the largest species expected to occur in both WEAs and have been observed feeding off the coast of California in the summer and fall (Appendix A). The species is listed as endangered under the ESA and thus, are of regulatory concern. Blue whales are occasionally documented in pot/trap fishery gear along the U.S. West Coast (Carretta et al. 2023) and considered to have a moderate vulnerability to entanglement (Southall et al. 2023). Unlike humpback whales, blue whales have a streamlined body with small, high aspect ratio flippers and flukes that make them efficient swimmers (Woodward et al. 2006). While they may have smaller appendages compared to humpback whales, blue whales may be more at risk of primary entanglement with mooring cables due to their large size. Similar to humpback whales, blue whales are susceptible to entanglement with gear around their mouths ('bridling') due to their lunge foraging behavior. As lunge feeders, they rapidly swim through a school of prey while diving (Goldbogen et al. 2011, 2012). High-resolution digital recording tags show that blue whales engage in 360° rolls while lunge feeding, when searching for prey between lunges, and during their ascents and descents (Goldbogen et al. 2012). This rolling behavior also contributes to their risk of becoming wrapped around the mooring cables (primary entanglement) or ensnared in derelict fishing gear on the moorings (secondary entanglement).

2.2.2 Odontocetes: Sperm Whales, Killer Whales, & Pacific White-sided Dolphins

Odontocetes—toothed whales, porpoises, and dolphins—sense objects in their environment using sound (i.e., echolocation). Because toothed whales can both see and echolocate obstacles in their path, they may be capable of detecting mooring cables in the water from a greater distance, and thus, may be less susceptible to primary entanglement than baleen whales (Benjamins et al. 2014). Despite their innate ability to acoustically survey their environment, odontocetes may fail to detect the moorings or fishing gear ensnared on the moorings during their juvenile stage or when engaged in foraging. As with other whales, odontocetes are typically long-lived and it takes time for juveniles to fully develop their sensory capacity in order to adequately react to hazards (Benjamins et al. 2014). Because they are more likely to be engaged in learning, juveniles are more likely to play with unfamiliar objects. It is also possible that foraging individuals are vulnerable to entanglement since they are distracted. The risk of entanglement is higher for feeding juvenile odontocetes since they are more likely to ignore undetected obstacles while pursuing prey around the FOSW structures.

Sperm whales are expected to occur in both WEAs with peaks in abundance in spring and fall, corresponding to their migration (Appendix A). The species is of special concern given that they are listed as endangered under the ESA. Risk of entanglement was determined to be low for most odontocete species by Southall et al. (2023); however, their relatively large size compared to the mooring cables in addition to their feeding behavior puts sperm whales at risk for entanglement, especially around their mouth. Sperm whales have a history of interactions with and entanglement in longlines and drift gill nets (Southall et al. 2023), as well as entanglement in submarine telecommunication cables, especially those located in deep water (> 119 meters) with excessive slack (Wood and Carter 2008). Sperm whales appear to be curious as evidenced by reports of sperm whales inspecting oil rig platforms and gear (Todd et al. 2020, J. Harvey pers. comm. 2024). For example, a study using ROV and commercial diver footage (globally, spanning 1998-2019) for documenting marine megafauna presence and potential feeding around subsea structures found three accounts of sperm whales interacting with structures in the Gulf of Mexico (Todd et al. 2020). Finally, their unique body shape and jaw morphology offer a good contrast from those of humpback and blue whales for assessing the models, making sperm whales a good candidate for the entanglement simulations.

Killer whales have been observed in both WEAs and could occur at both locations year-round (Appendix A). Multiple ecotypes of killer whales frequent the California coast, including the critically endangered Southern Resident DPS (ESA-listed), therefore killer whales are of regulatory concern. Their ability to echolocate would likely allow killer whales to avoid the mooring cables (Benjamins et al. 2014), however secondary entanglement could be a concern since killer whales have been found entangled in fishing gear in Alaska (Bolling et al. 2023). Killer whales can become entangled in fishing gear while they are actively depredating fish off longlines or in trawling nets (Bolling et al. 2023). Killer whales are also inquisitive, which may result in increased interactions with and entanglement in fishing gear ensnared around the mooring cables. Similar to sperm whales, Southall et al. (2023) estimated that killer whales have a relatively low risk of entanglement related to FOSW. Given that there is a non-zero probability of an endangered Southern Resident killer whale becoming entangled in the two WEAs, we determined that killer whales were an important candidate for the Project's entanglement simulations.

Pacific white-sided dolphins have been observed in both WEAs and are expected to have moderate to high density in both areas with the highest densities occurring in summer/fall

(Becker et al. 2020). Like other dolphin species, they are estimated to have low entanglement risk, however the risk in non-zero due to observed interactions with thresher shark and swordfish fisheries (Southall et al. 2023). The species is protected by the MMPA but has no additional protection. Pacific white-sided dolphins are smaller than sperm and killer whales, providing a good contrast for modeling in the entanglement simulations. The species is known to forage in the mesopelagic zone at depths of 200–1000 meters while offshore (Walker and Jones 1993), which could expose them to secondary entanglement hazards at greater depths.

2.2.3 Pinnipeds: California Sea Lions & Northern Elephant Seals

Pinnipeds are small relative to the size of the mooring cables, therefore primary entanglement is not expected to be an issue (Benjamins et al. 2014, J. Harvey pers. comm. 2024). Also, pinnipeds are able to detect objects using their vibrissae (whiskers) (Denhardt et al. 2001 and Hanke et al. 2013, as cited in Benjamins et al. 2014), which may allow them to detect wakes downstream of the mooring cables. Pinnipeds are more susceptible to secondary entanglement due to their small size and their curiosity. Otariids, or sea lions, in particular are curious about novel objects, and often become entangled when playing or exploring (Yoshida and Baba 1985 and Cawthorn 1985, as cited in Allyn and Scordino 2020). Most observed pinniped entanglements occurred during active fishing operations, with pinnipeds pursuing fish in nets and on lines (L. Saez pers. comm. 2024). Similar to odontocetes, juveniles are found entangled more often than adults likely due to their curiosity and inexperience (Dau et al. 2009, Stelfox et al. 2016). Entanglement typically occurs around the body or neck for pinnipeds.

California sea lions are the most abundant sea lion species in California (Lowry et al. 2021) and are commonly observed in both WEAs. California sea lions have no additional protections other than the MMPA, however their high likelihood of occurring in the WEAs made them an important candidate for the Project’s entanglement simulations. Southall et al. (2023) estimated that California sea lions have a moderate risk of entanglement. California sea lions are curious and may interact with mooring cables, especially any netting and or debris on the moorings that could attract prey, which puts them at greater risk for secondary entanglement. Based on a review on the impact of ghost gear on entanglement in marine megafauna, California sea lions were the second most entangled species (Stelfox et al. 2016).

Northern elephant seals are present in both WEAs and are a species of concern given that the species is fully protected under California law. They forage on mesopelagic and benthic prey in offshore slope and shelf habitats, and are deep divers, which could expose them to secondary entanglement hazards on deeper sections of the mooring cables. According to their SARs, they have a moderate risk of entanglement (Southall et al. 2023).

2.2.4 Sea Turtles: Leatherback Sea Turtle

Of the four sea turtle species that occur in the CCS, the most likely species to be present in both WEAs is the leatherback sea turtle. The species is of regulatory concern due to their listing as endangered under the ESA and the fact that their designated critical habitat overlaps with the Morro Bay WEA (NMFS 2012). Leatherback sea turtles are extremely vulnerable to entanglement in fishing gear, as evidenced by numerous documented interactions with longline gear in the Pacific (Lewison et al. 2004, Martin et al. 2020) and fixed fishing gear in the Atlantic (Dodge et al. 2022). All the entanglement events analyzed by Dodge et al. (2022) involved the head and/or front flippers, likely due to the turtles' large forelimbs which they use to propel themselves forward. Leatherbacks are also vulnerable to entanglement in horizontal and vertical lines (Hamelin et al. 2017, as cited in Bath et al. 2023). In 2008, NOAA held a workshop addressing species distribution in the northeast U.S. and interactions with vertical lines in fixed gear commercial fisheries, in addition to injury assessments and disentanglement techniques (Schwartz et al. 2008, as cited in Bath et al. 2023). It was suggested that some sea turtles become entangled in vertical lines by chance, either during foraging or due to curiosity. Lines that have more slack were determined to be more of a hazard since the line can wrap tightly around their flippers as the turtles attempt to escape. Because of their high vulnerability to entanglement (Southall et al. 2023) and listing status, leatherback sea turtles are an important species to include in the Project's entanglement simulations.

2.3 Key Species Behavioral and Morphological Information, and Force Calculations

The ultimate goal of the Project is to develop a sensor system that can detect collisions and entanglements with FOSW mooring cables. Therefore, it will be important to incorporate as much information about the key species as possible in the entanglement simulations. We collected species-specific behavioral and morphological information in addition to force estimates for the key species that will inform modeling of force transference and interaction behavior in the entanglement scenarios. This information will also contribute to the expected responses and active loading on mooring cables, which in turn will inform the sensor design criteria.

2.3.1 Behavioral Information

Quantitative information on dive depth and duration as well as swimming speed may be valuable for understanding where entanglements could occur along the mooring lines as well as how fast the animal may be moving when it comes into contact with the mooring lines. Information on transit speed (either while migrating or foraging), dive depth and duration along with other pertinent behavioral information from published studies on the eight key species is presented in Table 2 through Table 9. Since each source contained various types of information, the context of the study is provided to aid with interpretation of the reported results.

Table 2. Behavioral and Physiological Information for Sperm Whales

Traveling Speed	Dive Depth	Dive Duration	Other Related Information	Study Context	Source
Average velocity during dives: 1.77 m/s (SD = 0.39 m/s) (*n* = 137 dives) **Max swim velocity:** 4.2–9.6 m/s (*n* = 8 individual whales)	N/A	N/A	N/A	Two data loggers were attached to sperm whales off the Ogasawara Islands in Japan. Accurate swim speed data were obtained for individuals.	Aoki et al. 2007

Traveling Speed	Dive Depth	Dive Duration	Other Related Information	Study Context	Source
Average descent speed: 1.2 m/s **Average ascent speed**: 1.4 m/s	1200 m (range: 400–1200 m)	**Max dive duration**: 64 min **Average dive duration:** 45 min (range 14–64 min)	**Diving and foraging parameters:** Ascent and descent speed was calculated as the average vertical velocity divided by the average of the sine of the pitch angle. Female and immature sperm whales find food via active searching at depths between 400–1200 m. Whales maintained their foraging phase decreasing their transit time (and diving faster) during deeper foraging dives, presumably to maintain a consistent foraging effort at depth. During the average 45-minute dive time, sperm whales were exploiting food patches between 400 and 1200 m depth.	Watwood et al. (2006) attached time depth recording tags to sperm whales in the north-western Atlantic, Gulf of Mexico, and Ligurian Sea.	Watwood et al. 2006

Acronyms: m/s = meters per second; m = meters; max = maximum; SD = standard deviation; min = minute(s); TDR = time depth recorder; SE = standard error; m = meter.

Table 3. Behavioral and Physiological Information for Killer Whales

Traveling Speed	Dive Depth	Dive Duration	Other Related Information	Study Context	Source
Foraging Dives (*n* = 701) **Median descent velocity:** 0.66 m/s (IQR = 0.66 m/s) **Median ascent velocities:** 0.57 m/s (IQR = 0.76 m/s)	Foraging Dives **Max dive depth**: 34 m (IQR = 71.02 m)	Foraging Dives **Median dive duration**: 2.94 min	3D dive tracks demonstrated that foraging and non-foraging dives were distinct: foraging individuals dove deeper, were submerged longer, swam faster, and increased their path tortuosity more. Their max foraging dive depths reflect the deeper vertical distribution of Chinook salmon.	Dive behavior of northern resident killer whales (32 individuals) were recorded on biologging tags and compared to the distribution path of their prey.	Wright et al. 2017

Traveling Speed	Dive Depth	Dive Duration	Other Related Information	Study Context	Source
N/A	**Max dive depth**: 480 m **Median dive depth:** 41 m (CA whale) and 100 m (WA whale)	**Max dive duration:** 12.3 min (WA whale), 10.1 min (CA whale)	N/A	Pacific offshore killer whales tagged with satellite tags (two whales tagged off CA and one tagged off WA) traveled across the entire U.S. West Coast. Two of the tags provided data on diving behavior, including one on an individual tagged off CA (1,110 dives were analyzed).	Schorr et al. 2022

Acronyms: m/s = meters per second; IQR = inter-quartile range; m = meters; max = maximum; SD = standard deviation; min = minute(s); CA = California; WA = Washington.

Table 4. Behavioral and Physiological Information for Pacific White-sided Dolphins

Traveling Speed	Dive Depth	Dive Duration	Other Related Information	Study Context	Source
Mean speed: 7.6 km/h	**Max dive depth**: 1000 m	**Mean dive duration**: 24 s (SD = 2 s)	N/A	Three adult dolphins tracked via radio tags in Monterey Bay, CA. Additionally, most common prey are found between 500 m and 1000 m depth.	Black 1994 Allen et al. 2011

Acronyms: km/h = kilometers per hour; m = meters; s = seconds; SD = standard deviation; CA = California.

Table 5. Behavioral and Physiological Information for Humpback Whales

Traveling Speed	Dive Depth	Dive Duration	Other Related Information	Study Context	Source
Swim speed: 1.6–12 km/h **Sprint speed**: 12 km/h	N/A	N/A	Ford and Reeves (2008) report swimming and burst/sprint speeds of baleen whales. The exact source of a given speed can be referenced in Table 2 of Ford and Reeves (2008). The information included here represents the full range of values reported in the review, but is limited to data sourced from speeds measured via satellite tracking or GPS. Humpbacks were categorized as 'fight' species, owing to their robust body shape, being slow yet relatively maneuverable, migrating in areas where refuge	A comparative analysis of how baleen whales respond to predatory advances and attacks by killer whales, dividing whales into two response categories: flight or fight. For whales that respond via flight, it provides flee/flight speeds, defined as the high-speed swimming away from killer whales.	Ford and Reeves 2008

Traveling Speed	Dive Depth	Dive Duration	Other Related Information	Study Context	Source
			can be taken from predators, among other factors.		
Foraging Dives **Dive ascent speeds:** 1.4 m/s (SD = 0.2 m/s, *n* = 15 dives) and 1.5 m/s (SD = 0.3 m/s, *n* = 43 dives) **Gliding descent speeds:** 1.7 m/s (SD = 0.2 m/s, *n* = 15 dives) and 1.5 m/s (SD = 0.4 m/s, 43 dives)	Foraging Dives 156 m (SD = 29 m, *n* = 1 dive) and 139 m (SD = 25 m, *n* = 1 dive)	Foraging Dives 7.9 min (SD = 1.5 min) and 7.7 min (SD = 2.0 min)	Foraging dives are characterized by a gliding descent with up to 15 distinct lunges at depth, and an ascent via steady swimming. Longer dives are required to perform more lunges, and lunges target the shallowest section of the densest layer of krill. The maximum dive duration while foraging is around half the maximum dive duration of non-feeding humpbacks.	Two high resolution digital tags were placed on humpbacks off the coast of Point Reyes, CA. Data were collected during the summer months.	Goldbogen et al. 2008

Traveling Speed	Dive Depth	Dive Duration	Other Related Information	Study Context	Source
Average speed during migration: 4.0 km/h (± 2.3 km/h)	N/A	N/A	Information reported for migrating individuals. The average speed between all high-quality locations during migration was 4.0 ± 2.3 km/h. Average speed during migration was slower than non-migration travel (1.3 km/h ± 1.9 km/h). Average speeds in the winter breeding and Alaskan summer feeding areas were 1.2 km/h and 2.2 km/h (± 0.8 km/h and 0.6 km/h), respectively.	Eight whales were equipped with Argos satellite tags off Socorro Island, Mexico, while wintering, and then migrated (average of 444 km) offshore and north along the U.S. West Coast.	Lagerquist et al. 2008
Typical traveling speed by equal weighted average: 3.81	**Typical max dive depth** by equal weighted	**Typical dive duration** by equal weighted	The behavioral parameters of an adult-calf pair were measured as they were diving, traveling, or foraging. Dive depths, lengths, and surface intervals provided by adult	Technical report by Pacific Northwest National Laboratory for Bureau of Ocean Energy Management providing information that was used to	Copping and Grear 2018

Traveling Speed	Dive Depth	Dive Duration	Other Related Information	Study Context	Source
km/h (from Hawaii, Brazil and Australia) **Typical dive speed** by equal weighted average: 2.0 m/s **Typical foraging speed** by equal weighted average: 2.5 m/s	average = 132 m	average = 6.34 min	and adult-calf pair. The information reported here are aggregated dive and foraging times from Goldbogen et al. (2008), in addition to studies from Greenland and Alaska (Simon et al. 2012, Witteveen et al. 2015, and Kavanaugh et al. 2017, as cited in Copping and Grear 2018).	develop an animation of humpback whales encountering mooring cables and inter-array cables at a hypothetical floating offshore wind farm.	

Acronyms: km/h = kilometers per hour; km = kilometers m/s = meters per second; m = meters; SD = standard deviation; min = minute(s); CA = California.

Table 6. Behavioral and Physiological Information for Blue Whales

Traveling Speed	Dive Depth	Dive Duration	Other Related Information	Study Context	Source
Routine swim speed: 2.4–7.2 km/h **Sprint Speed**: 32–37 km/h	N/A	N/A	Ford and Reeves (2008) report swimming and burst/sprint speeds of baleen whales. The exact source of a given speed can be referenced in Table 2 of Ford and Reeves (2008). The information included here represents the full range of values reported in the review, but is limited to data sourced from speeds measured via satellite tracking or GPS. Blue whales were categorized as 'flight' species, potentially owing to their streamlined body, and presence in pelagic	A comparative analysis of how baleen whales respond to predatory advances and attacks by killer whales, dividing whales into two response categories: flight or fight. For whales that respond via flight, it provides flee/flight speeds, defined as the high-speed swimming away from killer whales.	Ford and Reeves 2008

Traveling Speed	Dive Depth	Dive Duration	Other Related Information	Study Context	Source
			habitats and calving grounds where it is more feasible to sprint away from a predator.		
Average area-restricted search/foraging speed: 1.05 km/h **Average transit speed**: 3.7 km/h	N/A	N/A	There was a southward movement during the winter to Baja CA and a region west of the Costa Rica Dome. Travel speeds via transit were significantly faster than during area-restricted search (i.e., foraging).	A switching state-space model was applied to satellite tracks of blue whales in the Northeast Pacific to better understand migratory (transiting) and foraging (area-restricted search) behaviors of this population. Argos tags were attached to 159 individuals, primarily off the coast of CA.	Bailey et al. 2009
Dive – Average median of descent speed:	**Average foraging dive depth**:	**Average foraging dive**	Foraging dives for blue whales were deeper and longer, and were distinguished from non-	Time-depth recorders were attached to 7 blue whales, and the foraging and non-	Croll et al. 2001

Traveling Speed	Dive Depth	Dive Duration	Other Related Information	Study Context	Source
2.2 m/s (SD = 0.38 m/s) **Dive – Average median of ascent speed**: 2.1 m/s (SD = 0.52 m/s) **Lunge – Average descent rate**: 1.5 m/s (SD = 0.38 m/s) **Lunge – Average ascent rate**: 2.4 m/s (SD = 0.93 m/s) **Dive – Max descent rate**: 2.7 m/s (SD = 1.2 m/s)	140 m (± 46.01 m) **Average non-foraging dive depth**: 67.6 m (± 51.46 m)	**duration**: 7.88 min (± 1.89 min) **Average non-foraging dive duration**: 4.9 min (± 2.53 min) **Max recorded dive duration**: 14.7 min	foraging dives by the presence of a series of vertical excursions/lunge feeding. A total of 231 dives were reviewed for blue whales.	foraging dive behavior was described, among other objectives. Whales were tagged in Bahia de La Paz and Bahia de Loreto, Mexico; Monterey Bay, CA; and the Channel Islands.	

Traveling Speed	Dive Depth	Dive Duration	Other Related Information	Study Context	Source
Dive – Max ascent rate: 3.0 m/s (SD = 1.3 m/s) **Lunge – Max descent rate**: 1.9 m/s (SD = 0.95 m/s) **Lunge – Max ascent rate:** 3.5 m/s (SD = 0.97 m/s)					
N/A	**Max dive depth**: 193 m (range: 142–193 m) **Average maximum**	**Average dive durations:** 8.8 min (± 0.8 min) and 8.3 min (± 1.4 min)	Tagged individuals displayed stereotypical patterns, diving consistently and directly into the 150–200 m layer in the water column and performing a	This study integrated ship and mooring oceanographic, hydroacoustic, and net sampling, sighting records and time depth recorder deployments to, in part,	Croll et al. 2005

Traveling Speed	Dive Depth	Dive Duration	Other Related Information	Study Context	Source
	dive depth: 155 m (±9.8 m) and 172 m (±14.7 m)		series of 1–4 or 20–30 m vertical excursions per dive.	explore the temporal and spatial links between the distribution, abundance and foraging behavior of blue whales in Monterey Bay, CA.	
N/A	**Max average dive depth:** 253.5 m (n = 8 blue whales)	**Max average dive duration:** 17.4 min (n = 8 blue whales)	All individuals dispersed as far as Cape Mendocino and as far south as Ensenada, Baja CA, Mexico. The summary information provided are of feeding bouts made while in Southern CA (near Point Mugu and San Miguel Island), as these whales stayed near the tagging location to feed for several days before dispersing.	Eight blue whales were instrumented with advanced dive behavior tags off CA. Feeding lunges were used to characterize feeding bouts (defined as a sequence of feeding dives with < 60 minutes of consecutive non-feeding dives), within-bout behavior, and spatial distribution of feeding.	Irvine et al. 2019

Traveling Speed	Dive Depth	Dive Duration	Other Related Information	Study Context	Source
Average descent speed: 2.6 m/s (SD = 0.5) **Average ascent speed**: 2.8 m/s (SD = 1.6 m/s) **Max descent speed**: 4.0 m/s **Max ascent speed**: 2.8 m/s	**Max dive depth**: 315 m; **Average dive depth**: 201 m (SD = 52 m)	**Max dive duration**: 15.2 min **Average dive duration**: 9.8 min (SD = 1.8 min)	The kinematics of these diving blue whales were similar to other baleen whales, where foraging dives consisted of a gliding descent (faster than ascent), multiple lunges at depth followed by an ascent with a steady swim speed. The speed during a lunge rapidly increased. All data reported here are from foraging dives.	Goldbogen et al. (2011) attached archival data loggers to the backs of blue whales off Monterey Bay, La Jolla, Santa Barbara Channel and San Nicolas Island in CA, and the Sea of Cortez and Tanner-Cortez Banks in Mexico. A total of 200 foraging dives including 654 lunges at depth were analyzed. This information was integrated with information on engulfment to better understand the energetics of their lunge-feeding.	Goldbogen et al. 2011

Acronyms: m/s = meters per second; m = meters; min = minute(s); SD = standard deviation; km/h = kilometers per hour; km = kilometers; CA = California.

Table 7. Behavioral and Physiological Information for Leatherback Sea Turtles

Traveling Speed	Dive Depth	Dive Duration	Other Related Information	Study Context	Source
Average water-related swim speeds: 18.6–62.2 cm/s	N/A	N/A	Average speeds calculated over 8-hour periods. It is unknown whether these values reflect the actual cruising speed of moving leatherbacks over shorter time frames. Findings suggest that leatherbacks actively swim throughout most of their migration as opposed to drifting passively.	A total of 15 leatherbacks were tracked via satellite tags during their movements between the Indian and North Atlantic oceans. The overall goal was to evaluate how individual turtles orient their water and ground-related movements in relation to ocean currents.	Galli et al. 2012
High foraging success areas (average): 17.2 ± 8.0 km/day Low foraging success areas	High foraging success areas (average): 53.6 m (SD = 33.1 m)	N/A	Individuals travel relatively slowly in areas where they have high foraging success and dive shallower compared to lower foraging success areas. Only post-nesting portions of tracks were analyzed.	Analysis of 21 leatherback turtles during their migration in the Northern Atlantic to assess spatio-temporal foraging patterns.	Fossette et al. 2010

Traveling Speed	Dive Depth	Dive Duration	Other Related Information	Study Context	Source
(average): 51 km/day (SD = 13.1 km/day)	Low foraging success areas (average): 81.8 m (SD = 56.2 m)				
21 km/day for those transiting in the Eastern Pacific (20–45 km/day for those transiting in the Atlantic)	N/A	N/A	Swim and transit speed may vary geographically and based on behavior. For example, leatherback sea turtles in transit may swim at greater speeds than when foraging on a prey patch. Travel speed of those in the Atlantic suggested two modes: < 15 km/day during periods of foraging to 20–45 km/day when transiting at high speed, whereas those in the Eastern Pacific displayed a single mode (21 km/day). Those in	Analyzed movement patterns and travel rates of leatherback turtles in the North Atlantic and Eastern Pacific (via Argos satellite tags) to identify differences in foraging behavior.	Bailey et al. 2012

Traveling Speed	Dive Depth	Dive Duration	Other Related Information	Study Context	Source
			the Eastern Pacific may lack a slower travel speed because they have more difficulty achieving high foraging success and spend most of their time searching for prey.		
Modal speeds: range from 0.56–0.84 m/s **Maximum speed range:** 1.9–2.8 m/s (164–242 km/day)	N/A	N/A	N/A	Swim speed of seven female leatherbacks during their inter-nesting intervals.	Eckert 2002
N/A	1280 m	68.5 min (for a dive to 1250 m)	The information reported here represents the maximum dive depth and duration for the individuals tagged in Doyle et al. (2008); however, dives may be shallower in	Satellite telemetry of movements and behavior of leatherbacks that were caught in fisheries off Ireland.	Doyle et al. 2008

Traveling Speed	Dive Depth	Dive Duration	Other Related Information	Study Context	Source
			oceanographic features that aggregate their jellyfish prey such as eddies and upwelling zones.		

Acronyms: km = kilometers; km/day = kilometers per day; m/s = meters per second; m = meters; cm/s = centimeters per second; SD = standard deviation; min = minute(s).

Table 8. Behavioral and Physiological Information for California Sea Lion

Traveling Speed	Dive Depth	Dive Duration	Other Related Information	Study Context	Source
10.8 km/h	N/A	N/A	N/A	N/A	Feldkamp 1985
32 km/h	N/A	N/A	N/A	N/A	Mate 1979
N/A	200 m	10 min	N/A	N/A	Feldkamp et al. 1991
N/A	Max dive depth: 274 m	Max dive duration: 9.9 min	A total of 17 feeding trips were identified covering 40.6 days at sea, with > 8,900 dives. The max values are provided, although most dives were < 3 min long and < 80 m deep.	Study observed diving patterns of 10 adult females during the summer breeding season.	Feldkamp et al. 1989

Traveling Speed	Dive Depth	Dive Duration	Other Related Information	Study Context	Source
Average transit rate (females): 0.84 m/s ± 0.1 m/s (range: 0.5–1.6 m/s, *n* = 26 animals)	**Average dive depth (females):** 84.6 m (± 8.4 m; range: 13.6–171.3 m; *n* = 25 animals) **Average dive depth (males):** 32.2 m (±44.3 m; range: 19–96 m)	**Average dive duration (males)**: 1.9 min (± 1.6 min) **Max dive duration (males)**: > 18 min	Refer to Tables 1–4 in Costa et al. (2007) for more detailed metrics.	The goal of this project was to explore the foraging and dive behavior of California sea lions (among over variables) along the California coast. Sea lions were tagged with satellite tracking and time depth recorders on San Nicolas Island, CA.	Costa et al. 2007

Acronyms: km/h = kilometers per hour; m = meters; m/s = meters per second; max = maximum; CA = California; min = minute(s).

Table 9. Behavioral and Physiological Information for Northern Elephant Seals

Traveling Speed	Dive Depth	Dive Duration	Other Related Information	Study Context	Source
0.91 to 1.66 m/s	N/A	N/A	Le Boeuf et al. (1992) also examined minimum and maximum dive speeds (range: 0.4 to 3.0 m/s for most dive segments).	Swim speeds were recorded from a tagged 8-year-old female elephant seal. Tag consisted of a speed-distance meter and a time-depth recorder. Mean swim speeds were calculated using distance covered in a set amount of time.	Le Boeuf et al. 1992
N/A	Max dive depth: 1,529 m	Max dive duration: 77 min	Dive depths and durations varied with the seasons with the longest dives recorded in early summer and the greatest depths recorded in spring. Dives were deepest during the day and shallower at night (likely following the diel vertical migration pattern of their prey).	Six adult male elephant seals were equipped with time-depth recorders. Males were tagged on San Miguel Island, CA. Dives were recorded during the spring and early summer.	DeLong et al. 1991

Acronyms: m/s = meters per second; max = maximum; m = meters; min = minute(s); CA = California.

2.3.2 Morphological Information

Additional morphological information that may be useful for the Project's modeling and simulation efforts for the eight key species is summarized in Table 10 through Table 15.

Table 10. Morphological Information for Blue Whales

Metric	Body Length (m)	Flipper Length to Body Length Ratio	Flipper Width to Body Length Ratio	Fluke Span to Body Length Ratio	Fluke Chord to Body Length Ratio	Max Girth* (m)
Average	24.72	0.132	0.037	0.215	0.051	0.493
Standard error	0.07	0.0005	0.0002	0.006	0.0002	0.009
Median	24.8	0.132	0.037	0.21	0.051	0.498
Min	20.02	0.102	0.27	0.185	0.039	0.476
Max	28.96	0.164	0.049	0.256	0.061	0.505
Sample size	448	249	292	13	366	3

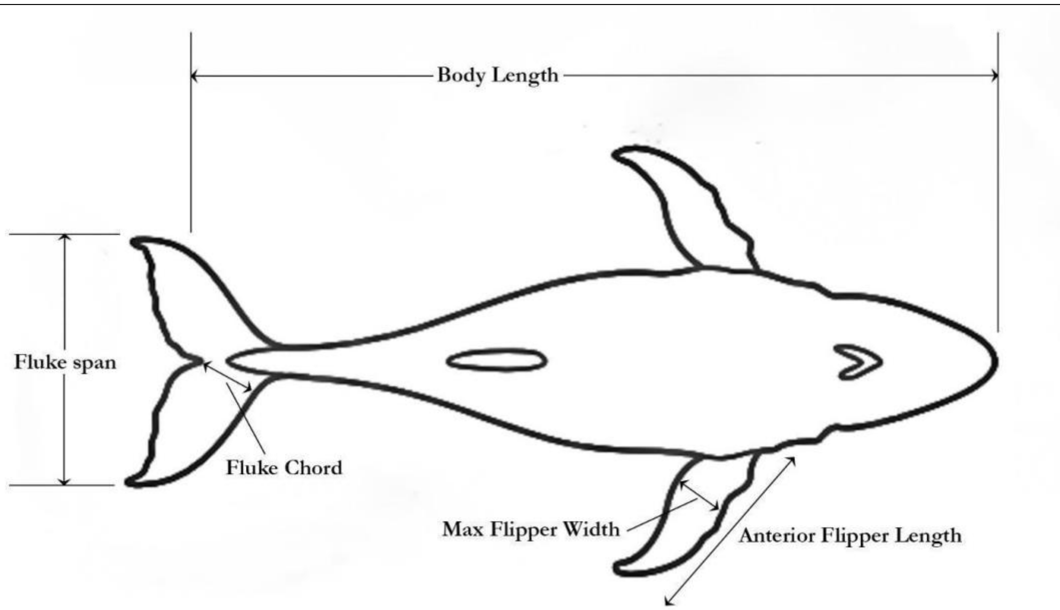

Source: Subset of Table 2 in Woodward et al. (2006).

Notes: Morphological measurements from whaling records and stranding events. The whale illustration provided beneath the table depicts what each measurement represents. Note that the illustration is a humpback whale, not a blue whale, and is included for reference to the body metrics only. *Max Girth = maximum body circumference divided by body length (position of girth measurement differed by species).

Table 11. Morphological Information for Humpback Whales

Metric	Body Length (m)	Flipper Length to Body Length Ratio	Flipper Width to Body Length Ratio	Fluke Span to Body Length Ratio	Fluke Chord to Body Length Ratio	Max Girth* (m)
Average	13.5	0.308	0.073	0.341	0.08	0.747
Standard error	0.08	0.002	0.0007	0.01	0.0009	0.02
Median	13.5	0.31	0.072	0.35	0.079	0.758
Min	11.58	0.265	0.058	0.283	0.067	0.521
Max	15.85	0.344	0.109	0.384	0.109	0.899
Sample size	128	60	94	14	75	29

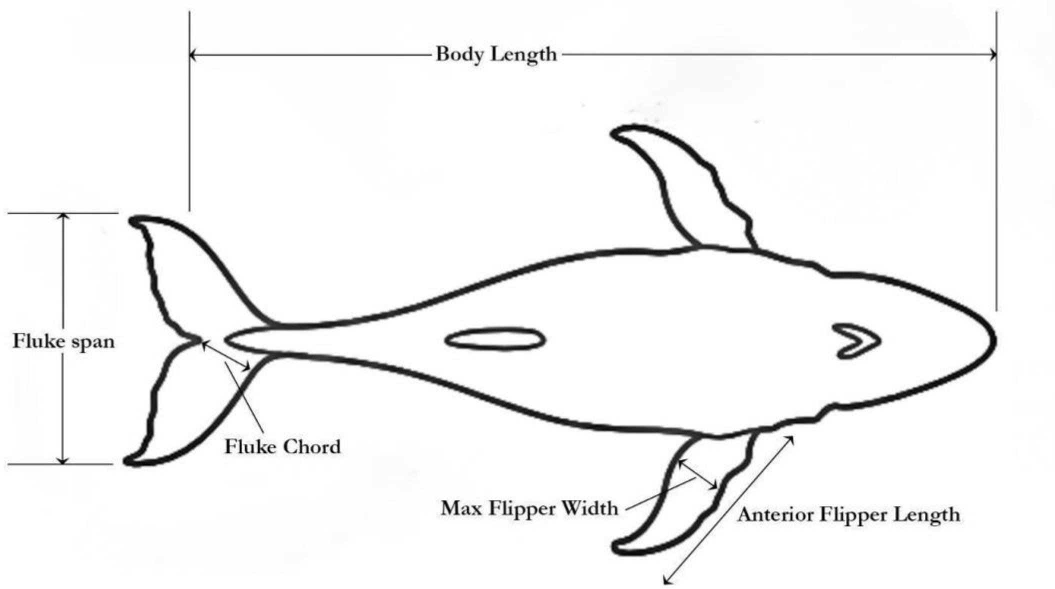

Source: Subset of Table 2 in Woodward et al. (2006)

Notes: Morphological measurements from whaling records and stranding events. The visualization provided beneath the table depicts what each measurement represents. *Max Girth = maximum body circumference divided by body length (position of girth measurement differed by species).

Table 12. Average Morphological Measurements for Adult Female and Calf Humpback Whales

Size Class	Metric	Measurement (m)
Adult female	Length	13.18
	Girth[1]	9.85
	Fluke length[2]	4.44
	Flipper length[3]	4.06
Calf	Length[4]	6.59
	Girth[1]	4.92
	Fluke length[2]	2.22
	Flipper length[3]	2.03

Source: Copping and Grear (2018)

Notes: [1] Girth = 0.747 multiplied by the length at the axilla; [2] Fluke length = 0.337 multiplied by length; [3] Flipper length = 0.308 multiplied by length; [4] Calf length = half of adult length.

Table 13. Morphological Measurements of a Mature Male Sperm Whale

Body Part	Measurement (m)
Total length	14.7
Snout to blowhole	0.8
Snout to dorsal fin base	8.98
Snout to gape	3.95
Snout to eye	4.4
Snout to flipper	5.8
Snout to umbilicus	8.4
Snout to anus	10.9
Maximum girth	8.8
Girth at anus	5.4
Flipper length anterior insertion to tip	1.4 L
Flipper length axilla to tip	0.82 L
Maximum width of flipper	0.69 L
Dorsal fin higher length	0.97
Dorsal fin lower length	0.52
Base of dorsal fin length	1.4
Caudal fin higher length	2.47 L
Caudal fin lower length	2.04 L
Caudal fin total length	4.12
Thickness of blubber, behind the blowhole	0.105
Thickness of blubber, mid dorsal	0.245
Thickness of blubber, anterior insertion of dorsal fin	0.175

Source: Adapted from Table 1 in Degrati et al. (2011)

Notes: Measurements are from a stranded >64-year-old male sperm whale. All measurements are in meters (m); L = left. Since the animal was lying on its right side, only its left pectoral flipper was accessible.

Table 14. Morphometric Measurements of an Adult Male and Female California Sea Lion

	Body Length (m)	Mass (kg)	Pectoral Flipper Area (m^2)	Pectoral Aspect Ratio	Pelvic Flipper Area (m^2)	Pelvic Aspect Ratio	Total Flipper Area (m^2)
Male	1.89	137.8	0.069	4.13	0.044	1.95	0.227
Female	1.72	88.2	0.061	4.16	0.028	1.85	0.18

Source: Adapted from Table 1 in Fish et al. (2003)

Notes: Body length is measured as the distance from the tip of the nose to the tip of the tail. Aspect ratio of the flippers is the length^2/projected flipper area. m = meters; kg = kilograms.

Table 15. External Morphological Measurements of an Adult Female Leatherback Turtle

Body Part	Measurement (m)
Maximum straight carapace length[1]	1.52
Minimum straight carapace length[2]	1.44
Curved carapace length	1.58
Straight carapace length	0.77
Curved carapace width	1.02
Head width	0.21
Head length	0.26
Body depth	0.49
Circumference	1.85
Straight plastron length	0.90
Curved plastron length	0.99
Total tail length[3]	0.28
Post cloacal tail length[4]	0.13
Foreflipper length I (left, insertion to tip)	0.91
Foreflipper length II (left, axilla to tip)	0.69
Maximum width of foreflipper	0.26
Hindflipper length I (left, insertion to tip)	0.60
Hindflipper length II (left, axilla to tip)	0.55
Maximum width of hindflipper	0.28

Source: Chang et al. (2003)

Notes: Measurements were obtained from a stranded sexually mature female. Additional measurements of the vertebrae, skull, ribs, and postcranial skeleton are available in Chang et al. (2003). m = meters. [1] From the anterior edge of the carapace to the posterior tip of the supracaudals; [2] From the anterior point at the midline to the posterior notch at the posterior tip of the supracaudals; [3] From the midline of the posterior margin of the plastron to the end of the tail; [4] From the mid-cloacal opening to the end of the tail.

2.3.3 Estimated Force Calculations

Cetaceans

Estimates of forward thrust force are useful biomechanical data for input into the entanglement simulations, which will ultimately inform sensor design criteria with respect to detection limits and anticipated force transference. Arthur et al. (2015) developed a method to estimate force output ranges for several cetaceans. This method used multiple studies (Williams et al. 1993, Goforth 1990, Fish et al. 2014) that measured the force of bottlenose dolphins and related the measured force to the size of their epaxial muscles (a bundle of muscles surrounding the spine that is responsible for most of the swimming force of cetaceans). To derive force estimates, Arthur et al. (2015) measured the vertebrae of cetacean specimens to estimate the cross-sectional area of their epaxial muscles and multiplied the area by muscle stress, or force per unit cross-sectional area of the muscles. Two different muscle stress values (low = 1.5 kPa and high = 6.1 kPa) denoting different levels of effort were used to generate minimum (also known as sub-maximum) and maximum forces for a given specimen while struggling in an anchored entanglement. Minimum forces represent the forces exhibited while exerting considerable effort over a sustained period of time (i.e., multiple minutes). In contrast, maximum forces are the strongest forces expected during brief bursts, such as large amplitude starts. The force estimation method developed by Arthur et al. (2015) forms the basis of the force calculations in Table 16.

Since Arthur et al. (2015) estimates the force output of specimens rather than species, we expanded upon their methods to calculate force estimates for each species, with the goal of modeling the minimum and maximum force each species is capable of producing. The authors found that total length had a negative allometric relationship with minimum and maximum force, such that as a specimen grew longer, they produced more force. Additionally, total length appears to be a more reliable predictor of both minimum and maximum force than body mass. Based on this finding, we collected additional cross-sectional area and total length measurements from museums throughout California and modeled the relationship between total length and force for various size classes. Species were divided into size classes of species that share a similar body shape, body length, and, where possible, a shared taxonomic group. The size classes include large whale, large dolphin, beaked whale, small dolphin or porpoise, and *Kogia* spp. Because many species of different body shapes (e.g., beaked whales and large dolphins) overlap in size, we did not adhere to strict length cutoffs. However, species that differed dramatically in size from members of the same taxonomic group, like the Baird's beaked whale (*Berardius bairdii*), were reorganized into a size class of species expected to produce a similar amount of force. Blue whales, humpback whales, and sperm whales were categorized as 'large whales,' killer whales were categorized as 'large dolphins,' and Pacific white-sided dolphins were categorized as 'small dolphins.' These groupings allowed us to model the total length-force relationship in the absence of sufficient data to model each species separately. Another way to organize groups could be by fineness ratio (body length divided by height), with species of similar fineness ratios belonging to the same group. Unfortunately, such data are more difficult to acquire, so this method was not used. Finally, we used these modeled relationships to predict the minimum and maximum force that a cetacean could produce if it were the length of the smallest free-swimming calf or the largest adult, respectively.

Of the 113 whale, dolphin, and porpoise specimens included in our analysis, 83 are from Arthur et al. (2015) and the various museum collections cited therein. The remaining 30 specimens were measured in 2023 and 2024 at the University of California, Berkeley Museum of Vertebrate Zoology (Berkeley, CA), Cal Poly Humboldt Vertebrate Museum (Arcata, CA), and the Noyo Center for Marine Science (Fort Bragg, CA). Specimens from these additional sources allowed us not only to put together a more robust dataset of species, but also provided the first measurements for two key species: killer whales and Pacific white-sided dolphins (Appendix B).

To extrapolate specimen force estimates (i.e., those generated by Arthur et al. 2015) to the species level, we needed to collate minimum and maximum total lengths for each species. Minimum and maximum length values were derived either from Allen et al. (2011) or NOAA (2023b).

Modeling of the size class-force relationship and the subsequent species-level extrapolations was conducted in the R statistical computing and data analysis software (R Core Team 2024). Scatterplots (specimen total length:minimum force and specimen total length:maximum force) were generated for each size class and visually examined as a first approach for determining which model types to test. Both linear and power regressions appeared plausible, so the following analyses were performed for both. Data for the power regression were log-transformed, and linear regressions were performed on both the minimum and maximum force datasets. Adjusted R^2, AIC values, and the Breusch-Pagan test for homoscedasticity for both models suggest that the power regression fits best, though both perform well (power regression *Adjusted* R^2 = 0.98*;* linear regression *Adjusted* R^2 = 0.93). As such, only power regression results are shown below (see Appendix C for full results). QQ plots of the residuals also showed the data were normally distributed.

With the relationships generated, we were then able to plot the modeled trendlines for the full range of expected lengths and calculate the corresponding force values for each species. When reporting the species minimum and maximum forces in Table 16, we list the maximum force of the largest adults exerting full effort (i.e., using the 6.1 kPa muscle stress value) and the minimum force of the smallest free-swimming juvenile exerting sub-maximum effort (i.e., using the 1.5 kPa muscle stress value). This is because our initial goal was to estimate the full range of force values expected for each species. However, the trends modeled and shown in Figures 2 and 3 allow us to estimate the maximum and minimum (sub-maximum) effort forces of whales of any size in between as well.

Minimum and maximum cetacean force trends based on the power regression model are found in Figure 2 and Figure 3, respectively. These forces reflect a cetacean's forward thrust force output based on the power regression model (Table 16; full methods in Appendix C). Note that the pinniped and sea turtle forces shown in Table 16 do not use the regression modeling methods described, and are instead derived from different methods and sources listed below. Forward thrust force may not always represent the behavior an animal exhibits when entangled. As described above, some species thrash, roll, and/or exhibit other behaviors distinct from straight-line swimming when entangled. Given this, the maximum forces described in Table 16 may be higher than what could be exerted on mooring cables. Similarly, the minimum forces listed show the sub-maximum forward thrust exerted by juveniles, meaning they represent a very low end estimate of forces potentially imparted on a mooring line. The estimated species-specific minimum and maximum force outputs will be used as additional inputs for a force transference model in the Project's computer modeling and simulation efforts. The simulations, in turn, will then be used to determine the design criteria for selecting the mooring cable sensor. Results for the linear regression model can be found in Appendix C.

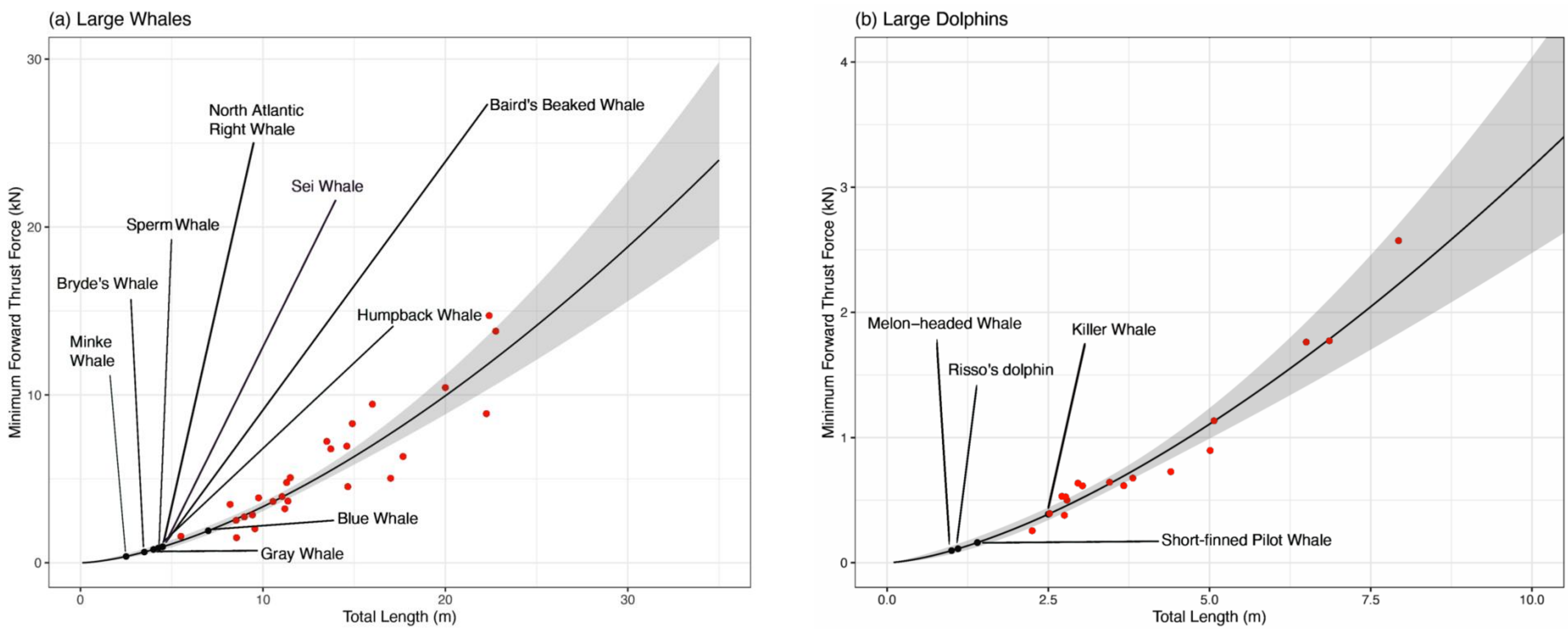

Figure 2. Minimum Cetacean Force Estimated by Power Regression

Notes: Red points = collected sub-maximum force data; Black points = modeled sub-maximum force for minimum-sized individuals (i.e., calves) of each key species. Shaded areas show the 95% confidence interval. Not all modeled species are labeled for readability. See Table C6 for full results. *Baird's beaked whale grouped with large whales due to its size.

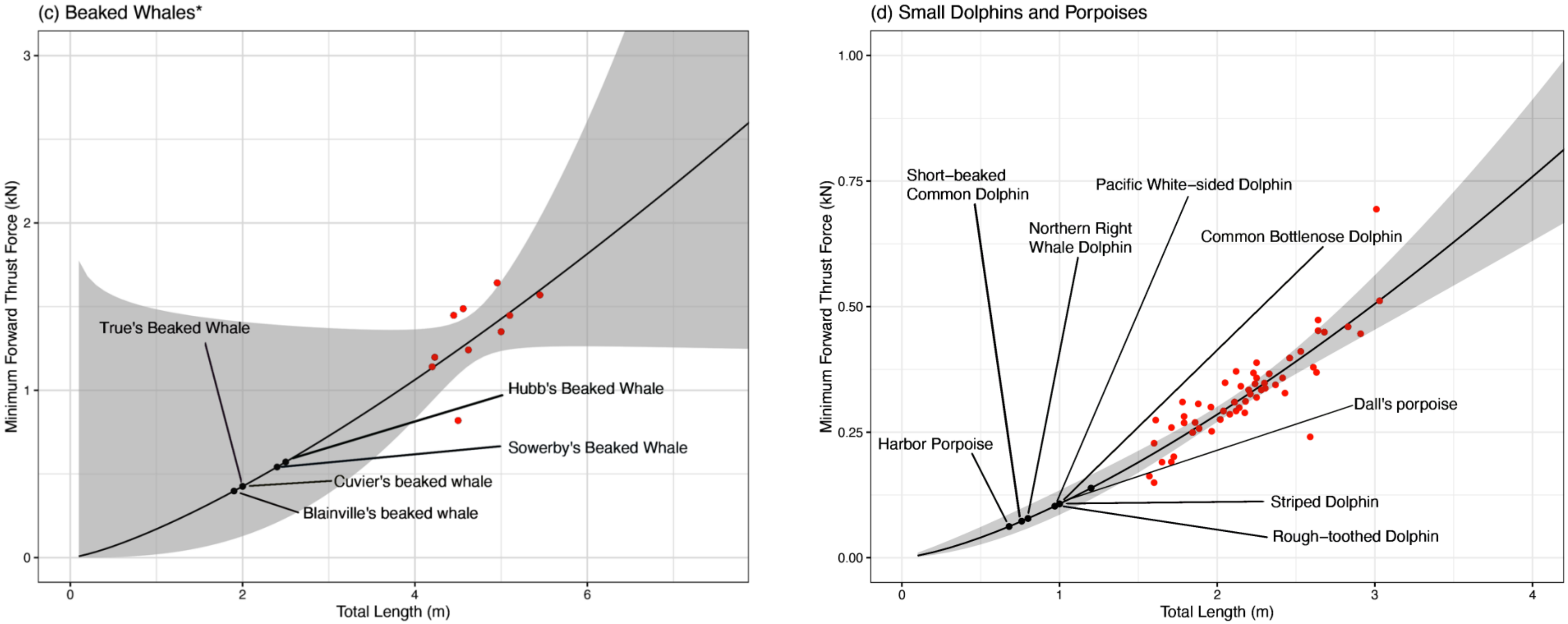

Figure 2. Minimum Cetacean Force Estimated by Power Regression (continued)

Notes: Red points = collected sub-maximum force data; Black points = modeled sub-maximum force for minimum-sized individuals (i.e., calves) of each key species. Shaded areas show the 95% confidence interval. Not all modeled species are labeled for readability. See Table C6 for full results.

*Baird's beaked whale grouped with large whales due to its size.

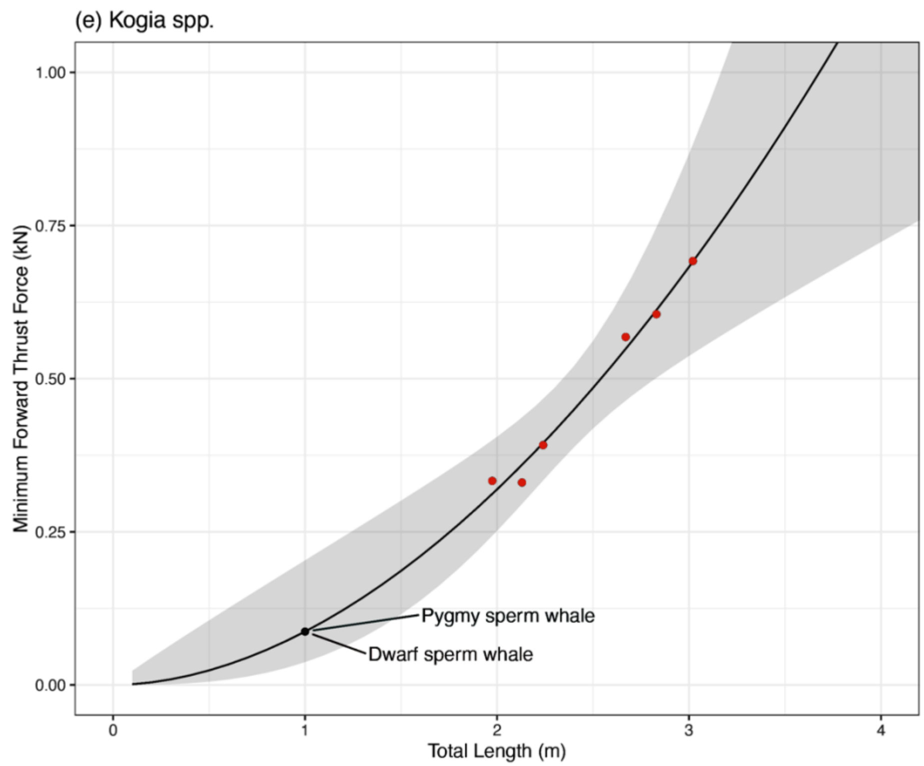

Figure 2. Minimum Cetacean Force Estimated by Power Regression (continued)

Notes: Red points = collected sub-maximum force data; Black points = modeled sub-maximum force for minimum-sized individuals (i.e., calves) of each key species. Shaded areas show the 95% confidence interval. Not all modeled species are labeled for readability. See Table C6 for full results.

*Baird's beaked whale grouped with large whales due to its size

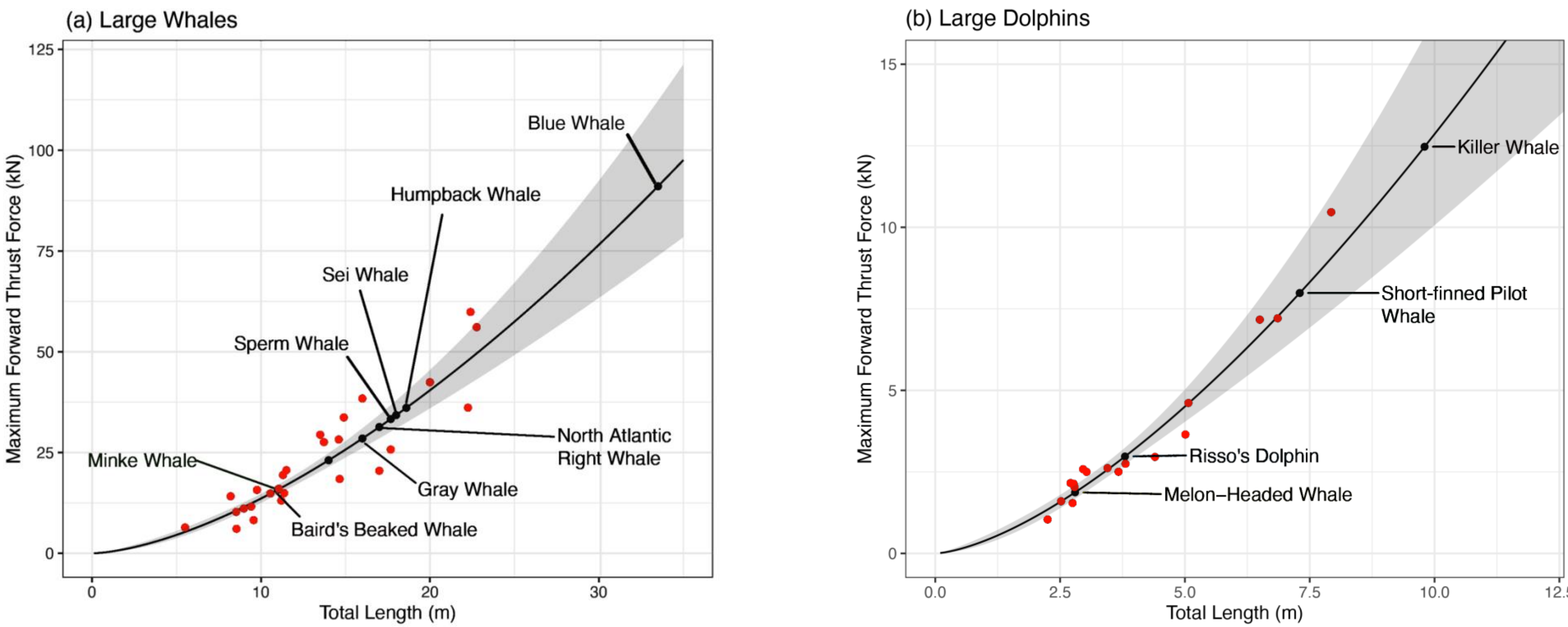

Figure 3. Maximum Cetacean Force Estimated by Power Regression

Notes: Red points = collected data; Black points = modeled maximums for each species. Shaded areas show the 95% confidence interval. Not all modeled species are labeled for readability. See Table C5 for full results. *Baird's beaked whale grouped with large whales due to its size.

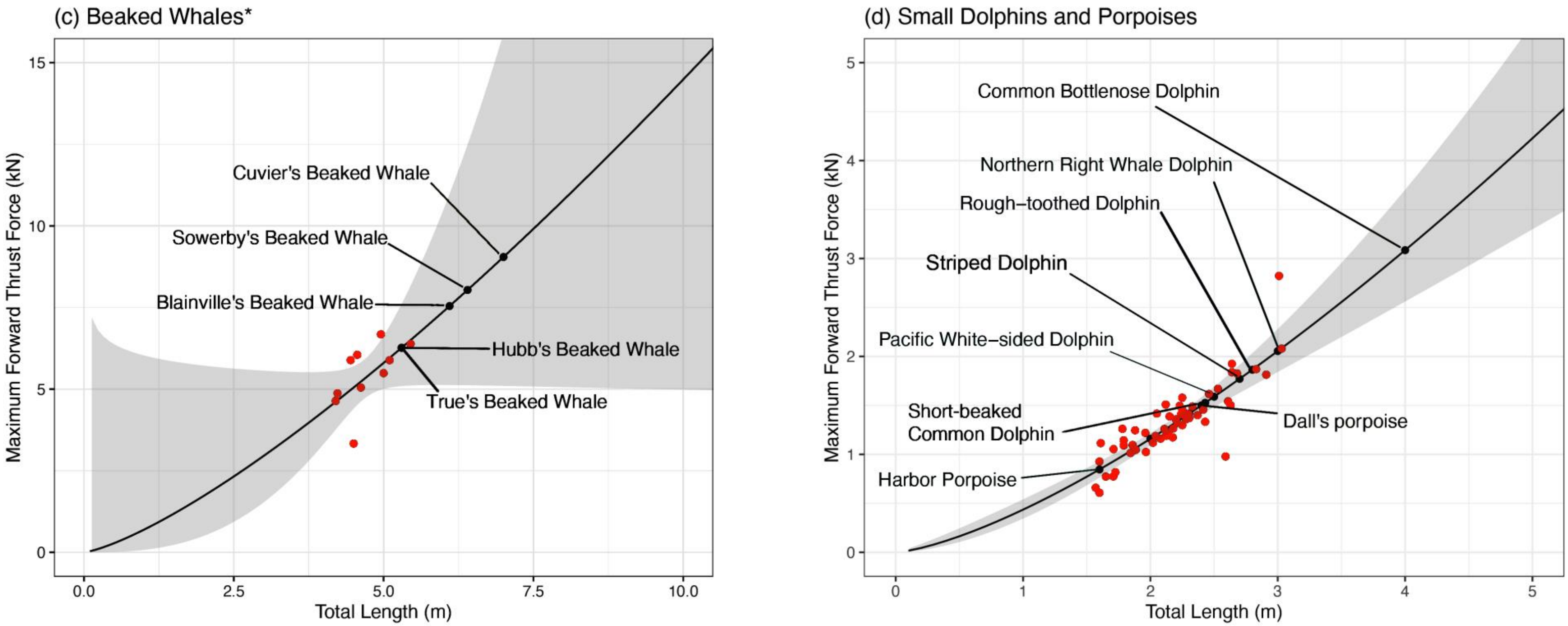

Figure 3. Maximum Cetacean Force Estimated by Power Regression (continued)

Notes: Red points = collected data; Black points = modeled maximums for each species. Shaded areas show the 95% confidence interval. Not all modeled species are labeled for readability. See Table C5 for full results. *Baird's beaked whale grouped with large whales due to its size.

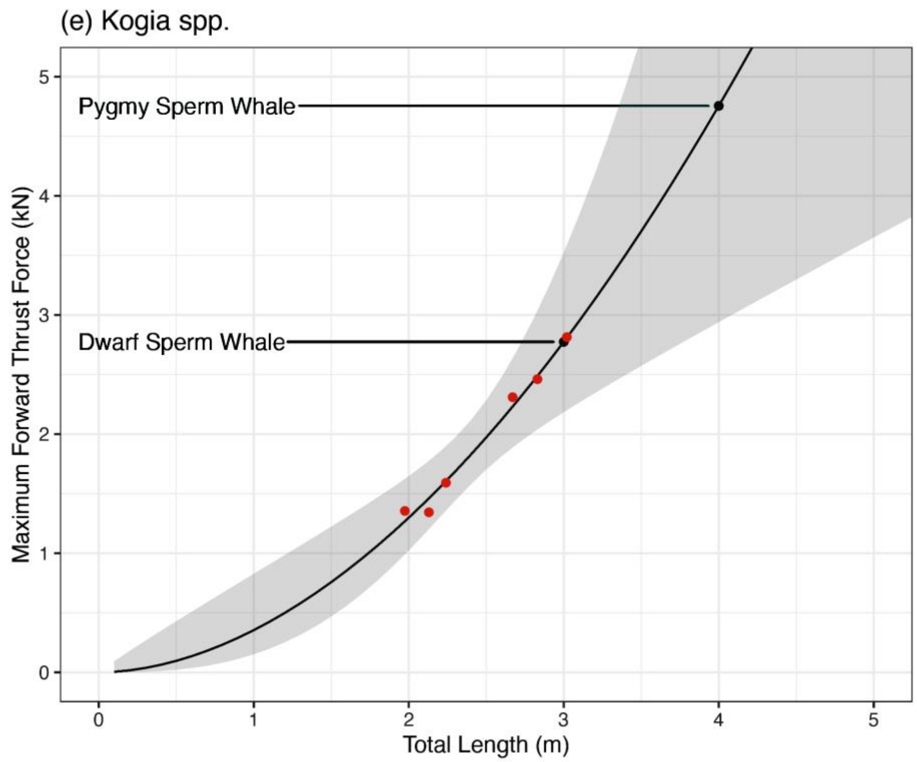

Figure 3. Maximum Cetacean Force Estimated by Power Regression (continued)

Notes: Red points = collected data; Black points = modeled maximums for each species. Shaded areas show the 95% confidence interval. Not all modeled species are labeled for readability. See Table C5 for full results. *Baird's beaked whale grouped with large whales due to its size.

Table 16. Calculated Key Species Force Estimates

Species	Min Length (juveniles) (m)	Max Length (m)	Min Mass (kg)	Max Mass (kg)	Min Force (kN), Power Regression	Max Force (kN), Power Regression
Blue Whale	7.0[1]	33.5[1]	5400[1]	150,000[2]	1.9	91
Humpback Whale	4.5[1]	18.6[1]	1350[1]	36,000[2]	0.95	36
Sperm Whale	4.0[1]	17.7[3]	575[4]	45,000[1]	0.79	33
Killer Whale	2.5[1]	9.8[1]	180[1]	11,000[1]	0.39	12
Pacific White-sided Dolphin	0.97[1]	2.5[1]	85[1]	150[1]	0.10	1.6
California Sea Lion	0.8[1]	2.5[1]	9[1]	400[1]	0.005	0.080
Northern Elephant Seal	1.0[1]	5.5 (males) [1]	589[2]	1996[2]	N/A	0.14[5]
Leatherback Turtle (adults)	1.22[6]	2.44[6]	273[6]	916[6]	N/A	N/A

Sources: [1] Allen et al. (2011); [2] NOAA Fisheries Species Directory (NOAA 2023b); [3] Arthur et al. (2015); [4] Glarou et al. (2022); [5] Aoki et al. (2011); [6] Stebbins and McGinnis (2012).

Notes: Minimum ('Min') force (measured in kilonewtons (kN) describes the estimated sub-maximum forward thrust force of a juvenile individual, and maximum ('Max') force describes the estimated maximum forward thrust force from a maximum length adult. The force estimates for cetaceans were calculated using a modified method based on Arthur et al. (2015), which provides force estimates for a specific specimen. To derive the reported species-specific force estimates, the minimum and maximum length (in meters [m]) were incorporated into a power regression. Additional details on this methodology can be found in the main text. Force estimates for the northern elephant seal and leatherback turtle have not been finalized due to the relative scarcity of relevant literature, but will be incorporated into the entanglement modeling simulation once finalized.

California Sea Lion

Cole (2020) developed a method of estimating the thrust output of California sea lions. This method used the species' mass, body shape, buoyancy, and drag force, among other morphological and environmental parameters, to arrive at a Newtons-per-kilogram (N/kg) thrust estimate for eight female California sea lions. A full description of the study methods can be found in the Cole (2020) paper. Using the N/kg estimates and Laake et al. (2016), we extrapolated minimum and maximum species force values using the mass of the smallest free-swimming juvenile and the largest adult male. These force values are reported in Table 16.

Northern Elephant Seal

Though literature on northern elephant seal thrust force is limited, Aoki et al. (2011) provides measurements that we include in Table 16. The authors captured three juvenile northern elephant seals, added weights to emulate different body conditions, released the weights remotely, and observed the differences in their swimming behavior and kinematics. Though the study did not focus principally on thrust, they estimated each individual's resistance force using similar methods to Cole (2020), which uses the organism's drag force, buoyancy force, and drag ratio, among other parameters. Figure S2 in Aoki et al. (2011) shows a maximum resistance force of at least 140 Newtons, with a mean of 87 Newtons. Because propulsive force must equal resistance force to maintain a constant speed, northern elephant seals may exceed the observed resistance force when accelerating. This aligns well with the Cole (2020) estimates for California sea lion forces, which are lower, but within one order of magnitude. Finally, it is important to note that force estimation or measurement methods vary considerably between pinnipeds and cetaceans, which may influence the reliability of direct comparisons. Future phases of this project will work to establish more realistic pinniped and leatherback sea turtle forward thrust values for entanglement simulations.

Section 3.0 Review of Fishing Gear and Biofouling

This section describes the characteristics of fishing gear which may wrap around the turbine mooring cables and create secondary entanglement hazards. We first describe how and why abandoned, lost, or otherwise discarded fishing gear (ALDFG) may contribute to entanglement. Then, we summarize findings on species-specific interactions with key fisheries in California. Lastly, we describe how the colonization of biofouling organisms pertains to the Project and should be considered in modeling and simulation efforts.

3.1 Abandoned, Lost, or otherwise Discarded Fishing Gear (ALDFG)

Historically, fishing gear was made of materials that quickly decomposed whereas modern day fishers now use gear made with plastics and synthetic materials such as nylon, polyethylene, and polypropylene which are more durable and do not biodegrade (Macfadyen et al. 2009, as cited in Stelfox et al. 2016). Because these sturdy fishing materials do not break down in marine environments, ALDFG can persist in the environment for decades and can continue to capture and ensnare marine life, a phenomenon referred to as “ghost fishing.” A review by Stelfox et al. (2016) highlights the threat of entanglement in ALDFG to marine mammals, sea turtles, and elasmobranchs (i.e., sharks and rays) worldwide, and identifies the type of gear that poses threats to these groups. While this review is global, the results provide insight into the types of gear typically associated with entanglements and how various taxa may become ensnared in ALDFG. First, it is not always possible to identify ALDFG because animals may shed gear prior to being found or an entanglement incident may be known only from photographs of entanglement scars. Stelfox et al. (2016) found that just over half of the ALDFG associated with entanglement incidents were identified. Of the 5,440 incidents, 55% were from fishing nets, 35% were monofilament lines externally entangled around an animal, and <10% consisted of lines from traps and pots, unknown rope, or a combination of nets and lines. Lines and ropes from traps and pots were the gear most likely to be entangled around cetaceans, whereas nets affected 56% of observed entangled pinnipeds and sea turtles. Again, the review by Stelfox et al. (2016) was global in scope, so the above percentages do not necessarily represent the composition of ALDFG for California or within the two WEAs. Also, a rebuttal by Asmutis-Silvia et al. (2017) found that not all of the entanglement cases reported in Stelfox et al. (2016) were with ALDFG but rather were with actively fished gear. Therefore, the results of Stelfox et al. (2016) should be viewed as entanglements related to both ALDFG and active gear.

A total of 70% of all entanglements reported in Stelfox et al. (2016) involved marine mammals, with humpback whales—a species found in both WEAs—being the most recorded entangled species. This observation is consistent with entanglement reports off the U.S. West Coast (Saez et al. 2021). Many cetaceans were observed with gear wrapped around their tails and juveniles were determined to be more at risk of mortality from entanglement compared to adults. Stelfox et al. (2016) found that fixed gear such as lobster pots and set gill nets were the primary source of whale entanglements, aligning with the observations of Johnson et al. (2005) and Saez et al. (2021). Of the pinnipeds included in the review by Stelfox et al. (2016), California sea lions were the second most commonly entangled species. California sea lions are likely to be present in both WEAs, and thus, are a species of concern. Most pinnipeds were observed with gear entangled around their neck or body, and most entangled individuals were juveniles.

A total of 27% of the entanglement reports reviewed by Stelfox et al. (2016) were sea turtles. Olive ridley sea turtles (*Lepidochelys olivacea*) were the most commonly entangled species (68%), however the species is unlikely to be present in either WEA. Olive ridley and leatherback sea turtles have a higher likelihood of entanglement in the open ocean because they spend more of their life cycle there compared to other sea turtles (Stelfox et al. 2016). Elasmobranchs were only 2% of entanglements, but it is likely that elasmobranch entanglements are underreported (Parton et al. 2019).

3.2 NMFS Entanglement Reports

Entanglement monitoring and reporting provides insight into the types of derelict gear that may form secondary entanglement hazards. A technical review was recently published of the historical record of large whale entanglements reported to NMFS for the U.S. West Coast, in addition to pertinent information from neighboring countries (Saez et al. 2021). Large whale entanglements included those pertaining to blue whales, fin whales, gray whales, humpback whales, killer whales, common minke whales (*Balaenoptera acutorostrata*), and sperm whales. More specifically, data covering entanglements between 1982 and 2017 were compiled into a single database and analyzed, in part to (1) determine spatial and temporal patterns and trends in entanglements of large whales from the U.S. West Coast, and (2) review the available information on fishing gear types and fisheries associated with entanglements. The results summarized below are most pertinent for the Project.

A confirmed entanglement is defined as an observation of a whale with human-made materials attached to it. The entanglement gear type was determined for 57% of the confirmed entanglement reports. The identified gear included various types of nets (34%), pot/trap gear (22%), hook and line gear (< 1%), and other types of gear (< 1%) (Saez et al. 2021). The remaining 43% of confirmed entanglement reports involved unknown gear types. There are also notable temporal trends, including a shift in the type of gear associated with entanglements over time. Starting in the 2000s, pot/trap gear has been the most common identified gear type (32%) followed by nets (16%). The percentage of entanglements with unknown gear also increased from 26% between 1982 and 1999 to 52% from 2000 through 2017. Saez et al. (2021) suspect this increase is due to a reduction in easily identifiable gear (such as nets) accompanied by an increase in harder-to-identify gear (such as entanglements with only some form of a line visible). These trends are visible in Figure 4 (Saez et al. 2021), which displays the types of fish gear associated with large whale entanglements between 1982 and 2017.

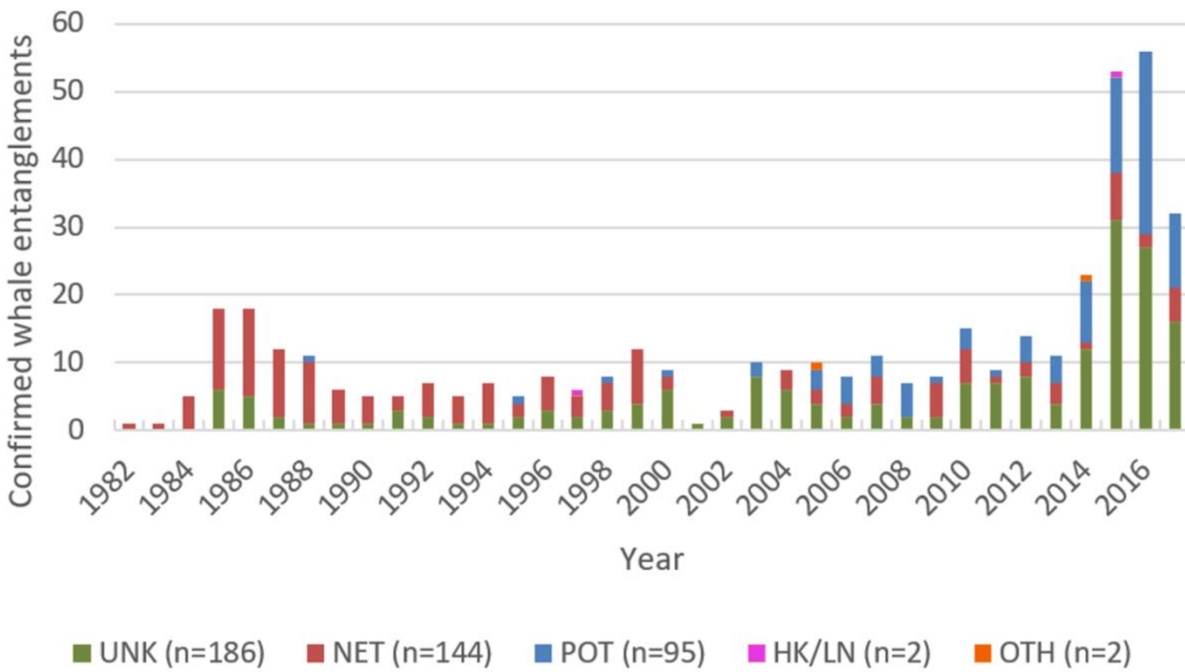

Figure 4. Confirmed Entanglement Reports from 1982–2017 By General Gear Type and Year

Source: Reproduced from Figure 12 in Saez et al. (2021)

Notes: Each bar represents a year; color coded sections represent the general gear type associated with the entanglement reports for that year (total of 429 reports). Unk = Unknown, NET = Netting, Gillnet, and Drift gillnet, POT = all trap/pot fisheries, HK/LN = Hook and line, OTH = Other.

Figure 4 also shows an overall increase in reported large whale entanglements over time, particularly for the period between 2014 and 2017. This increase may be due to a combination of increased entanglements and more frequent reporting. As such, this purported increase may be misleading since the trend could be explained by more reporting by the public along with changes in fishing effort and compliance with evolving standards, shifts in oceanographic conditions bringing whales and fish closer to shore and causing increased overlap, and somewhat recovered whale populations leading to greater exposure to entanglements.

From 1982 to 2017, gillnets were associated with the highest number of entanglement incidents, although none of the gillnets were connected back to a specific fishery (*n* = 82; Saez et al. 2021). Dungeness crab (*Metacarcinus magister*) pots and gear were involved in the highest number of entanglements where the gear was traced to a specific fishery (*n* = 73) and have become the most common confirmed entanglement gear type since 2000, while incidents with gillnets have decreased. Humpback whales were the species most frequently entangled in gear associated with the Dungeness crab fishery. Entanglements with commercial Dungeness crab gear have been recorded in each month of the year, with a peak between April and August (Figure 15 *in* Saez et al. 2021). Commercial spot prawn (*Pandalus platyceros*) (*n* = 9), commercial sablefish (*Anoplopoma fimbria*) (*n* = 5), commercial lobster (*n* = 3), recreational Dungeness crab (*n* = 3), commercial king crab, and commercial rock crab (*n* = 1, respectively) were the other gear types confirmed to be involved in entanglements.

Gray and humpback whales were the most frequently reported entangled large whale species, constituting ~45% and ~36% of the reports, respectively (Saez et al. 2021). Entanglement reports were highest between March and April, which corresponds to the presence of feeding humpback whales and the northern migration of gray whales along the U.S. West Coast. The risk of entanglement is greatest when there is overlap between whale presence and fishing effort, however whales can become entangled then swim away from the original location of the gear and be discovered after the fishing season closes. Gray and humpback whales may be the most reported entangled whale species due to the overlap between their nearshore distributions and Dungeness crabbing locations, the overlap between the whales' migration/feeding seasons and fishing seasons, and their increased population numbers (Saez et al. 2021). Note that migration pathways of gray whales are farther inshore than the two WEAs. As previously mentioned, when the entangling gear type is known, humpback whales are most often reported as entangled in pot gear. However, the majority of the pot gear is from commercial Dungeness crab fisheries (Figure 9 and 10 *in* Saez et al. 2021), which are far inshore of the WEAs. A smaller portion of humpback whale entanglements are from netting, gillnets, sablefish, and recreational Dungeness crab pots. Entanglements of blue whales, fin whales, minke whales, killer and sperm whales were also reported, though these species together constituted ~7% of the reports while unidentified whales made up ~10% of the reports (Saez et al. 2021).

3.3 Gear Overview and Key Fisheries in California

This section describes key fisheries that are associated with entanglements reported along the U.S. West Coast. An overview of gear types (pot/trap, net, and hook and line) involved in entanglements with large whales between 1982 and 2017 is also provided (Saez et al. 2021).

3.3.1 Pot/Trap Gear

The terms 'pot' and 'trap' refer to stationary baited enclosures lowered to the seafloor to catch fish and crustaceans (NMFS 2024). Pots/traps capture crustaceans and fish by luring them into one or more funnel-like entrances that allow organisms to enter but not exit. The enclosures are typically made from materials including wood, wicker, and metal, and are often covered with mesh netting with openings anywhere from ½ inch to 2 inches x 3 inches, depending on regional regulations. Baited pots/traps are weighted and may be strung together or fished individually on the bottom, and are typically connected via ropes/lines to a surface buoys (NMFS 2024). The pot/trap itself can take various shapes, including round, rectangular, conical, or barrel shape. A more detailed description with visualizations of a single pot/trap and multiple pots/traps is available on pages 24 and 25 *in* the NMFS (2024). Pots and traps have been involved in numerous large whale entanglements since 2000 (Saez et al. 2021), but have not been documented in entanglement cases involving pinnipeds (Stelfox et al. 2016).

Commercial Dungeness Crab Pot Fishery

Most large whale entanglements documented by NMFS on the U.S. West Coast between 1982 and 2017 were with Dungeness crab gear (Saez et al. 2021). Dungeness crabs are trapped along the entire U.S. West Coast and the gear is unlike other pots/traps used in other fisheries (e.g., sablefish, lobster). Commercial Dungeness crab gear can have different line markings and buoy colors, as well as different pot limits and fishing seasons depending on the state (regulations differ between California, Oregon, and Washington). The details reported here are for California gear, but are likely applicable to gear used in Oregon, and Washington. Dungeness crab traps in California are typically circular steel frames wrapped in rubber (Saez et al. 2013, NMFS 2024). These steel frames are between 3 and 4 feet (ft) in diameter, 1 ft high, and are wrapped with three to 4-inch diameter mesh made from ¾-inch stainless steel wire (NMFS 2005, as cited in Saez et al. 2013). Dungeness crab traps are not attached to one another and fishers typically deploy 15 pots per mile (NMFS 2005, as cited in Saez et al. 2013; NMFS 2024). The traps weigh between 60 and 120 pounds and have 2 rigid circular escape rings 4.25 inches inside diameter on the upper half of the trap to allow sub-legal sized crabs to exit the trap. The line used is synthetic rope (e.g., floating nylon or polyethylene, sinking lead-core), typically with diameters of 5/16 inches, 2/8 inches, or 7/16 inches (NMFS 2024). The commercial Dungeness crab pot fishery in California spans the entire coastline from Point Conception north to the California-Oregon border. Depths between 60 and 600 ft are commonly fished, which is shallower than both WEAs. However, crab pot line lengths are longer than the water depth to account for currents dragging ropes and buoys underwater. There are seasonal closures in northern California from approximately mid-July through December, and in southern California from June through mid-November. Seasonal closures vary year to year and are determined by CDFW based on the presence of large whales and the potential for whale entanglement.

Spot Prawn Trap Fishery

The spot prawn fishery was the second most common source fishery identified in large whale entanglements documented by NMFS between 1982 and 2017 (Saez et al. 2021). Nine large whale entanglements with spot prawn traps were confirmed. Note that trap/pot lines are uncommon causes of pinniped entanglement (Stelfox et al. 2016). Spot prawn trap fishing occurs along the entire West Coast of the U.S. and is also popular in Canada. In California, spiny lobster

(*Panulirus interruptus*) pots are used to target spot prawn, and the fishery operates in waters between 600 and 900 ft (Saez et al. 2013, NMFS 2024). These depths are inshore and shallower than both WEAs. The geographic range of this fishery is limited to central and southern California (south of San Francisco Bay) and the fishing season differs geographically but occurs year-round. Traps are either tapered, circular or rectangular and measure 3 ft by 1.5 ft by 1 ft. There are two chambers. The mesh size used is typically 7/8 inches to 1 inch x 1 inch. The traps are attached to a 5/16-inch ground line made from nylon or a polypropylene blend. Strings of 10 to 30 wire mesh traps are typically deployed and the string of traps can measure up to a mile long (Saez et al. 2013, NMFS 2024). Similar to Dungeness crab pots, the line from spot prawn traps to the surface is longer than the water depth fished to account for drag on the rope and buoy.

Sablefish Trap Fishery

The sablefish trap fishery was the third most common source fishery identified in large whale entanglements documented by NMFS between 1982 and 2017, with five confirmed entanglements reported (Saez et al. 2021). Sablefish are targeted with trapezoid, conical, or rectangular steel frame traps wrapped in a 3.5-inch nylon webbing (NMFS 2005, as cited in Saez et al. 2013, NMFS 2024). Common size traps are 36 inches and 72 inches in diameter, and between 28 inches to 32 inches high (NMFS 2024). In California, traps cannot be >72 inches in diameter. A common ground line connects multiple traps (length of this line is unknown), and the material is often nylon, polypropylene-blend, or nylon blend and 5/16 inches or 3/8 inches in diameter, but can be larger (NMFS 2024). The traps are connected to a buoy at the surface with line lengths greater than the depth of the pots to account for drag. The nylon mesh openings on the traps are 2 inches x 2 inches. Trapezoidal traps and conical pots commonly weigh 55 pounds while rectangular traps are the largest and can weigh up to 100 pounds (NMFS 2005, as cited in Saez et al. 2013). The geographic range of this fishery extends along the entire U.S. West Coast and to depths between 600 and 2,250 ft (NMFS 2024), overlapping with both WEAs. The fishery is open throughout the entire year (for all states) but is managed as a limited entry fishery.

Recreational Dungeness Crab

Recreational Dungeness crab gear were identified in a smaller portion of the large whale entanglements between 1982 and 2017 (Saez et al. 2021). Compared to at least 73 commercial Dungeness crab pot entanglements, only three recreational entanglements were observed from 1982–2017 by NMFS (Saez et al. 2021). The lines used are not standardized and traps may be crab traps, hoop nets, or crab loop trays. Typical fishing depths are between 60 and 300 ft (NMFS 2024), which is shallower than both WEAs. The season varies depending on the state and similar to the commercial crab fishery, there can be delayed openings and seasonal closures. The season typically extends from November 7 through June 20 in central California and through July 30 in Northern California (NMFS 2024).

California Spiny Lobster Pot Fishery

Gear from the California spiny lobster pot fishery was involved in three confirmed large whale entanglements documented by NMFS between 1982 and 2017 (Saez et al. 2021). California spiny lobster traps are rectangular shaped and made of wire or plastic. The wire mesh is 2 inches x 4 inches, and the inside measurement of the mesh is no less than 1.5 inches x 3.5 inches. The dimensions of the traps vary from 28 inches x 26 inches x 14 inches to 26 inches x 48 inches x 20 in. A single trap is set per line and the line usually consists of 3/8-inch polypropylene blend. The geographic range of the fishery extends from Point Conception south and the maximum depth fished is 300 ft, out of the range of both WEAs. The general fishing season runs from October through March. Despite not occurring near either of the WEAs, lobster pot gear, like most pot/trap gear, has the potential to be moved from their set location by storms or boat collisions, and float throughout the CCS.

California Rock Crab

California rock crab (*Romaleon antennarium*) gear was identified in only one confirmed large whale entanglement documented by NMFS between 1982 and 2017 (Saez et al. 2021). Common trap dimensions are 24 inch by 24 inch by 12 inch with wire mesh (either 1 inch x 1 inch, 2 inch x 2 inch, or 2 inch x 4 inch). Traps typically have an entry funnel at the top made of a 6-inch diameter PVC pipe and some entry funnels made of wire mesh on the sides. There is usually one single trap with a single buoy, but a single line may contain up to 25 traps. The line commonly consists of a polypropylene blend or nylon with a 5/16-inch or ⅜-inch width. The fishery extends along the entire California coastline and includes offshore islands such as the Channel Islands. Common depths fished are between 60 and 210 ft, which is shallower than both WEAs and the fishery is open year-round.

Other Pot/Trap Fisheries

There are other trap/pot fisheries that have not been documented in entanglements but that could form secondary entanglement hazards. The geographic range, seasonality, and depth of the fishery may vary; however, lost gear could travel throughout the CCS and ensnare on mooring lines. These fisheries include, but are not limited to, the hagfish trap fishery (fished along the entire West Coast of the U.S., but concentrated in coastal Washington, Oregon and northern California at depths of 300–750 ft [shallower than both WEAs]), shrimp pots from Washington or Oregon (fished coastally between 230 and 330 ft or inland [shallower than both WEAs]), California tanner crab pots (at depths of 1,800–6,000 ft, potentially offshore of the WEAs). Other examples include the California nearshore finfish trap fishery, California coonstripe shrimp (*Pandalus danae*) pot, and Washington and Puget Sound Dungeness crab.

3.3.2 Net Gear

There are multiple different types of net gear, including trawls and gillnets. Gillnets were associated with 43.6% of the confirmed gear type entanglement records between 1982 and 2017 (Table 3 *in* Saez et al. 2021). Net entanglements are also the most common type of entanglement for pinnipeds (n = 631) (Stelfox et al. 2016). Gillnets consist of fine mesh monofilament or multifilament nylon webbing with mesh openings large enough for fish to get their heads stuck (or ‘gilled’), entangled, or enmeshed in the netting (NMFS 2024). Gillnets can be used for fishing on the surface, in midwater, or on the bottom and are typically long (e.g., hundreds of meters to kilometers in length). Gillnets are either set on the seafloor with anchors and vertical lines attached to marker buoys, or are set to drift attached to or near a boat for a set period of time. Gillnet fishing has been banned in California state waters along the coast, but it remains legal in federal waters and in state waters around the Channel Islands, and in tribal river fisheries for salmon (Pfeiffer et al. 2024). Trawl nets are cone- or funnel-shaped nets towed through the water, either on the seafloor (bottom trawling) or in the midwater/pelagic zone. Midwater trawls target whiting/hake (*Mercluccius productus*) and midwater rockfish, whereas bottom trawls target groundfish, particularly Dover sole (*Microstomus pacificus*), thornyheads (*Sebastolobus*), sablefish, and shrimp (Pfeiffer et al. 2024). Trawls have a wide opening (mouth) at the front but taper to a closed end where the fish are collected.

3.3.3 Hook and Line

There are multiple different types of hook and line gear, and each configuration targets different species. Examples include dinglebar, longline, pelagic longline, and benthic/bottom set long. Longline fishing consists of short lines carrying hooks attached to a longer main line at regular intervals (NMFS 2024). The hooks are generally attached to the main line using a gangion, which are either permanently attached to the main line/set gear or attached when the gear is set and removed during the haul. Longlines are laid either at the bottom with anchors, or suspended horizontally at a predetermined depth, depending on the target species (NMFS 2024). There are usually surface markers with buoys or floats attached to each end of the gear. Pelagic longlines target tuna and other pelagic fishes, and benthic/bottom set longlines target groundfish including Pacific halibut (*Hippoglossus stenolepis*), sablefish, Pacific cod (*Gadus macrocephalus*), and other flatfish, rockfish, and skates (Pfeiffer et al. 2024).

Salmon troll gear is another type of hook and line gear. Of entanglement events that had a confirmed gear type recorded between 1982 and 2017, two humpback whales were observed entangled in salmon troll gear. Salmon trollers target Chinook (*Oncorhynchus tshawytscha*) and/or coho salmon (*Oncorhynchus kisutch*) off the coasts of California, Oregon, Washington, Canada, and Alaska. The troll consists of a stainless-steel wire connected to each outrigger on a boat, and two to six lines are deployed with up to four monofilament leaders/spreads per line. Each leader culminates in a lure and each line is sunk to a specific depth using a 10–15-pound weight. The wire leaders are 1/16 inch in diameter and can be of varying lengths depending on how far the troll is set behind the vessel. The leaders/spreads are made of solid braided nylon cord. Lures can be fished from just below the surface to 980 ft or deeper (Pfeiffer et al. 2024). Vessels troll for salmon up to 50 nautical miles from shore but on average fish within 10 nautical miles from shore. For California, trolling is concentrated along the central and northern coast but does extend into the Southern California Bight. Salmon trolling typically occurs in the summer and fall but the regulations differ by year. Monofilament line entanglements, which can comprise both hook and line and high seas fisheries gear types, are the second-most common type of pinniped entanglement (n = 430) besides net gear entanglements (n = 631) (Stelfox et al. 2021).

3.3.4 High Seas Fisheries

Although gear utilized by fisheries operating in the high seas (i.e., waters extending seaward of 200 miles) has not been identified in large whale entanglement reports along the U.S. West Coast (Saez et al. 2021), gear from these fisheries could drift inshore into the WEAs and form secondary entanglement hazards. Summaries of specific key fisheries are not detailed here as many gear types (e.g., trawls, gillnets, and pelagic longlines) used in the Western and Central Pacific are similar to those used in California fisheries. However, high sea operations often differ in scale and resulting net tonnage, thus additional forces enacted on the mooring cables may be incorporated into the simulation models.

3.4 Biofouling

Biofouling is a term that refers to the 'undesirable' settlement and growth of sedentary and semi-sedentary organisms, and fixing organisms (e.g., bacteria, plants, algae, or animals) on artificial structures in marine and estuarine environments (Tiron et al. 2012, Yang et al. 2017). The effects of biofouling are relevant to the Project because of its biological implications, influence on the drag dynamics of the mooring lines, and its effect on the structural integrity/fatigue life of FOSW moorings.

3.4.1 Biological Implications

FOSW moorings and inter-array cables have the potential to provide vertical habitat in deep water locations off the California coast that are otherwise devoid of vertical structure. These structures can support a diversity of sessile invertebrate communities comprised of anemones, hydroids, bryozoans, sponges, mussels, barnacles, and corals, which in turn, could attract motile invertebrates (Guerin 2009; Langhamer and Wilhelmsson 2009; McLean et al. 2017; Meyer et al. 2018; Todd et al. 2018, 2019, as cited in Todd et al. 2020). The invertebrate assemblage would then provide a foraging base for fish populations (Todd et al. 2020), and in turn, could attract marine megafauna, increasing the potential for entanglement. Additionally, biofouling on the mooring lines would increase the surface roughness and diameter of the lines, making them more likely to snag a drifting net or fishing line, thus increasing the risk for secondary entanglement (Benjamins et al. 2014, Maxwell et al. 2022).

3.4.2 Drag Dynamics, Structural Integrity, and Mooring Life Fatigue

Biofouling is also important to consider for the Project because of its potential impact on both the drag dynamics and the structural integrity of the mooring lines. For example, when developing a monitoring and mitigation system that detects collisions, it may be important to account for changes in movement of the lines as well as fatigue and tension caused by biofouling since these communities can add significant bulk and weight to the lines, and thus, increase the drag (Yang et al. 2017, Marty et al. 2021). If the growth of organisms on the lines is relatively constant over time, it is likely that any additional weight caused by biofouling could be filtered out as “baseline” conditions. A select few studies also demonstrated that biofouling could be a cause of rupture and fatigue in mooring lines and inter-array cables (Gueguen 2016 and Johanning et al. 2011, as cited in Yang et al. 2017). Yang et al. (2017) found that biofouling on wave energy converters can decrease the fatigue life of the moorings up to 76% in some cases. Tables 6–7 and Figures 6–8 in Yang et al. (2017) provide useful quantitative information that may be considered in the Project’s sensor development.

Section 4.0 Met-Ocean Conditions

This section presents the Project's approach for defining met-ocean conditions that will be used in simulating baseline and entanglements scenarios. The framework is based on the American Bureau of Shipping (ABS) standards, which define design load cases (DLCs) specific to the design and installation of FOSW turbines. The DLCs are intended to verify the design adequacy of FOSW turbines subjected to various operational, environmental, and electrical network conditions, among other factors. As such, the DLCs provide a wide range of conditions including a variety of mooring and turbine failure cases. For this Project, we focus on the DLCs representing an intact floating turbine system and typical power generation, which is the most likely operational state for a deployed system, and therefore represents the most probable condition for entanglement to occur. The DLCs that include system faults are important in the ABS framework as this is meant to guide the design of these systems, which will undoubtedly experience faults in situ. These ABS standards rely heavily on the International Electrotechnical Commission (IEC) 61400 standards. Both ABS and IEC standards are referenced in this approach.

Table 17 below is an excerpt for the ABS guide and presents typical power generation DLCs. These DLCs will be utilized to define met-ocean conditions for these simulations (except for DLC 1.4 and 1.5). DLC 1.4 represents a brief strong gust of wind which is non-aligned to the existing flow field. DLC 1.5 similarly represents an extreme wind shear event. Both of these wind behaviors are highly transient in nature, and thus, were not considered in the framework. Buoy data from deployments in the two WEAs are being compiled and analyzed (see Section 4.1 for more details on the data source). Initial findings suggest that we will be able to match site-specific environmental conditions to established, standard DLC conditions, which is necessary for establishing baseline conditions in the simulation and will ensure modeled assumptions align with standardized engineering design criteria. To date, site-specific data from AXYS Technologies WindSentinel™ buoys ("AXYS buoy") deployments in both WEAs has been analyzed and reviewed for use in the modeling simulation. These instrument-laden buoys were deployed at each WEA for a period of approximately one year, providing time series data. The buoys and data are described in greater detail in Section 4.1.

4.1 Data Sources

These ABS standards suggest using measured site-specific data to determine the met-ocean conditions associated with each of the DLCs defined in Table 17. The site-specific data are from Pacific Northwest National Laboratories' (PNNL) Light Detection and Ranging (LiDAR) Buoy Program (AXYS buoys). This program deployed two LiDAR buoys designed to improve understanding of the offshore wind resources in the Humboldt and Morro Bay WEAs, as well as advance FOSW farm technology. Each of the two AXYS buoys were outfitted with a suite of sensors to monitor met-ocean conditions near the sea surface. The main instrument on these buoys is a wind profiling LiDAR sensor (Leosphere Windcube 888). This sensor utilizes a five-beam configuration with four inclined beams (28°) and a single vertical beam. It measures wind speeds at 12 heights from 40 to 250 m above the sea surface with an accuracy of 0.1 m/s (PNNL 2020, Leosphere 2020). In addition to these LiDAR sensors, the AXYS buoys are outfitted with a range of accelerometers to measure wave spectra. Finally, the buoys are equipped with a Nortek, Signature 250 acoustic doppler current profiler, which measures current speed and direction down to 200 m below the sea surface.

Table 17. Conditions and Parameters for Design Load Criteria for Floating Offshore Wind Turbines

DLC	Wind Condition	Waves	Wind & Wave Directionality	Sea Currents	Water Level	Type of Analysis	Safety Factor
1.2	NTM $V_{in} \leq V_{hub} \leq V_{out}$	NSS Joint Probability Distribution of H_s, T_p, V_{hub}	MIS, MUL	NCM	NWLR or ≥ MSL	F	FDF
1.3	ETM $V_{in} \leq V_{hub} \leq V_{out}$	NSS $H_s = E[H_s \mid V_{hub}]$	MIS, MUL	NCM	MSL	S	N
1.4	ECD $V_{hub} = V_r \pm 2$ m/s (6.6 ft/s)	NSS $H_s = E[H_s \mid V_{hub}]$	MIS, wind direction change	NCM	MSL	S	N
1.5	EWS $V_{in} \leq V_{hub} \leq V_{out}$	NSS $H_s = E[H_s \mid V_{hub}]$	MIS, MUL	NCM	MSL	S	N
1.6	NTM $V_{in} \leq V_{hub} \leq V_{out}$	SSS $H_s = H_{s,SSS}$	MIS, MUL	NCM	NWLR	S	N

Source: Excerpt from American Bureau of Shipping (ABS 2024)

Notes: Design load criteria (DLCs) are defined to verify the design adequacy of FOSW turbines subjected to various operational conditions, environmental conditions, and electrical network conditions, among other factors. The DLCs provided here are for turbines producing power (see column one). DLC 1.4 and 1.5 were not considered for the Project. All equations can be referenced in ABS (2024). Wind turbulence conditions are based on either the normal turbulence model (NTM) or the extreme turbulence model (ETM). Wave conditions are defined by the normal sea state (NSS) or severe sea state (SSS). Wind and wave directionality is defined by either the misaligned wind and wave directions (MIS), or multi-directional wind and wave (MUL). Sea currents are defined by the normal current model (NCM). Water levels are determined based on mean sea level (MSL) or normal water level range (NWLR). These DLCs are subject to strength (S) and fatigue (F) analysis and are used in structural assessments under normal design conditions (N) and fatigue design factor (FDF). V_{in} and V_{out} are the cut-in and cut-out wind speeds, respectively. V_R denotes a given reference wind speed. Other definitions: ECD = extreme coherent gust and direction change; EWS = extreme wind shear.

The PNNL LiDAR Buoy Program intended to deploy each of the two buoys for a year in the WEAs (Krishnamurthy et al. 2023). However, due to a system fault, the buoy in the Humboldt WEA was towed to shore and repaired a few months into deployment. This resulted in an extended deployment with non-contiguous measurements. Figure 5 shows the percent of time that valid LiDAR wind speed measurements were recorded in the Humboldt and Morro Bay WEAs, respectively. This graphic demonstrates the effects of fog or heavy precipitation, which prevent the LiDAR sensor from making a measurement (black sections), as well as clearly showing the time for which the Humboldt AXYS buoy was not onsite.

A previous analysis of the LiDAR wind speed data showed that missing values tend to occur at lower wind speeds. It is believed that most of these missing data (aside from those missing due to buoy system failure) result from fog and precipitation obscuring the LiDAR sensor. This assumption is supported by the fact that missing values occur at lower wind speeds and more frequently at distances farther from the sensor.

To address the fact that these wind speeds are not missing at random and to remove bias from this analysis, we extrapolate missing wind speeds where possible based on cup anemometer data (10-m height) and a linear regression to correlate the two. These linear regressions fit well with adjusted R-squared values of 0.90 and 0.79 for the Morro Bay and Humboldt deployment locations, respectively.

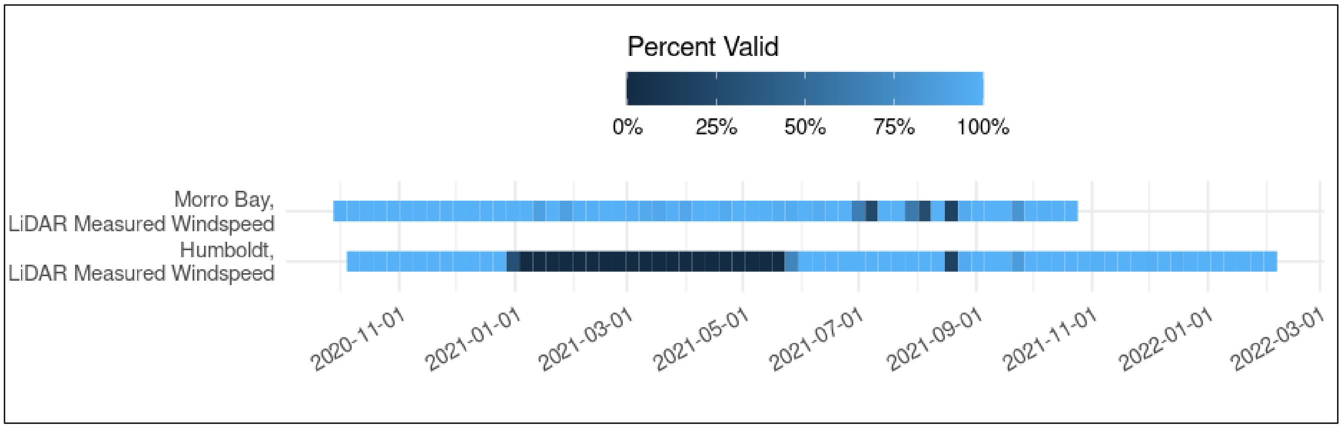

Figure 5. AXYS Buoy Deployments and LiDAR Measured Wind Speed

Source: Schatz Energy Research Center

Notes: For each of the two AXYS buoy deployments (in Morro Bay and Humboldt WEAs), the percentage for which there are valid measures is provided (by week). For the light detection and ranging (LiDAR) measured wind speed, a reference elevation of 140 m was used. Dates are in the format YYYY-MM-DD.

4.2 Wind

The ABS standards define the wind conditions in several facets: wind speeds at hub height, wind speed profile, and turbulent characteristics. This section addresses each and covers the approach to determine the specific values for modeling. Measured wind speed data at 150 m height are summarized in Figure 6.

There are three distinct wind speeds to be modeled between the four considered DLC conditions: (1) average conditions; (2) severe conditions with one-year return intervals (return interval is the average number of years between floods [events] of a certain size, also referred to as the “return period” [Dinicola 1997]); and (3) severe conditions with 50-year return intervals. While the ABS standards suggest using site specific information to define these three values, the IEC 64100 standards (referred to hereafter as ‘IEC standards’) provides simple equations based on turbine classifications to calculate these values. At this early phase of the modeling and simulation development, we used statistical extrapolation techniques in conjunction with the buoy data to determine representative wind speeds. In the interim period, suggested values from the IEC standards were considered. Wind speeds are summarized in Table 18.

Statistical extrapolation used was to fit a Weibull distribution to the existing data and reference this distribution at probabilities representing the 10-minute interval (inherent to the measurement data) and one-year and 50-year return intervals. Determining extreme probabilities (e.g., 50-year return) using a one-year dataset is not ideal and extreme wind cases are transient, therefore, the Weibull distribution is a simple approach for our purpose. Figure 7 (Humboldt WEA) and Figure 8 (Morro Bay WEA) visualize both the fit distribution (left panel) and the observed distribution (right panel) of wind speeds.

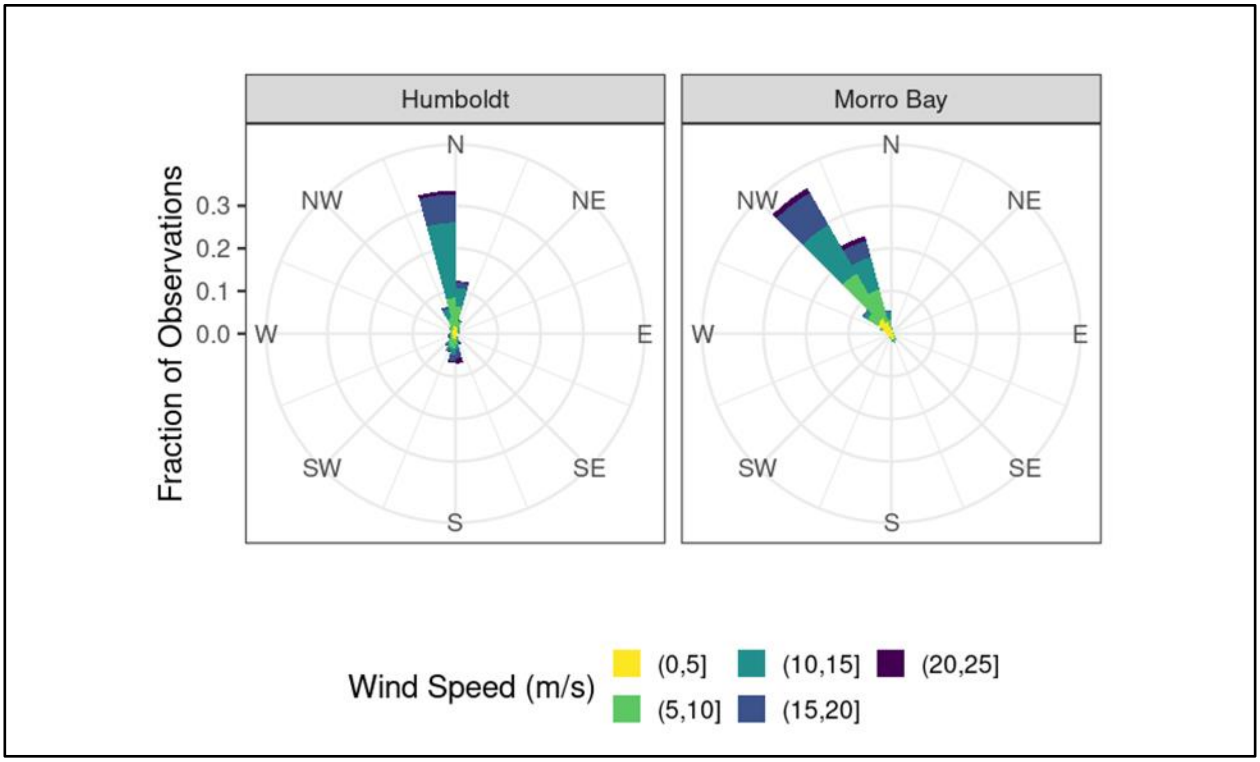

Figure 6. Wind Speed and Direction for Humboldt and Morro Bay WEAs

Source: Schatz Energy Research Center

Notes: These wind roses display the fractional observations of wind speed and direction for the Humboldt and Morro Bay Wind Energy Areas (WEAs). Wind speed is measured in meters per second (m/s) and the color scale represents various wind speeds. Note that the spokes of the wind roses show how often wind blows from that direction.

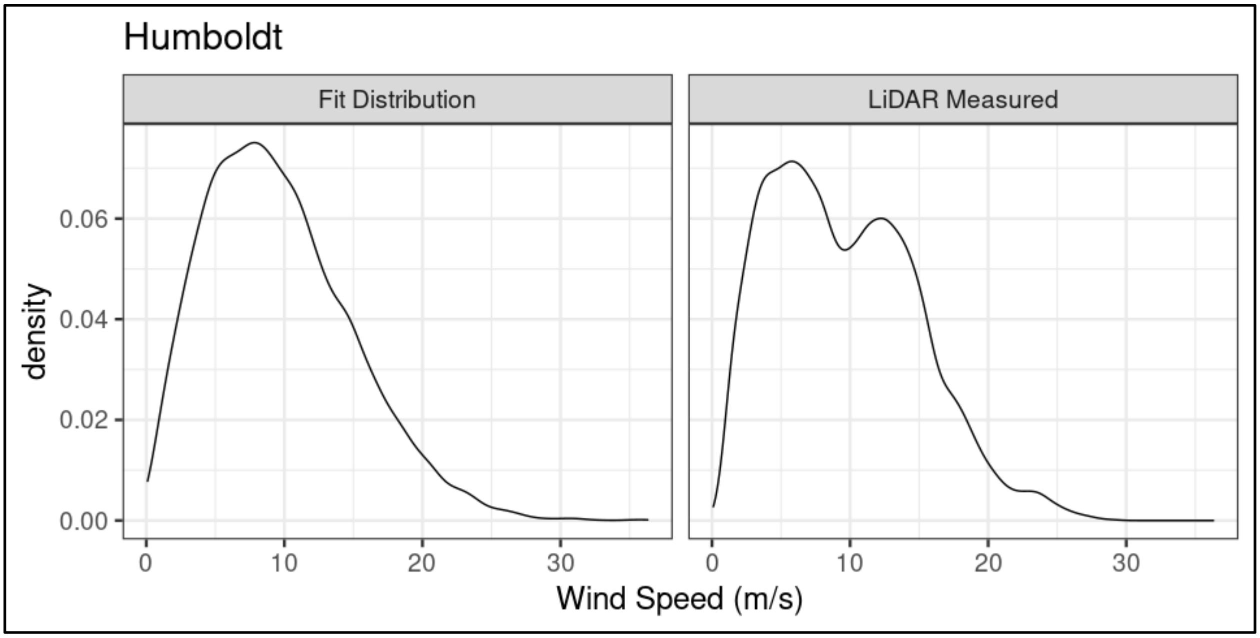

Figure 7. Fit Distribution vs. Measured Wind Speed in the Humboldt WEA

Source: Schatz Energy Research Center

Notes: The modeled fit distribution shows average density of wind speeds (left) compared to a plot of the light detection and ranging (LiDAR) measured wind speed data (right) for the Humboldt Wind Energy Area (WEA). The modeled distribution shows a high density of wind speeds slightly lower than the rated speed for the reference turbines (11 meters per second [m/s]). The plot with observed data displays a bi-modal distribution of two distinct peaks clustered around the rated wind speed for the reference turbines.

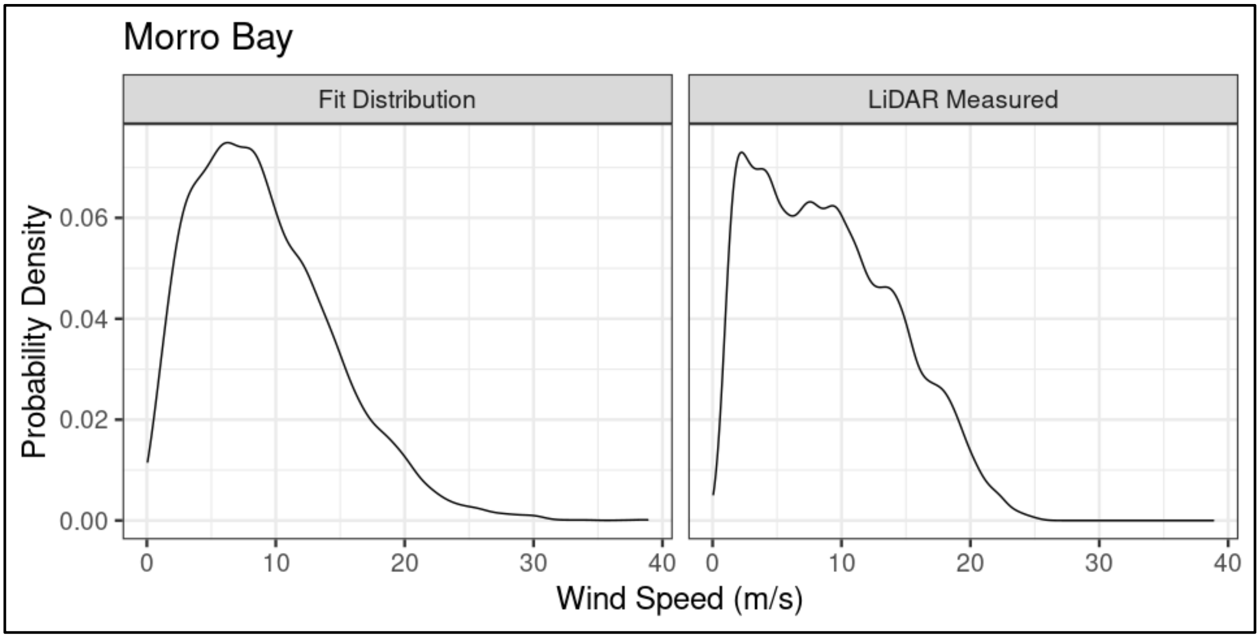

Figure 8. Fit Distribution vs. Measured Wind Speed in the Morro Bay WEA

Source: Schatz Energy Research Center

Notes: The modeled fit distribution shows average density of wind speeds (left) compared to a plot of the light detection and ranging (LiDAR) measured wind speed data (right) for the Morro Bay Wind Energy Area (WEA). The fit distribution shows high density of wind speeds near the rated speed for the reference turbines [11 meters per second (m/s)]. The plot with observed data displays a multi-modal distribution of several peaks clustered around the rated wind speed for the reference turbines.

Table 18. Wind Speeds (m/s) in the Humboldt and Morro Bay WEAs

Location	Average Wind Speed Measured	1-Year Extrapolated Wind Speed	50-Year Extrapolated Wind Speed	IEC – Typical Wind Speed	IEC – 1-Year Wind Speed	IEC – 50 Year
Humboldt	9.62	38.55	45.40	10	56	70
Morro Bay	8.97	40.55	48.55	10	56	70

Source: Schatz Energy Research Center

Notes: Average wind speeds including extrapolated averages for 50-year wind speeds, and International Electrotechnical Commission (IEC)- standard values are provided for the Humboldt and Morro Bay Wind Energy Areas (WEAs).

4.2.1 Wind Speed Profile

The wind speed profile to be modeled is provided by following ABS equation:

(4) $V(z) = V_{hub}(z/z_{hub})^{\alpha}$

Where:

$V(z)$ = wind profile of the 10-minute mean wind speed as a function of height (z) above the Still Water Level (SWL), in m/s (ft/s)

V_{hub} = 10-minute mean wind speed at turbine hub height, in m/s (ft/s)

α = power law exponent, values of which are given by ABS (dimensionless)

z = height above the SWL in m (ft)

z_{hub} = hub height above the SWL in m (ft)

For our applications, the power exponent (α) is given as 0.14 and our turbine hub height is 150 m.

4.2.2 Turbulent Characteristics

Both ABS and IEC standards refer to a standard deviation of turbulence. While the ABS standards imply calculating this value from site specific measurements, the IEC standards provide simple linear relations with wind speed. Due to data limitations (higher time resolution would be required) we chose to use the IEC standards.

(5) $\sigma_1 = I_{ref}(0.75V_{hub} + b)$

where:

σ_1 is the standard deviation of turbulence

I_{ref} for a class b turbine is 0.14

b is given as 5.6 m/s

V_{hub} is the wind speed in meters per second

4.3 Waves

The ABS standards define waves based on significant wave height and time period between peaks (wave period). Similar to the wind conditions, wave height and period are defined in three categories: typical, one-year, and 50-year return intervals. These wave conditions are largely wind driven so the ABS guide suggests using a joint probability distribution conditional on relevant wind speeds. Figure 9 demonstrates the overall probability distribution for wave height and wave period.

To make this analysis of wave parameters conditional for a specific wind speed, one approach is to form the same joint probability distribution but only use input data for periods when the wind speeds were near the average values (to define typical wave action). Results of this analysis imply simulating a ~1.6 m wave with a 6.5 second interval in the Humboldt WEA and a ~2 m wave with a ~8 second interval in the Morro Bay WEA (Figure 10). Additional effort to define this joint probability for extreme wind speed cases is ongoing by the Schatz modeling team.

4.3.1 Wave Directionality

The ABS standards provide minimal guidance for determining the orientation of wind and waves to model. However, it is mentioned in the standards that the misalignment between wind and waves should be considered. Figure 11 shows the distribution of wave directions for the two WEAs. The waves in the Humboldt WEA predominantly originate between West and West by North-West, while the Morro Bay WEA has much less spread of directions with waves predominantly originating from West by North-West. When comparing this distribution of wave directions to the average wind directions presented in Figure 6, it is apparent that the wave and wind misalignment in the Humboldt WEA would be expected to be around ~45 to 90 degrees with primarily northerly and northwesterly winds. In the Morro Bay WEA, wave and wind misalignment would typically be ~25 to 30 degrees with primarily northwesterly winds.

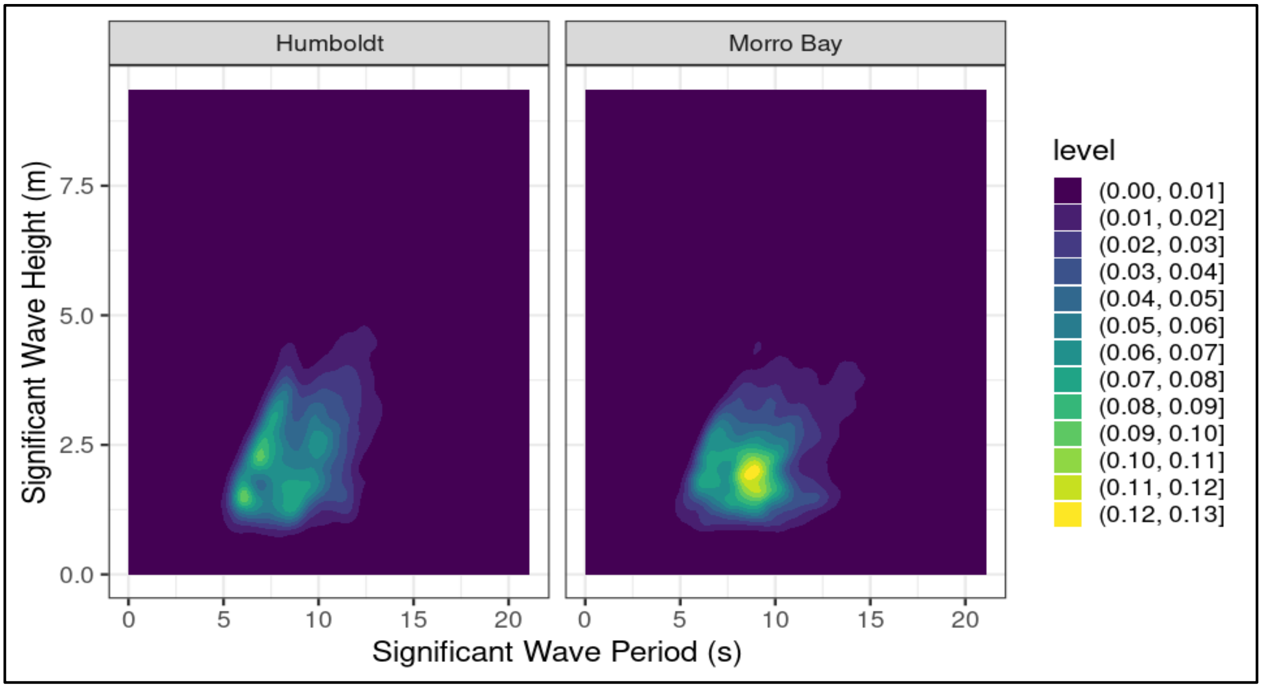

Figure 9. Joint Probability Distribution for Wave Height and Wave Period

Source: Schatz Energy Research Center

Notes: Purple-colored portions display areas of the solution space that rarely (or never) occur while yellow areas show the most common occurrences. m = meters; s = seconds.

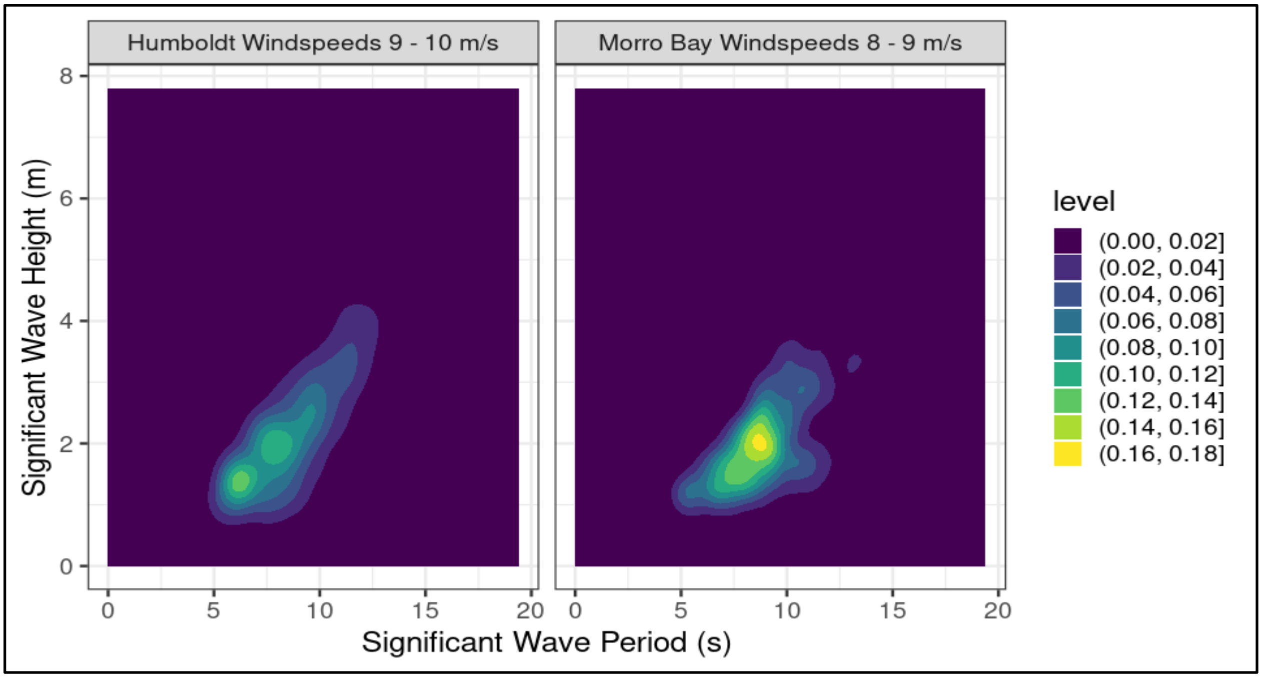

Figure 10. Conditional Probability Distribution for Wave Height and Wave Period

Source: Schatz Energy Research Center

Notes: Joint probability distribution using input data only where wind speeds are near to the typical values to define typical wave action. This figure displays a simulation of a ~1.6-meter (m) wave with a 6.5 second (s) interval in the Humboldt WEA and a ~2 m wave with a ~8 s interval in the Morro Bay WEA. m/s = meters per second.

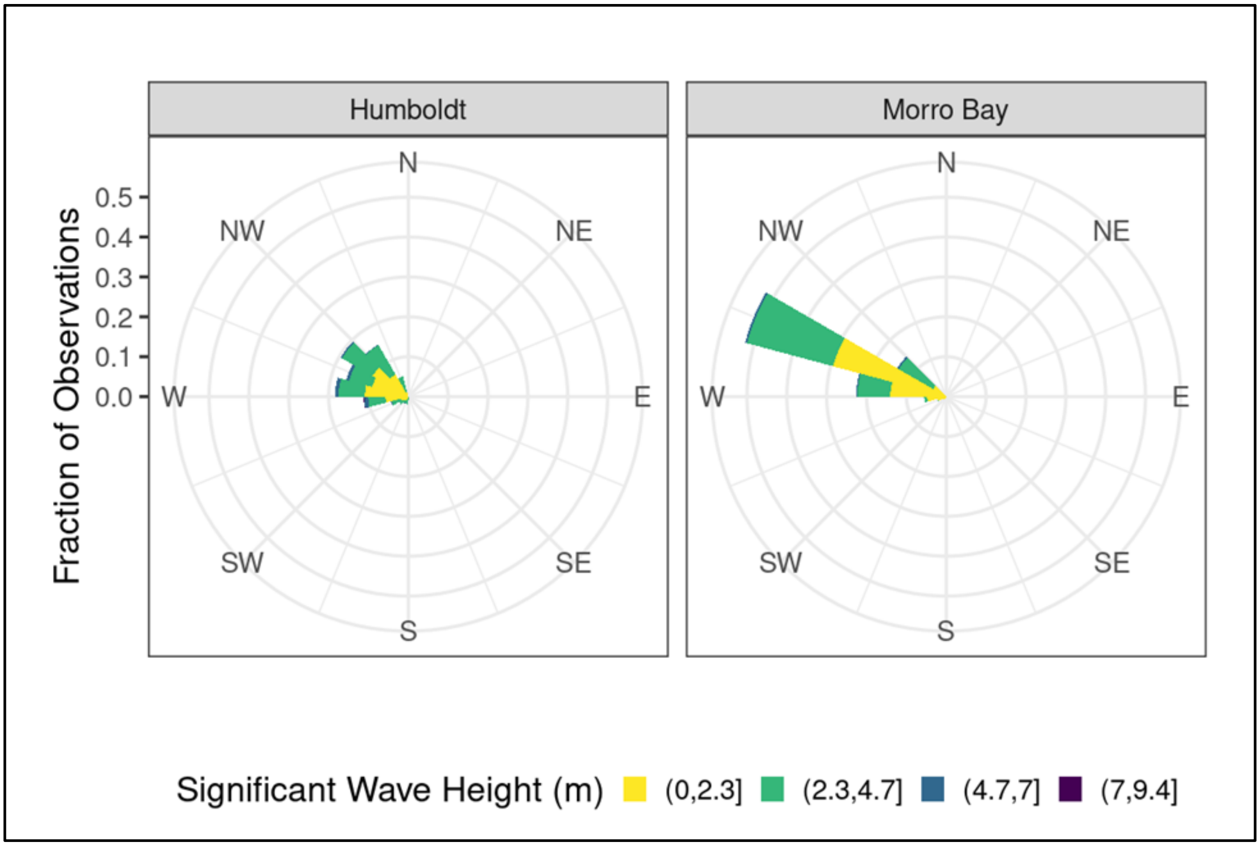

Figure 11. Wave Height and Direction for Humboldt and Morro Bay WEAs

Source: Schatz Energy Research Center

Notes: The color scale represents various wave height ranges. m = meter.

4.4 Currents

The ABS standards document suggests that typical current data be measured in situ, but it provides minimal guidance on how to relate these measurements to the specific modeling parameters. While the current profilers on the AXYS buoys take measurements at multiple depth intervals, we focus on the depth with the fastest current speed measurement. Since currents are largely wind driven, the strongest currents are typically measured near the surface. It is important to note that the current bins nearest the sea surface may contain erroneous measurements as a result of wave or other surface activity. The rose plot in Figure 12 visualizes the fastest currents (among depths measured) and associated directions. The average current speed (at the depth with highest current) was 35 centimeters per second (cm/s) in Humboldt and 40.8 cm/s in Morro Bay. Figure 13 shows average current speed observed by the buoys as a function of depth.

Another interesting analysis is to determine the depths with fastest currents. Figure 14 displays counts for how many timesteps each depth was found to have the fastest current. Note, there is potential bias in this graphic because the profiler tends to have more non-missing measures for surface currents than for deeper currents. This record of current speeds has a larger proportion of missing values below 90 m depth than above. However, we can conclude the upper water column (depths <90 m) has the fastest current speeds. Additional data considerations and datasets are being explored to further validate assumptions and ensure that the most representative met-ocean conditions as feasible are modeled for the Project’s simulation efforts.

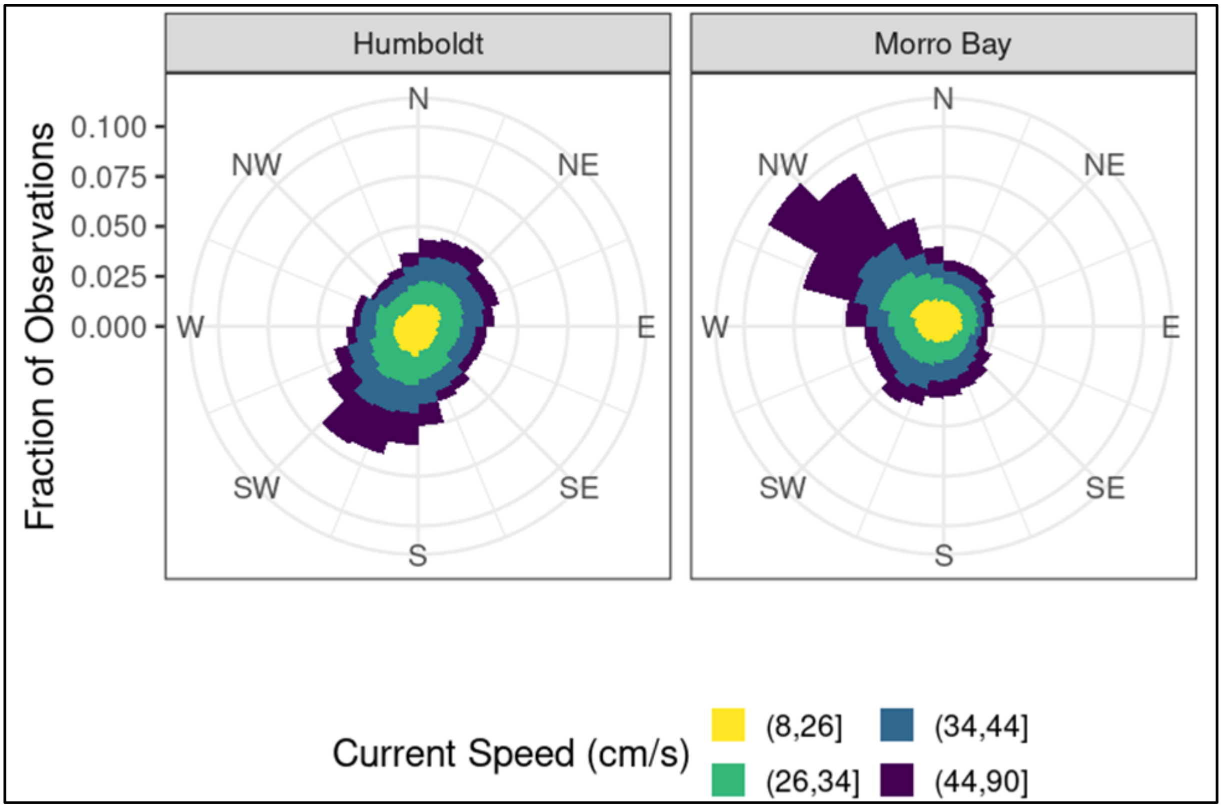

Figure 12. Current Speeds and Associated Directions for Humboldt and Morro Bay WEAs

Source: Schatz Energy Research Center

Notes: Current speeds are given in centimeters per second (cm/s). The color scale represents various current speed ranges.

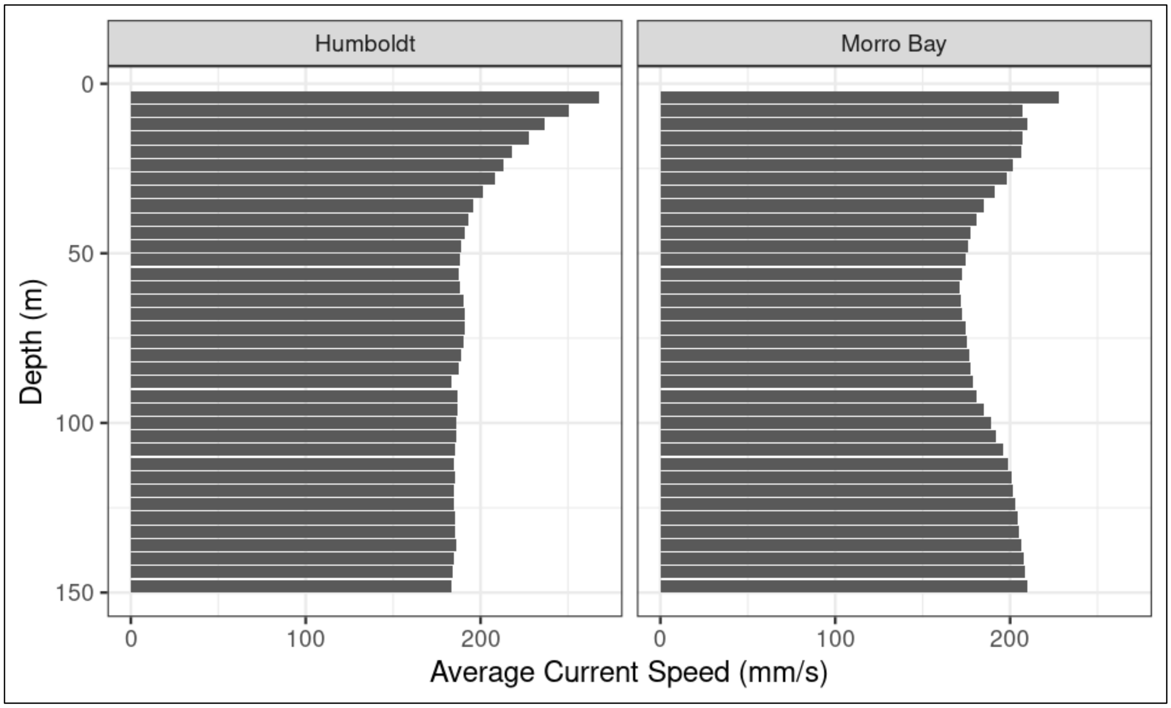

Figure 13. Average Current Speed as a Function of Depth for Humboldt and Morro Bay WEAs

Source: Schatz Energy Research Center

Notes: Current speeds are given in millimeters per second (mm/s). Depth is shown in meters (m).

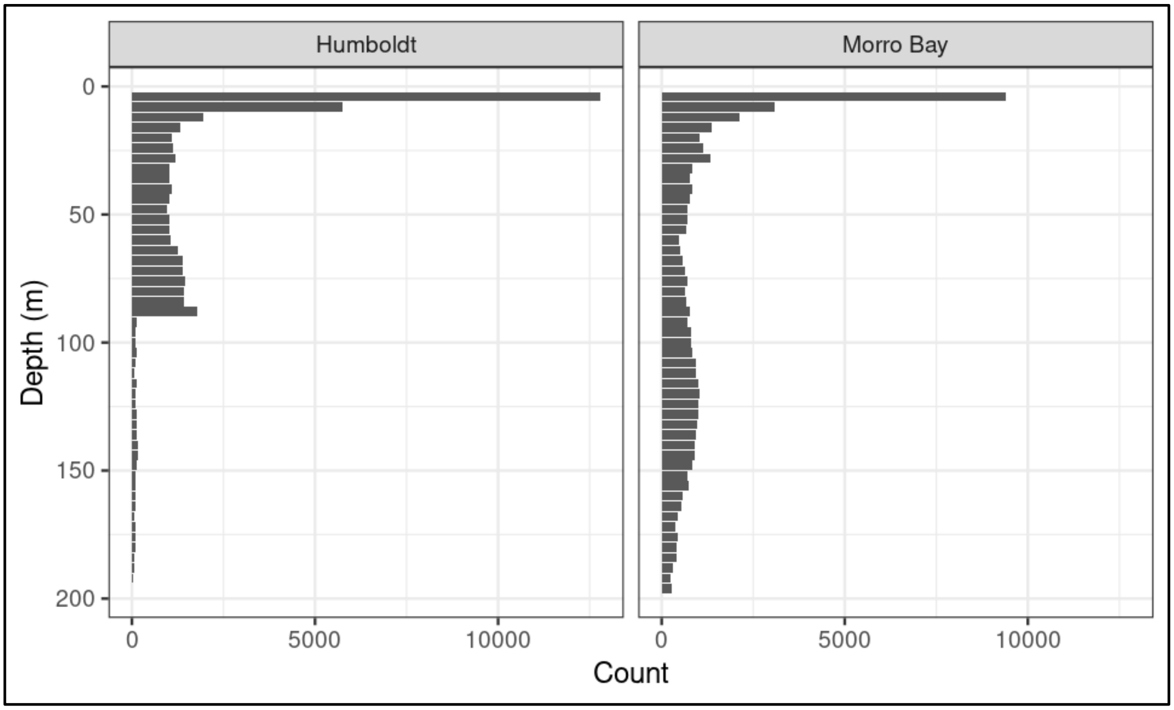

Figure 14. Depth of Peak Current Velocity

Source: Schatz Energy Research Center

Notes: Depth is shown in meters (m).

Section 5.0 References

Adams, J., J. Felis, J. W. Mason, and J. Y. Takekawa. 2014. Pacific Continental Shelf Environmental Assessment (PaCSEA): Aerial Seabird and Marine Mammal Surveys off Northern California, Oregon, and Washington, 2011–2012. OCS Study BOEM 2014-003. U.S. Department of the Interior, Bureau of Ocean Energy Management, Pacific OCS Region, Camarillo, California.

Allen, S. G., J. Mortenson, and S. Webb. 2011. Field Guide to Marine Mammals of the Pacific Coast. University of California Press.

Allyn, E. M., and J. J. Scordino. 2020. Entanglement rates and haulout abundance trends of Steller (*Eumetopias jubatus*) and California (*Zalophus californianus*) sea lions on the north coast of Washington state. PloS One 15(8).

[ABS] American Bureau of Shipping. 2024. Guide for Building and Classing: Floating Offshore Wind Turbines. January. Spring, Texas. https://ww2.eagle.org/content/dam/eagle/rules-and-guides/current/offshore/195-guide-for-building-and-classing-floating-offshore-wind-turbines/195-fowt-guide-jan24.pdf.

Antonelis, G. A., and C. H. Fiscus. 1980. The pinnipeds of the California Current. California Cooperative Oceanic Fisheries Investigations Reports 21:68–78.

Aoki, K., Watanabe, Y. Y., Crocker, D. E., Robinson, P. W., Biuw, M., Costa, D. P., Miyazaki, N., Fedak, M. A., and Miller, P. J. O. 2011. *Northern elephant seals adjust gliding and stroking patterns with changes in buoyancy: validation of at-sea metrics of body density.* The Journal of Experimental Biology. 214, 2973–2987.

Aoki, K., M. Amano, N. Sugiyama, H. Muramoto, M. Suzuki, M. Yoshioka, K. Mori, et al. 2007. Measurement of swimming speed in sperm whales. IEEE:467–471.

Arthur, L. H., W. A. McLellan, M. A. Piscitelli, S. A. Rommel, B. L. Woodward, J. P. Winn, C. W. Potter, et al. 2015. Estimating maximal force output of cetaceans using axial locomotor muscle morphology. Marine Mammal Science 31(4):1401–1426.

Asmutis-Silvia, R., S. Barco, T. Cole, A. Henry, A. Johnson, A. Knowlton, S. Landry, et al. (2017). Rebuttal to published article "A review of ghost gear entanglement amongst marine mammals, reptiles and elasmobranchs" by M. Stelfox, J. Hudgins, and M. Sweet. Marine Pollution Bulletin 117(1–2):554–555. https://doi.org/10.1016/j.marpolbul.2016.11.052

Bailey, H., B. R. Mate, D. M. Palacios, L. Irvine, S. J. Bograd, and D. P. Costa. 2009. Behavioural estimation of blue whale movements in the Northeast Pacific from state-space model analysis of satellite tracks. Endangered Species Research 10(1):93–106.

Bailey, H., S. Fossette, S. J. Bograd, G. L. Shillinger, A. M. Swithenbank, J. Y. Georges, P. Gaspar, et al. 2012. Movement patterns for a critically endangered species, the leatherback turtle (*Dermochelys coriacea*), linked to foraging success and population status. PloS One7(5):1–8.

Baird, R. W. 2008. Risso's dolphin, *Grampus griseus*. Pages 975–976 *in* W. F. Perrin, B. Wursig, and J. G. M. Thewissen, editors, The Encyclopedia of Marine Mammals. Second edition. Academic Press, San Diego, California.

Barlow, J., and K. A. Forney. 2007. Abundance and population density of cetaceans in the California Current ecosystem. Fishery Bulletin 105(4):509–526.

Bath, G. E., C. A. Price, K. L. Riley, and J. A. Morris. 2023. A global review of protected species interactions with marine aquaculture. Reviews in Aquaculture 15(4):1–34.

Becker, E. A., K. A. Forney, D. G. Foley, R. C. Smith, J. E. Moore, and J. Barlow. 2014. Predicting seasonal density patterns of California cetaceans based on habitat models. Endangered Species Research 23(1):1–22.

Becker, E. A., K. A. Forney, P. C. Fiedler, J. Barlow, S. J. Chivers, C. A. Edwards, A. M. Moore, et al. 2016. Moving towards dynamic ocean management: How well do modeled ocean products predict species distributions? Remote Sensing 8(149):2–26.

Becker, E. A., K. A. Forney, D. L. Miller, P. C. Fiedler, J. Barlow, and J. E. Moore. 2020. Habitat-Based Density Estimates for Cetaceans in the California Current Ecosystem Based on 1991–2018 Survey Data. NOAA Technical Memorandum. December. NOAA Technical Memorandum NMFS-SWFSC-638. Prepared by U.S. Department of Commerce, National Oceanic and Atmospheric Administration, National Marine Fisheries Service, Southwest Fisheries Science Center, La Jolla, California.

Benjamins, S., V. Harnois, H. C. M. Smith, L. Johanning, L. Greenhill, C. Carter, and B. Wilson. 2014. Understanding the Potential for Marine Megafauna Entanglement Risk from Marine Renewable Energy Developments. Scottish Natural Heritage. Commissioned Report No. 791.

Benson, S. R., K. A. Forney, J. T. Harvey, J. V. Carretta, and P. H. Dutton. 2007. Abundance, distribution, and habitat of leatherback turtles (*Dermochelys coriacea*) off California, 1990–2003. Fishery Bulletin 105:337–347.

Benson, S. R., T. Eguchi, D. G. Foley, K. A. Forney, H. Bailey, C. Hitipeuw, B. P. Samber, R. F. Tapilatu, V. Rei, P. Ramohia, J. Pita, and P. H. Dutton. 2011. Large-scale movements and high-use areas of western Pacific leatherback turtles, *Dermochelys coriacea*. Ecosphere 2(7):art84. https://doi.org/10.1890/ES11-00053.1.

Black, N.A. 1994. Behavior and ecology of Pacific white-sided dolphins (*Lagenorhynchus obliquidens*) in Monterey Bay, California. M.Sc. thesis, San Francisco State University.

Black, N. A. 2008. Pacific white-sided dolphin. Pages 817–819 *in* W. F. Perrin, B. Wursig, and J. G. M. Thewissen, editors, The Encyclopedia of Marine Mammals. Second edition. Academic Press, San Diego, California.

Bolling, Z. M., S. K. Wright, S. S. S. Teerlink, and E. G. Lyman. 2023. Killer Whale Entanglements in Alaska: Summary Report 1991–2022. U.S. Department of Commerce, NOAA Technical. Memorandum. NMFS-f/AKR-32, 45 p.

Burns, J. J. 2008. Harbor seal and spotted seal *Phoca vitulina* and *P. largha*. 533–542 *in* W. F. Perrin, B. Wursig, and J. G. M. Thewissen, editors, The Encyclopedia of Marine Mammals. Academic Press, San Diego, California.

Burtenshaw, J. C, E. M. Oleson, J. A. Hildebrand, M. A. McDonald, R. K. Andrew, B. M. Howe, and J. A. Mercer. 2004. Acoustic and satellite remote sensing of blue whale seasonality and habitat in the Northeast Pacific. Deep Sea Research Part II: Topical Studies in Oceanography 51(10–11):967–986.

Calambokidis, J. 2009. Sightings of Eleven Species of Marine Mammals during Thirty Surveys from 1991–2007. Cascadia Research, Olympia, Washington.

Calambokidis, J., and J. Barlow. 2020. Updated Abundance Estimates for Blue and Humpback Whales along the U.S. West Coast Using Data through 2018. NOAA-TM-NMFS-SWFSC-634. Prepared by U.S. Department of Commerce, National Oceanic and Atmospheric Administration, National Marine Fisheries Service, Southwest Fisheries Science Center.

Calambokidis, J., G. H. Steiger, C. Curtice, J. Harrison, M. C. Ferguson, E. Becker, M. DeAngelis, et al. 2015. Biologically important areas for selected cetaceans within U.S. waters – West Coast Region. Aquatic Mammals 41(1):39–53.

Calambokidis, J., M. A. Kratofil, D. M. Palacios, B. A. Lagerquist, G. S. Schorr, M. B. Hanson, R. W. Baird, K. A. Forney, E. A. Becker, R. C. Rockwood, and E. L. Hazen. 2024. Biologically Important Areas II for cetaceans within U.S. and adjacent waters – West Coast Region. Frontiers in Marine Science 11:1283231. https://doi.org/10.3389/fmars.2024.1283231.

Carretta, J. V., E. M. Oleson, K. A. Forney, D. W. Weller, A. R. Lang, J. Baker, A. J. Orr, et al. 2023. U.S. Pacific Marine Mammal Stock Assessments: 2023. NOAA Technical Memorandum NMFS. July. NOAA-TM-NMFS-SWFSC-684. U.S. Department of Commerce, National Oceanic and Atmospheric Administration, National Marine Fisheries Service, Southwest Fisheries Science Center.

Chang, C. H., C. M. Jang, and C. Yen-Nien. 2003. The latest record of the leatherback sea turtle (*Dermochelys coriacea*) from Eastern Taiwan. Collection and Research 16.

Checkley, D. M., and J. A. Barth. 2009. Patterns and processes in the California Current System. Progress in Oceanography 83(1–4):49–64.

Cole, M. R. 2020. Detecting Feeding and Estimating the Energetic Costs of Diving in California Sea Lions (*Zalophus californianus*) Using 3-Axis Accelerometers. Master's Thesis. San Jose State University, 5141. DOI: https://doi.org/10.31979/etd.hfrt-ee52.

Copping, A., and M. Grear. 2018. Humpback Whale Encounter with Offshore Wind Mooring Lines and Inter-Array Cables. Report No. PNNL-27988. Report by Pacific Northwest National Laboratory. Report for Bureau of Ocean Energy Management.

Costa, D. P., C. Kuhn, and M. Weise. 2007. Foraging Ecology of the California Sea Lion: Diet, Diving Behavior, Foraging Locations, and Predation Impacts on Fisheries Resources. Research Completion Reports. Paper Coastal 07-03. California Sea Grant College Program, San Diego.

Croll, D. A., A. Acevedo-Gutiérrez, B. R. Tershy, and J. Urbán-Ramírez. 2001. The diving behavior of blue and fin whales: is dive duration shorter than expected based on oxygen stores? Comparative Biochemistry and Physiology Part A: Molecular & Integrative Physiology 129(4):797–809.

Croll, D. A., B. Marinovic, S. R. Benson, F. P. Chavez, N. Black, R. Ternullo, and B. R. Tershy. 2005. From wind to whales: Trophic links in a coastal upwelling system. Marine Ecology Progress Series 289:117–130.

Dahlheim, M. E., A. Schulman-Janiger, N. Black, R. Ternullo, D. Ellifrit, and K. C. Balcomb III. 2008. Eastern temperate North Pacific offshore killer whales (*Orcinus orca*): Occurrence, movements, and insights into feeding ecology. Marine Mammal Science 24(3):719–729.

Dau, B. K., K. V. K. Gilardi, F. M. D. Gulland, A. Higgins, J. B. Holcumb, J. S. Leger, and M. H. Ziccardi. 2009. Fishing gear-related injury in California marine wildlife. Journal of Wildlife Disease 45(2):355–362.

Degrati, M., N. Garcia, M. F. Grandi, M. S. Leonardi, R. L. de Castro, D. G. Vales, S. L. Dans, et al. 2011. New record of a stranded sperm whale (*Physeter macrocephalus*) and a review of strandings along the continental Argentine coast. Mastozoología Neotropical 18(2):307–313.

DeLong, R. L., and B. S. Stewart. 1991. Diving patterns of northern elephant seal bulls. Marine Mammal Science 7(4):369–384. https://doi.org/10.1111/j.1748-7692.1991.tb00112.x.

Dinicola, K. 1997. The "100-year flood" - Fact Sheet 229-96. U.S. Geological Survey. https://www.usgs.gov/publications/100-year-flood.

Dodge, K., S. Landry, B. Lynch, C. Innis, K. Sampson, D. Sandilands, and B. Sharp. 2022. Disentanglement network data to characterize leatherback sea turtle *Dermochelys coriacea* bycatch in fixed-gear fisheries. Endangered Species Research 47:155–170.

Doyle, T., J. Houghton, P. F. O'Súilleabháin, V. Hobson, F. Marnell, J. Davenport, and G. Hays. 2008. Leatherback turtles satellite-tagged in European waters. Endangered Species Research 4:23–31.

Eckert, S. A. 2002. Swim speed and movement patterns of gravid leatherback sea turtles (*Dermochelys coriacea*) at St Croix, US Virgin Islands. Journal of Experimental Biology 205:3689–3697.

[ESRI] Environmental Systems Research Institute, Inc. 2019. ArcGIS Desktop: Release 10.7.1. Redlands, CA: Environmental Systems Research Institute.

Falcone, E. A., and G. S. Schorr. 2014. Distribution and Demographics of Marine Mammals in SOCAL through Photo-Identification, Genetics, and Satellite Telemetry. Technical Report. December. NPS-OC-14-005CR. Chief of Naval Operations, Energy and Environmental Readiness Division. Prepared by Naval Postgrad School, Monterey, California.

Falcone, E. A., E. L. Keene, J. Barlow, J. Steward, T. Cheeseman, C. Hayslip, and D. M. Palacios. 2022. Movements and residency of fin whales (*Balaenoptera physalus*) in the California Current System. Mammalian Biology 102(4):1445–1462.

Feldkamp, S. D. 1985. Swimming and Diving in the California Sea Lion, *Zalophus californianus*. Dissertation. University of California, San Diego.

Feldkamp, S. D., R. L. DeLong, and G. A. Antonelis. 1989. Diving patterns of California sea lions, *Zalophus californianus*. Canadian Journal of Zoology 67(4):872–883.

Feldkamp, S. D., R. L. DeLong, and G.A. Antonelis. 1991. Effects of El Niño 1983 on the foraging patterns of California sea lions (*Zalophus californianus*) near San Miguel Island, California.

Pages 146–155 *in* F. Trillmich and K. A. Ono, editors, Pinnipeds and El Niño: Responses to Environmental Stress. 146–155. Ecological Studies, Springer-Verlag, Berlin.

Fish, F. E., J. Hurley, and D. P. Costa. 2003. Maneuverability by the sea lion *Zalophus californianus*: Turning performance of an unstable body design. Journal of Experimental Biology 206:667–674.

Fish, F. E., P. Legac, T. M. Williams, and T. Wei. 2014. Measurement of hydrodynamic force generation by swimming dolphins using bubble DPIV. Journal of Experimental Biology 217(2):252–260.

Ford, J. K. B., G. M. Ellis, L. G. Barrett-Lennard, A. B. Morton, R. S. Palm, and K. C. Balcomb. 1998. Dietary specialization in two sympatric populations of killer whales (*Orcinus orca*) in coastal British Columbia and adjacent waters. Canadian Journal of Zoology 76(8):1456–1471.

Ford, J. K. B., and R. R. Reeves. 2008. Fight or flight: Antipredator strategies of baleen whales. Mammal Review 38(1):50–86.

Forman, P., D. Goley, and C. Nasr. 2018. Emerging Northern Elephant Seal Colony in the King Range National Conservation Area 2017–2018. April 1. Winter Breeding Season Report. Bureau of Land Management.

Forney, K. A., and J. Barlow. 1998. Seasonal patterns in the abundance and distribution of California cetaceans, 1991–1992. Marine Mammal Science 14(3):460–489.

Forney, K. A., M. C. Ferguson, E. A. Becker, P. C. Fiedler, J. V. Redfern, J. Barlow, I. L. Vilchis, et al. 2012. Habitat-based spatial models of cetacean density in the eastern Pacific Ocean. Endangered Species Research 16:112–133.

Fossette, S., V. J. Hobson, C. Girard, B. Calmettes, P. Gaspar, J. Y. Georges, and G. C. Hays. 2010. Spatio-temporal foraging patterns of a giant zooplanktivore, the leatherback turtle. Journal of Marine Systems 81(3):225–234.

Galli, S., P. Gaspar, S. Fossette, B. Calmettes, G. C. Hays, J. R. E. Lutjeharms, and P. Luschi. 2012. Orientation of migrating leatherback turtles in relation to ocean currents. Animal Behaviour 84(6):1491–1500.

Glarou, M., S. Gero, A. Frantzis, J. M. Brotons, F. Vivier, P. Alexiadou, M. Cerda, et al. 2022. Estimating body mass of sperm whales from aerial photographs. Marine Mammal Science 39(1):251–273.

Goforth, H. 1990. Ergometry (exercise testing) of the bottlenose dolphin. Pages 559–574 *in* S. Leatherwood and R. Reeves, editors, The Bottlenose Dolphin. Academic Press, San Diego, California.

Goldbogen, J. A., J. Calambokidis, D. A. Croll, J. T. Harvey, K. M. Newton, E. M. Oleson, G. Schorr, et al. 2008. Foraging behavior of humpback whales: Kinematic and respiratory patterns suggest a high cost for a lunge. Journal of Experimental Biology 211(23):3712–3719.

Goldbogen, J. A., J. Calambokidis, E. M. Oleson, J. Potvin, N. D. Pyenson, G. S. Schorr, and R. E. Shadwick. 2011. Mechanics, hydrodynamics and energetics of blue whale lunge feeding: efficiency dependence on krill density. Journal of Experimental Biology 214:131–146.

Goldbogen, J. A., J. Calambokidis, A. S. Friedlaender, J. Francis, S. L. DeRuiter, A. K. Stimpert, E. Falcone, et al. 2012. Underwater acrobatics by the world's largest predator: 360 rolling maneuvers by lunge-feeding blue whales. Biology Letters 9(20120986).

Goley, D., and J. T. Harvey. 2010. Retrospective Analysis of Marine Mammal Ecological Data and Baseline Marine Mammal Monitoring in Northern California. Final report to CH 2 M Hill.

Gorton, A., and G. Harker-Klimes. 2020. International, national, and regional perspectives and projects for U.S. offshore wind development. *In* Potential Effects of Offshore Renewable Energy: Knowledge and Resources, POET Webinar Series, Pacific Ocean Energy Trust. https://pacificoceanenergy.org/wp-content/uploads/2020/04/POETWebinar_20200415_PNNL.pdf.

Heath, C. B., and W. F. Perrin. 2008. California, Galapagos, and Japanese sea lions, *Zalophus californianus*, *Z. wollebaeki*, and *Z. japonicas*. Pages 170–176 *in* W. F. Perrin, B. Wursig, and J. G. M. Thewissen, editors, The Encyclopedia of Marine Mammals. Academic Press, San Diego, California.

Herder, M. J. 1986. Seasonal Movements and Hauling Site Fidelity of Harbor Seals, *Phoca vitulina richardsi*, Tagged at the Klamath River, California. Master's thesis. Humboldt State University, Arcata, California.

Herman, D. P., D. G. Burrows, P. R. Wade, J. W. Durban, C. O. Matkin, R. G. LeDuc, L. G. Barrett-Lennard, et al. 2005. Feeding ecology of eastern North Pacific killer whales *Orcinus orca* from fatty acid, stable isotope, and organochlorine analyses of blubber biopsies. Marine Ecology Progress Series 302:275–291.

Irvine, L. M., B. R. Mate, M. H. Winsor, D. M. Palacios, S. J. Bograd, D. P. Costa, and H. Bailey. 2014. Spatial and temporal occurrence of blue whales off the U.S. west coast, with implications for management. PLoS One 9(7):e102959.

Irvine, L., D. M. Palacios, B. A. Lagerquist, and B. R. Mate. 2019. Scales of blue and fin whale feeding behavior off California, USA, with implications for prey patchiness. Frontiers in Ecology and Evolution 7(338):1–16.

Johnson, A., G. Salvador, J. Kenney, J. Robbins, S. Kraus, S. Landry, and P. Clapham. 2005. Fishing gear involved in entanglements of right and humpback whales. Marine Mammal Science 21(4):635–645.

Jones, M. L., and S. L. Swartz. 2008. Gray whale *Eschrichtius robustus*. Pages 503–511 *in* W. F. Perrin, B. Wursig, and J. G. M. Thewissen, editors, The Encyclopedia of Marine Mammals. Second edition. Academic Press, San Diego, California.

Krahn, M. M., M. J. Ford, W. F. Perrin, P. R. Wade, R. P. Angliss, M. B. Hanson, B. L. Taylor, et al. 2004. 2004 Status Review of Southern Resident Killer Whales (*Orcinus orca*) under the Endangered Species Act. NOAA Technical Memorandum NMFS-NWFSC-62. U. S. Department of Commerce, National Marine Fisheries Service, Northwest Fisheries Science Center, Seattle, Washington.

Krahn, M. M., D. P. Herman, C. O. Matkin, J. W. Durban, L. Barrett-Lennard, D. G. Burrows, M. E. Dahlheim, et al. 2007. Use of chemical tracers in assessing the diet and foraging regions of eastern North Pacific killer whales. Marine Environment Research 63:91–114.

Krishnamurthy, R., C. García Medina, B. Gaudet, W. I. Gustafson Jr., E. I. Kassianov, J. Liu, R. K. Newsom, et al. 2023. Year-long buoy-based observations of the air–sea transition zone off the US west coast. Earth System Science Data 15:5667–5699.

Laake, J. L., S. R. Melin, A. J. Orr, D. J. Greig, K. C. Prager, R. L. DeLong, and J. D. Harris. 2016. California Sea Lion Sex- and Age-specific Morphometry. U.S. Dep. Commer., NOAA Tech. Memo. NMFS-AFSC-312, 21 p. http://dx.doi.org/10.7289/V5/TM-AFSC-312.

Lagerquist, B. A., B. R. Mate, J. G. Ortega-Ortiz, M. Winsor, and J. Urban-Ramirez. 2008. Migratory movements and surfacing rates of humpback whales (*Megaptera novaeangliae*) satellite tagged at Socorro Island, Mexico. Marine Mammal Science 24(4):815–830.

Le Boeuf, B. J., Y. Naito, T. Asaga, D. Crocker, and D. P. Costa. 1992. Swim speed in a female northern elephant seal: metabolic and foraging implications. Canadian Journal of Zoology 70:786–795.

Leosphere. 2020. Windcube Buoy 2019. Windcube Buoy User Guide. Saclay, France.

Lewison, R. L., S. A. Freeman, and L. B. Crowder. 2004. Quantifying the effects of fisheries on threatened species: the impact of pelagic longlines on loggerhead and leatherback sea turtles. Ecology Letters 7(3):221–231.

Lowry, M. S., and K. A. Forney. 2005. Abundance and distribution of California sea lions (*Zalophus californianus*) in central and northern California during 1998 and summer 1999. Fishery Bulletin 103(2):331–343.

Lowry, M. S., J. V. Carretta, and K. A. Forney. 2008. Pacific harbor seal census in California during May-July 2002 and 2004. California Fish and Game 94(4):180–193.

Lowry, M. S., W. L. Perryman, M. S. Lynn, R. L. Westlake, and F. Julian. 1996. Counts of northern elephant seals, *Mirounga angustirostris*, from large-format aerial photographs taken at rookeries in southern California during the breeding season. Fishery Bulletin 94:176–185.

Lowry, M. S., R. Condit, B. Hatfield, S. G. Allen, R. Berger, P. A. Morris, B. J. Le Boeuf, et al. 2014. Abundance, distribution, and population growth of the northern elephant seal (*Mirounga angustirostris*) in the United States from 1991 to 2010. Aquatic Mammals 40(1):20–31.

Lowry, M. S., S. R. Melin, and J. L. Laake. 2017. Breeding Season Distribution and Population Growth of California Sea Lions, *Zalophus californianus*, in the United States during 1964-2014. NOAA Technical Memorandum. April. NOAA-TM-NMFS-SWFSC-574. Prepared by the U.S. Department of Commerce, National Oceanic and Atmospheric Administration, National Marine Fisheries Service, Southwest Fisheries Science Center, La Jolla, California.

Lowry, M. S., E. M. Jaime, and J. E. Moore. 2021. Abundance and distribution of pinnipeds at the Channel Islands in southern California, central and northern California, and southern Oregon during summer 2016–2019. U.S. Department of Commerce, NOAA Technical Memorandum NMFS-SWFSC-656. https://doi.org/10.25923/6qhf-0z55.

Maniscalco, J. M., K. M. Wynne, K. W. Pitcher, M. B. Hanson, S. R. Melin, and S. Atkinson. 2004. The occurrence of California sea lions (*Zalophus californianus*) in Alaska. Aquatic Mammals 30(3):427–433.

Martin, S. L., Z. Siders, and T. Eguchi. 2020. Update to Assessing the Population-Level Impacts of North Pacific Loggerhead and Western Pacific Leatherback Turtle Interactions, Inclusion of the Hawaii-Based Deep-Set and American Samoa-Based Longline Fisheries. https://doi.org/10.25923/PNF2-2Q77.

Marty, A., C. Berhault, G. Damblans, J.-V. Facq, B. Gaurier, G. Germain, T. Soulard, and F. Schoefs. 2021. Experimental study of hard marine growth effect on the hydrodynamical behaviour of a submarine cable. Applied Ocean Research 114:102810. https://doi.org/10.1016/j.apor.2021.102810.

Mason Cole. 2020. Detecting Feeding and Estimating the Energetic Costs of Diving in California Sea Lions (Zalophus Californianus) Using 3-Axis Accelerometers. San José State University ProQuest Dissertations & Theses. 28262875.

Mate, B. 1979. California sea lion. Pages 5–8 *in* FAO Advisory Committee on Marine Resource Research Working Party on Marine Mammals, editors, Mammals in the Sea. Volume 2. Pinniped Species Summaries and Report on Sirenians. Food and Agriculture Organization of the United Nations, Rome, Italy.

Maxwell, S. M., F. Kershaw, C. C. Locke, M. G. Conners, C. Dawson, S. Aylesworth, R. Loomis, et al. 2022. Potential impacts of floating wind turbine technology for marine species and habitats. Journal of Environmental Management 307(114577).

Mead, J. G. 2008. Beaked whales, overview, Ziphiidae. Pages 94-97 *in* W. F. Perrin, B. Wursig, and J. G. M. Thewissen, The Encyclopedia of Marine Mammals. Second edition. Academic Press, San Diego, California.

[NMFS] National Marine Fisheries Service. 2008. Endangered and threatened species: Designation of critical habitat for North Pacific right whale. Federal Register 73(68):19000–19014.

[NMFS] National Marine Fisheries Service. 2012. Endangered and threatened species: Final rule to revise the critical habitat designation for the endangered leatherback sea turtle. Federal Register 77(17):4169–4201.

[NMFS] National Marine Fisheries Service. 2021a. Endangered and threatened wildlife and plants: Revision of critical habitat for the southern resident killer whale distinct population segment. Federal Register 86(145):41668–41698.

[NMFS] National Marine Fisheries Service. 2021b. Endangered and Threatened Wildlife and Plants: Designating Critical Habitat for the Central America, Mexico, and Western North Pacific Distinct Population Segments of Humpback Whales. Federal Register 86(75):21082.

[NMFS] National Marine Fisheries Service. 2022. Takes of Marine Mammals Incidental to Specific Activities; Taking Marine Mammals Incidental to Weapons Testing at Vandenberg Air Force Base, California. Federal Register 87(4):762–776.

[NMFS] National Marine Fisheries Service. 2024. Guide for Identifying Gear from Marine Mammal Entanglements in the U.S. West Coast and Alaska. U.S. Department of Commerce, National Oceanic and Atmospheric Administration, National Marine Fisheries Service. <https://www.fisheries.noaa.gov/resource/document/guide-identifying-gear-marine-mammal-entanglements-us-west-coast-and-alaska>

[NMFS] National Marine Fisheries Service, and [USFWS] U.S. Fish and Wildlife Service. 2014. Olive Ridley Sea Turtle (*Lepidochelys olivacea*) 5-Year Review: Summary and Evaluation. June. National Marine Fisheries Service, Office of Protected Resources, Silver Spring, Maryland, and U.S. Fish and Wildlife Service, Southeast Region, Jacksonville, Florida.

[NMFS] National Marine Fisheries Service, and [USFWS] U.S. Fish and Wildlife Service. 2020a. Endangered Species Act Status Review of the Leatherback Turtle (*Dermochelys coriacea*). Status Review. National Marine Fisheries Service Office of Protected Resources and U.S. Fish and Wildlife Service.

[NMFS] National Marine Fisheries Service, and [USFWS] U.S. Fish and Wildlife Service. 2020b. Loggerhead Sea Turtle (*Caretta caretta*) North Pacific Ocean DPS 5-Year Review: Summary and Evaluation. 5-Year Status Review.

[NOAA] National Oceanic and Atmospheric Administration. 2023a. West Coast Large Whale Entanglement Response Program. W. C. R. Office, Marine Mammal Protection. Website. https://www.fisheries.
noaa.gov/west-coast/marine-mammal-protection/west-coast-large-whale-entanglement-response-program. Accessed 2024-01-13.

[NOAA] National Oceanic and Atmospheric Administration Fisheries. 2023b. NOAA Fisheries Species Directory. United States Department of Commerce. <https://www.fisheries.noaa.gov/species-directory>.

[PNNL] Pacific Northwest National Laboratory. 2020. LiDAR Buoy Program. PNNL-SA-156916. U.S Department of Energy.

Parton, K.J., Galloway, T.S., Godley, B.J., 2019. Global review of shark and ray entanglement in anthropogenic marine debris. Endangered Species Research 39:173–190. <https://doi.org/10.3354/esr00964>.

Pfeiffer, L., C. Alkire, J.L. Ise. 2024. Socioeconomic characterization of west coast fisheries in relation to offshore wind energy development. Camarillo (CA): U.S. Department of the Interior, Bureau of Ocean Energy Management. 109 p. Report No.: OCS Study BOEM 2024-054. Interagency Agreement Number M22PG00032.

Pitman, R. 2008. Mesoplodont whales, *Mesoplodon* spp. Pages 721–726 in W. F. Perrin, B. Wursig, and J. G. M. Thewissen, editors, The Encyclopedia of Marine Mammals. Second edition. Academic Press, San Diego, California.

Point Blue Conservation Science. 2022a. Environmental Data Catalog for the Morro Bay Wind Energy Area. Unpublished Report to the California Ocean Protection Council. Point Blue Conservation Science (Contribution No. 2397), Petaluma, California.

Point Blue Conservation Science. 2022b. Environmental Data Catalog for the Humboldt Wind Energy Area. Unpublished Report to the California Ocean Protection Council. Point Blue Conservation Science (Contribution No. 2387), Petaluma, California.

R Core Team (2024). _R: A Language and Environment for Statistical Computing_. R Foundation for Statistical Computing, Vienna, Austria. <https://www.R-project.org/>.

Rice, D. W. 1974. Whales and whale research in the eastern North Pacific. Pages 170–195 *in* W. E. Schevill, editor, The Whale Problem. Harvard University Press, Cambridge, Massachusetts.

Rykaczewski, R. R., and D. M. Checkley. 2008. Influence of ocean winds on the pelagic ecosystem in upwelling regions. Proceedings of the National Academy of Sciences of the United States of America 105(6):1965–1970.

Saez, L., D. Lawson, and M. DeAngelis. 2013. Understanding the Co-Occurrence of Large Whales and Commercial Fixed Gear Fisheries Off the West Coast of the United States. September. NOAA-TM-NMFS-SWR-044. Prepared by U.S. Department of Commerce, National Oceanic and Atmospheric Administration, National Marine Fisheries Service, Southwest Region Office, Long Beach, California.

Saez, L., D. Lawson, and M. DeAngelis. 2021. Large Whale Entanglements Off the U.S. West Coast, from 1982-2017. NOAA Technical Memorandum March. NMFS-OPR-63A. Prepared by U.S. Department of Commerce, National Oceanic and Atmospheric Administration, National Marine Fisheries Service.

Scales, K. L., G. S. Schorr, E. L. Hazen, S. J. Bograd, D. L. Miller, R. D. Andrews, A. N. Zerbini, et al. 2017. Should I stay or should I go? Modelling year-round habitat suitability and drivers of residency for fin whales in the California Current. Biodiversity Research 23:1204–1215.

Schorr, G. S., M. B. Hanson, E. A. Falcone, C. K. Emmons, S. M. Jarvis, R. D. Andrew, and E. M. Keene. 2022. Movements and diving behavior of the eastern north Pacific offshore killer whale (*Orcinus orca*). Frontiers in Marine Science 9(854893).

Seminoff, J. A., C. D. Allen, G. H. Balaza, P. H. Dutton, T. Eguchi, H. L. Haas, S. A. Hargrove, et al. 2015. Status Review of the Green Turtle (*Chelonia mydas*) Under the Endangered Species Act. Technical Memorandum. March. NOAA-TM-NMFS-SFWSC-539. Prepared by the U.S. Department of Commerce, National Oceanic and Atmospheric Administration, National Marine Fisheries Service, Southwest Fisheries Science Center.

Southall, B., R. Mazurek, and R. Erikksen. 2023. Vulnerability Index to Scale Effects of Offshore Renewable Energy on Marine Mammals and Sea Turtles Off the U.S. West Coast (VIMMS). Report No OCS Study BOEM 2023-057. U.S. Department of the Interior, Bureau of Ocean Energy Management, Camarillo, California.

Starbird, C., A. Baldridge, and J. Harvey. 1993. Seasonal occurrence of leatherback sea turtles (*Dermochelys coriacea*) in the Monterey Bay region, with notes on other sea turtles, 1986-1991. California Fish and Game 79:54–62.

Stebbins, R. C., and S. M. McGinnis. 2012. Field Guide to Amphibians and Reptiles of California. 1. California Natural History Guides. University of California Press.

Stelfox, M., J. Hudgins, and M. Sweet. 2016. A review of ghost gear entanglement amongst marine mammals, reptiles and elasmobranchs. Marine Pollution Bulletin 111(1-2):6–17.

Sullivan, R. M. 1980. Seasonal occurrence and haul-out use in pinnipeds along Humboldt County, California. Journal of Mammalogy 61(4):754–760.

Tiron, R., C. Pinck, E. G. Reynaud, and F. Dias. 2012. Is biofouling a critical issue for wave energy converters? Proceedings of the Twenty-Second International Offshore and Polar Engineering Conference, June 17-22, 2012, Rhodes, Greece.

Todd, V. L. G., L. Lazar, L. D. Williamson, I. T. Peters, A. L. Hoover, S. E. Cox, I. B. Todd, P. I. Macreadie, D. L. McLean. 2020. Underwater visual records of marine megafauna around offshore anthropogenic structures. Frontiers in Marine Science 7(230):1–16.

Urban, R. J., A. Jaramillo, L. A. Aguayo, P. L. De Guevara, Z. M. Salinas, C. Alvarez, L. Medrano-Gonzalez, et al. 2000. Migratory destinations of humpback whales wintering in the Mexican Pacific. Journal of Cetacean Research and Management 2(2):101–110.

[USFWS] U.S. Fish and Wildlife Service. 2011. Endangered and threatened species; Determination of nine distinct population segments of loggerhead sea turtles as endangered or threatened; Final rule. Federal Register 76(184):58868–58951.

U.S. Offshore Wind Synthesis of Environmental Effects Research. 2022. Risk to Marine Life from Marine Debris & Floating Offshore Wind Cable Systems. Report by National Renewable

Energy Laboratory and Pacific Northwest National Laboratory for the U.S. Department of Energy, Wind Energy Technologies Office. https://tethys.pnnl.gov/seer.

Walker, W. A., and L. L. Jones. 1993. Food habits of northern right whale dolphin, Pacific white-sided dolphin, and northern fur seal caught in the high seas driftnet fisheries of the North Pacific Ocean, 1990. Bulletin of the International North Pacific Fisheries Commission 53:285–295.

Watwood, S. L., P. J. O. Miller, M. Johnson, P. T. Madsen, and P. L. Tyack. 2006. Deep-diving foraging behaviour of sperm whales (*Physeter macrocephalus*). Journal of Animal Ecology 75(3):814–825.

Weinrich, M. 1999. Behavior of a humpback whale (*Megaptera novaeangliae*) upon entanglement in a gill net. Marine Mammal Science 15(2):559–563.

Williams, R., and D. P. Noren. 2009. Swimming speed, respiration rate, and estimated cost of transport in adult killer whales. Marine Mammal Science 25(2):327–350.

Williams, T., W. Friedl, and J. Haun. 1993. The physiology of bottlenose dolphins (*Tursiops truncatus*): heart rate, metabolic rate and plasma lactate concentration during exercise. Journal of Experimental Biology 179:31-46.

Wood, M. P., and L. Carter. 2008. Whale entanglements with submarine telecommunication cables. IEEE Journal of Oceanic Engineering 33(4):445–450.

Woodward, B. L., J. P. Winn, and F. E. Fish. 2006. Morphological specializations of baleen whales associated with hydrodynamic performance and ecological niche. Journal of Morphology 267(11):1284–1294.

Wright, B. M., J. K. B. Ford, G. M. Ellis, V. B. Deecke, A. D. Shapiro, B. C. Battaile, and A. W. Trites. 2017. Fine-scale foraging movements by fish-eating killer whales (*Orcinus orca*) relate to the vertical distributions and escape responses of salmonid prey (*Oncorhynchus* spp.). Movement Ecology 5(1):3.

Yang, S. H., J. W. Ringsberg, E. Johnson, and Z. Hu. 2017. Biofouling on mooring lines and power cables used in wave energy converter systems - Analysis of fatigue life and energy performance. Applied Ocean Research 65:155–177.

Appendix A. Megafauna Species Potentially Present in the Wind Energy Areas

Table A1. Megafauna Species Potentially Present in the Wind Energy Areas

Species	Listing Status[1]	Likelihood of Presence[2]	Seasonality	Habitat Association	Vulnerability Index[3]
Cetaceans—Odontocetes					
Northern right-whale dolphin (*Lissodelphis borealis*)—California-Oregon-Washington (COW) stock	MMPA	Humboldt WEA: Present Morro Bay WEA: Present	Northern right-whale dolphins conduct seasonal movements along the U.S. West Coast, moving into California waters during the cold winter months and moving northward to Oregon and Washington in spring and summer (Allen et al. 2011). Within California, they move from northern waters in late spring and summer to the Southern California Bight	Endemic to temperate waters throughout the North Pacific. Primarily seen in waters overlying the outer continental shelf, shelf break and beyond (Barlow and Forney 2007, Carretta et al. 2023). Depth and sea surface temperature (SST) are key predictors of their presence (Becker et al. 2020). Their	Low risk; non-zero because of their bycatch risk in thresher shark and swordfish fisheries.

Species	Listing Status[1]	Likelihood of Presence[2]	Seasonality	Habitat Association	Vulnerability Index[3]
			during the winter (Becker et al. 2014, Carretta et al. 2023). Densities in the two WEAs are predicted to be highest in the summer/fall (Becker et al. 2020; Point Blue Conservation Science 2022a, b).	core population in the eastern Pacific can be found in central California between Point Conception in the south and Point Sur to the north (Allen et al. 2011).	
Pacific white-sided dolphin (*Lagenorhynchus obliquidens*)—COW, Northern and Southern stock	MMPA	Humboldt WEA: Present Morro Bay WEA: Present	Year-round; however, they conduct seasonal movements throughout their range, and are abundant along the coast of Southern California from April to November and along the coasts of Oregon and Washington in spring and summer as SST increases (Allen	Occur across the North Pacific Ocean both in the open ocean, and along the outer continental shelf and shelf break over depths of 1,000 meters (m) (Black 2008, Allen et al. 2011).	Low risk; non-zero because of their bycatch risk in thresher shark and swordfish fisheries.

Species	Listing Status[1]	Likelihood of Presence[2]	Seasonality	Habitat Association	Vulnerability Index[3]
			et al. 2011, Carretta et al. 2023). Densities in the two WEAs are predicted to be highest in the summer/fall (Becker et al. 2020; Point Blue Conservation Science 2022a, b).		
Risso's dolphin (*Grampus griseus*)—COW stock	MMPA	Humboldt WEA: Present Morro Bay WEA: Present	Year-round presence in California, with seasonal movements along the U.S. West Coast. Their distribution shifts northward as water temperatures increase. More individuals spotted in California waters in winter than in summer (Allen et al. 2011).	They are typically seen in large groups along the continental shelf break in waters 400–1000 m deep (Barlow and Forney 2007, Baird 2008, Allen et al. 2011). Observed in high densities in the Southern California Bight (Becker et	Low risk.

Species	Listing Status[1]	Likelihood of Presence[2]	Seasonality	Habitat Association	Vulnerability Index[3]
				al. 2020, Carretta et al. 2023).	
Dall's porpoise (*Phocoenoides dalli*)—COW stock	MMPA	Humboldt WEA: Present Morro Bay WEA: Present	Year-round. Though the COW population appears to conduct seasonal north-south movements within their range based on oceanographic conditions (Carretta et al. 2023). For example, they are seen off Southern California in the winter. The highest densities in the Humboldt WEA occur in the summer/fall, and in higher densities compared to elsewhere in the CCS (Becker et al. 2020, Point Blue Conservation Science 2022b).	Dall's porpoises have been sighted over, along, and beyond the continental shelf (Carretta et al. 2023), as well as in nearshore environments. They occur in higher abundance near the shelf break.	Low risk; non-zero risk because there is limited evidence of entanglement in longline and gillnet fisheries.

Species	Listing Status[1]	Likelihood of Presence[2]	Seasonality	Habitat Association	Vulnerability Index[3]
			The highest densities in the Morro Bay WEA are also in the summer/fall, but these densities are lower than those found in the Humboldt WEA (Becker et al. 2020, Point Blue Conservation Science 2022a).		
Sperm whale (*Physeter macrocephalus*)—COW stock	MMPA; ESA–E	Humboldt WEA: Present Morro Bay WEA: Present	Year-round. They reach peak abundance from April and mid-June and again from the end of August through mid-November (Rice 1974, Carretta et al. 2023). Rice (1974) suggested that peaks in sightings in May and September correspond to seasonal movements north and south, respectively.	Most abundant offshore > 3,000 m deep compared to coastal regions Forney et al. (2012) and Becker et al. (2020).	Low risk; non-zero risk because of limited evidence of entanglement in longline and gillnet fisheries.

Species	Listing Status[1]	Likelihood of Presence[2]	Seasonality	Habitat Association	Vulnerability Index[3]
Short-beaked common dolphin (*Delphinus delphis*)—COW stock	MMPA	Humboldt WEA: Present Morro Bay WEA: Present	Their abundance is seasonally and inter-annually variable, and often increases during warm periods (Forney and Barlow 1998, Carretta et al. 2023).	The most abundant cetacean off California and are widely distributed from the coastline to at least 300 nautical miles offshore (Carretta et al. 2023). Its distribution is typically concentrated off the continental shelf (Carretta et al. 2023) and farther offshore of the Humboldt Bay WEA. Compared to more northern waters, they are observed along the continental slope and closer to shore in more central and southern areas of	Low risk.

Species	Listing Status[1]	Likelihood of Presence[2]	Seasonality	Habitat Association	Vulnerability Index[3]
				California (including the Morro Bay WEA).	
Long-beaked common dolphin (*Delphinus capensis*)—California stock	MMPA	Humboldt WEA: Rare Morro Bay WEA: Present	Year-round. There may be seasonal shifts in abundance, with densities higher in the summer/fall months (although still low compared to the Southern California Bight; Becker et al. 2020).	Distribution overlaps with the short-beaked common dolphin, but long-beaked common dolphins are found closer to shore, typically within 50 nautical miles of the coast along the continental shelf. Their predicted densities peak directly south of the Morro Bay WEA in the Southern California Bight (Becker et al. 2020).	Low risk.

Species	Listing Status[1]	Likelihood of Presence[2]	Seasonality	Habitat Association	Vulnerability Index[3]
Common bottlenose dolphin (*Tursiops truncatus*)—California Coastal Stock	MMPA	Humboldt WEA: Rare Morro Bay WEA: Rare	North-south movements, influenced by oceanographic conditions (Carretta et al. 2023).	Exclusively coastal, typically found close to shore throughout its range (Carretta et al. 2023).	Moderate risk due to observations of entangled bottlenose dolphins in other contexts and their potential attraction to industrial offshore operations.
Common bottlenose dolphin (*Tursiops*	MMPA	Humboldt WEA: Rare	Year-round, without an apparent seasonality in their distribution (Carretta et al. 2023).	Typically observed farther offshore of both WEAs, however, there are high predicted densities in the	Moderate risk due to observations of entangled

Species	Listing Status[1]	Likelihood of Presence[2]	Seasonality	Habitat Association	Vulnerability Index[3]
truncatus)—COW offshore stock		Morro Bay WEA: Rare		Southern California Bight (Becker et al. 2020, Carretta et al. 2023).	bottlenose dolphins in other contexts and their potential attraction to industrial offshore operations.
Striped dolphin (*Stenella coeruleoalba*)—COW stock	MMPA	Humboldt WEA: Rare Morro Bay WEA: Rare	Information on seasonality is lacking since surveys that cover their offshore habitats have only been conducted in the summer/fall (Carretta et al. 2023).	Striped dolphins are globally distributed in tropical and warm-temperate pelagic waters (Carretta et al. 2023). In California, they are typically observed offshore when temperatures are high,	N/A

Species	Listing Status[1]	Likelihood of Presence[2]	Seasonality	Habitat Association	Vulnerability Index[3]
				further west of the WEAs. Their abundance varies annually based on ocean conditions. Depth, SST, and mixed layer depth are important predictors for their occurrence (Becker et al. 2020).	
Cuvier's beaked whale (*Ziphius cavirostris*)—COW stock	MMPA	Humboldt WEA: Rare Morro Bay WEA: Rare	Along the U.S. West Coast, they are the most frequently encountered beak whale; however, there are no seasonal changes in distribution at this stage (Carretta et al. 2023) and compared to other cetaceans, are relatively data deficient.	Cuvier's beaked whales are distributed throughout deep waters of all oceans. Abundance estimates have been difficult to determine using aerial and ship-based surveys because of their cryptic behavior. Cuvier's beaked whales, among	Low risk.

Species	Listing Status[1]	Likelihood of Presence[2]	Seasonality	Habitat Association	Vulnerability Index[3]
				other beaked whales, have been identified in the Southern California Bight and the Channel Islands using hydroacoustics (e.g., Falcone and Schorr 2014).	
Baird's beaked whale (*Berardius bairdii*)—COW stock	MMPA	Humboldt WEA: Rare Morro Bay WEA: Rare	Found along the entire coast of California, primarily along the continental slope between late spring and early fall; however, they are farther offshore and occupy colder waters between November and April (Carretta et al. 2023).	Distributed throughout the temperate edge of the North Pacific (Carretta et al. 2023).	Low risk.
Killer whale (*Orcinus rectipinnus*)—	MMPA	Humboldt WEA: Present	Year-round. Travel long distances in small groups in pursuit of marine mammals,	This stock generally occupies the continental shelf and slope but may be	Relatively low risk.

Species	Listing Status[1]	Likelihood of Presence[2]	Seasonality	Habitat Association	Vulnerability Index[3]
North Pacific Transient population		Morro Bay WEA: Rare	their exclusive prey (Ford et al. 1998, Herman et al. 2005, Krahn et al. 2007).	found in offshore and nearshore environments as well. While possibly present in the Humboldt WEA, their occurrences may be sporadic given their low population numbers and immense home range.	
Killer whale (*Orcinus orca*)—Eastern North Pacific (ENP) Offshore population	MMPA	Humboldt WEA: Rare Morro Bay WEA: Rare	Most surveys within their range have observed them off southern and central California between September and March (Dahlheim et al. 2008), but their distribution is more so determined by prey.	Offshore, past the continental shelf. They frequent waters beyond the continental slope from southern California to the Aleutian Islands (Dahlheim et al. 2008) to feed on fish and marine mammals.	Relatively low risk.

Species	Listing Status[1]	Likelihood of Presence[2]	Seasonality	Habitat Association	Vulnerability Index[3]
Killer whale (*Orcinus ater*)—Southern Resident Distinct Population Segment (DPS)	MMPA; ESA–E	Humboldt WEA: Rare Morro Bay WEA: Rare	Seasonality is influenced by the timing of salmon returns to different river systems (Point Blue Conservation Science 2022a, b) and their distribution is primarily linked to presence and abundance of prey. Little is known about their fall, winter, and spring movements. It is possible they travel at infrequent intervals in winter or spring through habitats further inshore of the two WEAs.	<u>Critical Habitat</u>: First designated in Puget Sound, then revised in 2021 to include six additional coastal regions along the U.S. West Coast to Point Sur, California (NMFS 2021a). The critical habitat extends longitudinally from Monterey Bay north through Oregon, between the 6.1 m and 200 m depth contour, where the essential features include prey and passage; however, it does not overlap with the Humboldt WEA. No critical	Relatively low risk.

Species	Listing Status[1]	Likelihood of Presence[2]	Seasonality	Habitat Association	Vulnerability Index[3]
				habitat exists near Morro Bay WEA (the nearest Critical Habitat is at Point Sur, where essential features include water quality, sufficient prey, and passage conditions). <u>Habitat Associations</u>: Satellite tagging, opportunistic observations, and acoustic recordings suggest that this DPS spends nearly all its time on the continental shelf, within 34 kilometers (km) of the coastline and in water < 200 m deep (Carretta et al.	

Species	Listing Status[1]	Likelihood of Presence[2]	Seasonality	Habitat Association	Vulnerability Index[3]
				2023). In recent years, the K and L pods have been seen as far south as central California, presumably searching for Chinook salmon (Krahn et al. 2004), their primary prey.	
Harbor porpoise (*Phocoena phocoena*)—Northern COW, and Morro Bay Stock	MMPA	Humboldt WEA: Rare Morro Bay WEA: Rare	Year-round.	Biologically Important Area (BIA): There are small resident population BIAs, including the Morro Bay Small Resident population that extends from Point Conception to Point Sur,	Low risk; but non-zero because of limited evidence of documented entanglement.

Species	Listing Status[1]	Likelihood of Presence[2]	Seasonality	Habitat Association	Vulnerability Index[3]
				from the coastline to the 200-m isobath. The WEAs are outside of the BIA. <u>Habitat Associations</u>: Primarily present in waters < 200 m deep and from the coastline to 92 m isobath (Calambokidis et al. 2015).	
Pygmy and dwarf sperm whale (*Kogia breviceps and Kogia sima*)—COW Stock	MMPA	Humboldt WEA: Rare Morro Bay WEA: Rare	Data deficient due to their cryptic behavior. Available information is insufficient to identify seasonality (or distribution; Carretta et al. 2023).	Globally distributed throughout deep oceanic waters along continental slopes. Pelagic.	Low risk; but non-zero.
Short-finned pilot whale (*Globicephala*	MMPA	Humboldt WEA: Rare	Data deficient.	Limited distribution in shelf and oceanic areas, highly cryptic and pelagic.	Low risk.

Species	**Listing Status**[1]	**Likelihood of Presence**[2]	**Seasonality**	**Habitat Association**	**Vulnerability Index**[3]
macrorhynchus)—COW Stock		Morro Bay WEA: Rare		Abundance and distribution are influenced by oceanographic conditions (Carretta et al. 2023). They were once common off Southern California, but sightings and presence in and around either WEA is rare, especially after the 1983 El Niño.	
Mesoplodont Beaked Whales					
Six species known to occur in the North Pacific, including the Blainville's	MMPA	Humboldt WEA: Rare Morro Bay WEA: Rare	There are insufficient sighting records to determine spatial and/or	Mesoplodont beaked whales occupy deep waters and along the continental slope of the North Pacific Ocean. All	N/A

Species	Listing Status[1]	Likelihood of Presence[2]	Seasonality	Habitat Association	Vulnerability Index[3]
beaked whale (*Mesoplodon denisirostris*), Perrin's beaked whale (*M. perrini*), lesser beaked whale (*M. peruvianus*), Stejneger's beaked whale (*M. stejnegeri*), Gingko-toothed beaked whale (*M. gingkodens*), and Hubbs' beaked whale (*M. carlhubbsi*).			seasonal patterns of these whales, and they are not easily distinguishable at-sea (Carretta et al. 2023). Since they're not easily distinguishable, they are treated as a single group. They have low densities in the two WEAs (Becker et al. 2020).	beaked whales forage for squid and fish and are most frequently sighted in pelagic and continental margin habitats (Mead 2008, Pitman 2008). Due to their prolonged periods at depth, low surfacing profiles, and similar appearances among species, mesoplodont beaked whales are difficult to detect and conclusively identify during visual surveys.	

Species	Listing Status[1]	Likelihood of Presence[2]	Seasonality	Habitat Association	Vulnerability Index[3]
Cetaceans—Mysticetes					
Humpback whale (*Megaptera novaengliae*)—COW stock, comprised of Central American DPS and Mexico DPS	MMPA; Central American DPS (ESA–E); Mexico DPS (ESA–T)	Humboldt WEA: Present Morro Bay WEA: Present	Year-round in both WEAs, with seasonal peaks in the spring to fall. The COW stock migrates south during the winter to the coast of Mexico and Central America to breed, and migrates north to feeding grounds in the summer. Migration is less synchronized than that of the gray whale (Urban et al. 2000, Calambokidis 2009, Calambokidis and Barlow 2020). Distribution in the cooler months (January through April) extends farther offshore than in	Critical Habitat: Designated critical habitat for the Central American and Mexico DPS encompasses almost the entire U.S. West Coast. Both WEAs are within Critical Habitats, where the essential biological feature is prey (i.e., krill) (NMFS 2021b). BIA: Humpback feeding BIAs overlap with both WEAs (Calambokidis et al. 2024). Feeding humpback whales are expected to occur in both WEAs during	High risk because of many reported fishing gear interactions.

Species	Listing Status[1]	Likelihood of Presence[2]	Seasonality	Habitat Association	Vulnerability Index[3]
			the summer and fall periods (Becker et al. 2016, 2017; NMFS 2021b). Humpbacks have been observed and detected from passive acoustic recorders off the coast of northern California in the winter (Calambokidis et al. 2015, 2024) and are thus likely to be present year-round, although in lower numbers during the winter (Adams et al. 2014). Becker et al. (2020) estimates that the highest densities occur in both WEAs during the summer and fall, which is low	the summer and early fall months (June–November) with whales arriving as early as March in the core areas (Calambokidis et al. 2024). Habitat Associations: Prefer nearshore and continental shelf habitats. Stick closer to shore while migrating. Latitude:longitude ratio, year, depth, SST, and mixed layer depth are key predictors for the presence of humpbacks (Becker et al. 2020).	

Species	Listing Status[1]	Likelihood of Presence[2]	Seasonality	Habitat Association	Vulnerability Index[3]
			to moderate (in Morro Bay) and low (in Humboldt) compared to the maximum densities in the CCS.		
Blue whale (*Balaenoptera musculus*)—ENP stock	MMPA; ESA–E	Humboldt WEA: Present Morro Bay WEA: Present	Seasonal; Satellite tracking indicates that the ENP stock's range extends from the Gulf of Alaska through Baja California, Mexico, and Costa Rica (Bailey et al. 2009, Carretta et al. 2023). They travel northward in response to spring t increases in primary productivity (Burtenshaw et al. 2004). They are most likely to be observed off California between the summer and fall (Carretta et al.	<u>BIA</u>: Feeding BIAs are centered near the shelf and overlap with both WEAs (Calambokidis et al. 2024). Feeding blue whales are expected to occur in both WEAs during the summer and early fall months (June–November)(Calambokidis et al. 2024). <u>Habitat Associations</u>: Most commonly observed along the continental shelf break	Moderate risk because of documented cases of entanglement in NMFS SARs, although fewer documented cases than other taxa.

Species	Listing Status[1]	Likelihood of Presence[2]	Seasonality	Habitat Association	Vulnerability Index[3]
			2023): blue whales tend to occupy the area off northern California during the latter part of their feeding season in late summer and fall (Irvine et al. 2014). Habitat density estimates suggest that the highest densities of blue whales in both the WEAs occur in the summer and fall, but the densities in these areas are low relative to the entire CCS (Becker et al. 2020).	and shelf break, and other bathymetric features near productive coastal upwelling regions that support dense concentrations of pelagic euphausiids (i.e., krill) (Burtenshaw et al. 2004, Croll et al. 2005). They also occur inshore while in transit or feeding. Habitat preferences are strongly influenced by SST, seafloor topography, and subsurface water properties (Point Blue Conservation Science 2022a, b).	

Species	Listing Status[1]	Likelihood of Presence[2]	Seasonality	Habitat Association	Vulnerability Index[3]
Fin whale (*Balaenoptera physalus*)—COW stock	MMPA; ESA–E	Humboldt WEA: Present Morro Bay WEA: Present	Year-round with seasonal peaks in the summer and fall. There are resident, smaller year-round subpopulations and also populations that participate in long-range seasonal migrations along the coastline (Falcone et al. 2022). A recent study conducted by Scales et al. (2017) used a multi-scale modeling framework to identify biophysical influences on habitat suitability throughout the CCS. Using tracking information from 67 fin whales and environmental data from	BIA: A feeding BIA for fin whales overlaps the Morro Bay WEA where fin whales are expected to occur in June–November (Calambokidis et al. 2024). Habitat Associations: Occur in both nearshore and pelagic waters where they feed primarily on krill and fish. Highest densities of fin whales occur in waters between 14°C and 18°C (Becker et al. 2020).	Moderate risk because of documented cases of entanglement in the SARs, although fewer documented cases than other taxa.

Species	Listing Status[1]	Likelihood of Presence[2]	Seasonality	Habitat Association	Vulnerability Index[3]
			the study region, generalized additive models were used to evaluate habitat suitability across seasons. Especially in the Morro Bay WEA, habitat suitability increases (and populations generally peak) between June and November (Scales et al. 2017) suggesting that populations generally peak in the summer. Becker et al. (2020) estimates that the highest densities of fin whales in both WEAs would occur in the summer and fall. Densities in the Humboldt WEA are low compared to offshore		

Species	Listing Status[1]	Likelihood of Presence[2]	Seasonality	Habitat Association	Vulnerability Index[3]
			areas, and regions between the Channel Islands and Morro Bay. Predictions suggest they are concentrated south of Monterey Bay to northern Channel Islands, ranging from coastal to offshore habitats.		
Minke whale (Balaenoptera acutorostrata)—COW stock	MMPA	Humboldt WEA: Rare Morro Bay WEA: Present	Year-round. Their presence in the Humboldt WEA is considered rare, although they are also data deficient.	Minke whales are generally observed over the continental shelf and nearshore. Minke whales in central California appear to have small home ranges. The most critical predictor variables in determining habitat density of minke whales include distance to	Moderate risk because given some limited instances reported within the SAR.

Species	Listing Status[1]	Likelihood of Presence[2]	Seasonality	Habitat Association	Vulnerability Index[3]
				the continental shelf, SST, and longitude:latitude ratio (Becker et al. 2020).	
Gray whale (*Eschrichtius robustus*)—ENP Stock and Pacific Coast Feeding Group	MMPA	Humboldt WEA: Rare Morro Bay WEA: Rare	Seasonal. Gray whales undergo one of the longest annual migrations of any mammal, transiting through the CCS on their biannual migrations to and from their feeding and wintering grounds. Migrations occur closer to shore than the WEAs. The southbound migration to Mexico from October through March, peaking in December through March, consists of all age classes (Calambokidis et al.	<u>BIA:</u> There are multiple migratory BIAs and one reproductive BIA along the West Coast of the United States (Calambokidis et al. 2015, 2024). None of the BIAs overlap with either WEA (Calambokidis et al. 2024). <u>Habitat Associations</u>: Nearshore, continental shelf.	Moderate risk.

Species	Listing Status[1]	Likelihood of Presence[2]	Seasonality	Habitat Association	Vulnerability Index[3]
			2015, 2024). Following the calving season, the whales begin their northbound migration, which is more prolonged and consists of two phases (Jones and Swartz 2008). The first northbound phase (northbound phase A) consists of adults and juveniles and occurs in late January through July, peaking in April to July. The second northbound phase (northbound phase B) occurs between March and July and consists of mother/calf pairs (Calambokidis et al. 2015).		

Species	Listing Status[1]	Likelihood of Presence[2]	Seasonality	Habitat Association	Vulnerability Index[3]
Sei whale (Balaenoptera borealis)—ENP Stock	MMPA; ESA–E	Humboldt WEA: Rare Morro Bay WEA: Rare	N/A	Occurs in temperate waters in all major oceans, usually far out to sea (Carretta et al. 2023). Highly pelagic.	No reported incidents of entanglements in recent SARs.
North Pacific right whale (*Eubalaena japonica*)—ENP Stock	MMPA; ESA–E	Humboldt WEA: Rare Morro Bay WEA: Rare	Species is data-deficient and their migration patterns are unknown. North Pacific right whales are believed to spend the summer in their northern feeding grounds in the Bering Sea and then migrate south to warmer waters during the winter (NMFS 2008).	<u>Critical Habitat</u>: Exists only in waters in the Gulf of Alaska and the Southeast Bering Sea (NMFS 2008). <u>Habitat Associations</u>: At present, the greatest concentrations exist in the Bering Sea and south of Kodiak Islands, but there have been sightings as far south as central Baja California, Mexico. They are	High risk, largely because of their conservation concerns. Also, entanglement is well documented in North Atlantic right whales.

Species	Listing Status[1]	Likelihood of Presence[2]	Seasonality	Habitat Association	Vulnerability Index[3]
				highly pelagic in nature and occur in very low numbers off California and Mexico.	
Pinnipeds (Phocids and Otariids)					
Northern elephant seal (*Mirounga angustirostris*)—California breeding stock	MMPA; CA–FP	Humboldt WEA: Present Morro Bay WEA: Present	Northern elephant seals migrate four times annually, traveling to and from breeding/pupping and molting areas (NMFS 2022). Peak abundance in California occurs during the breeding season, between January and February, then again in April to July to molt (Lowry et al. 2014, 2017; NMFS 2022).	Offshore, slope, shelf, coastal, beach. Northern elephant seals breed in large colonies, many of which have historically been on islands between mid-Baja California and the Farallon Islands (Antonelis and Fiscus 1980). More recently, the growing population has extended breeding colonies to	Moderate risk based on SARs noting interactions with fishing gear and vessels.

Species	Listing Status[1]	Likelihood of Presence[2]	Seasonality	Habitat Association	Vulnerability Index[3]
				mainland beaches near island colonies and new colonies have formed on mainland beaches in central California north to Humboldt County (Lowry et al. 1996, Forman et al. 2018). They primarily give birth on offshore islands in California and Baja California, Mexico.	
Harbor seal (*Phoca vitulina richardii*)—ENP subspecies, California stock	MMPA	Humboldt WEA: N/A Morro Bay WEA: N/A	Year-round. Present along the coastline, and not in the WEAs. Abundance peaks in the summer during pupping and molting, then declines in the winter when individuals	Coastal and nearshore. Harbor seals can be expected along the Humboldt County coast and coast near the Morro Bay WEA; however, their range	Moderate risk based on reports of interactions with vessels in SARs and

Species	Listing Status[1]	Likelihood of Presence[2]	Seasonality	Habitat Association	Vulnerability Index[3]
			disperse (Sullivan 1980, Herder 1986, Goley and Harvey 2010).	is restricted to coastal waters, river mouths, and bays and they are not expected in offshore areas (Burns 2008, Lowry 2008).	documented cases of entanglement in fishing gear and entrainment in power plants.
Guadalupe fur seal (*Arctocephalus townsendi*)—N/A	MMPA; ESA–E; CESA–T; CA–FP	Humboldt WEA: Rare Morro Bay WEA: Rare	Forage seasonally, otherwise non-migratory and typically occur in subtropical waters of southern California and Mexico. Satellite tagged individuals have been observed traveling as far north as Vancouver Island (Norris et al. 2015 as cited *in* Carretta et al. 2023) so	Oceanic, continental slope.	Moderate risk.

Species	Listing Status[1]	Likelihood of Presence[2]	Seasonality	Habitat Association	Vulnerability Index[3]
			presence is possible, although would be rare.		
Northern fur seal (*Callorhinus ursinus*)—California stock	MMPA; CA–FP	Humboldt WEA: Present Morro Bay WEA: Present	Seasonal, when not at their summer breeding grounds.	Oceanic, continental slope. Considered pelagic, foraging in waters off the continental shelf (when not at their summer breeding grounds; there are two in California, one on San Miguel Island in southern California and one on the Farallon Islands [Carretta et al. 2023]).	Moderate risk.
Northern (Steller) sea lion (*Eumetopias	MMPA	Humboldt WEA: Rare	Year-round.	<u>Critical Habitat</u>: includes all major rookeries and associated air and aquatic zones in California. Given	Moderate risk.

Species	Listing Status[1]	Likelihood of Presence[2]	Seasonality	Habitat Association	Vulnerability Index[3]
jubatus)—Eastern DPS		Morro Bay WEA: Rare		that they have been delisted, this critical habitat is currently being reviewed. Habitat Associations: Coastal, continental shelf and slope. Typically forage over the continental shelf at night, within 12 miles of their colonies. Their preferred habitat is in nearshore coastal waters and open oceans, as well as rocks and beach haul-outs. Año Nuevo Island is the southernmost rookery, > 200 miles from the Morro	

Species	Listing Status[1]	Likelihood of Presence[2]	Seasonality	Habitat Association	Vulnerability Index[3]
				Bay WEA. They breed along the Humboldt County coast.	
California sea lion (*Zalophus californianus*)—U.S. Stock	MMPA	Humboldt WEA: Present Morro Bay WEA: Present	Year-round. There may be two seasonal peaks of CSLs observed along the California coast, one during the fall northward migration and one during spring (mid-April) as they return to breeding colonies in the south (Sullivan 1980, Lowry and Forney 2005). During the nonbreeding season (i.e., beginning in late summer), adults and subadults migrate northward along the California coastline to Washington (Lowry and Forney 2005). Females and	Coastal, continental shelf and slope. During the summer months, CSLs congregate near rookery islands and open-water areas (Lowry and Forney 2005, Lowry et al. 2017, Carretta et al. 2023). Breeding colonies only occur on islands off southern California, along the western side of Baja California, and in the Gulf of California (Heath and Perrin 2008). Some of the primary	Moderate risk based on SARs and observations of entanglement from stranding facilities.

Species	Listing Status[1]	Likelihood of Presence[2]	Seasonality	Habitat Association	Vulnerability Index[3]
			juveniles disperse as well, but generally stay in the southern California region.	rookeries are in the Channel Islands. When not at rookeries, CSLs are found in the open ocean and coastal waters, over the continental shelf and slope. Dispersal from breeding colonies is sex-biased with males leaving in late summer and fall and migrating as far north as British Columbia, Canada, and Alaska (Maniscalco et al. 2004, Heath and Perrin 2008). Female sea lions from San Nicolas Island breeding colonies, fitted	

Species	Listing Status[1]	Likelihood of Presence[2]	Seasonality	Habitat Association	Vulnerability Index[3]
				with satellite positioning tags, tended to remain around the Channel Islands, though some traveled as far north as Monterey Bay (Costa et al. 2007). Males from the same colonies regularly traveled along the coast to Oregon.	
Sea Turtles					
Leatherback sea turtle (*Dermochelys coriacea*)—Western Pacific DPS	ESA–E	Humboldt WEA: Rare Morro Bay WEA: Present (estimated due to	Seasonal. Can be regularly seen pursuing jellyfish along the coasts of California and Oregon in summer and early fall (July through October; Starbird et al. 1993; Benson et al. 2007, 2011). Telemetry studies have	Critical Habitat: Designated in 2012 (NMFS 2012), including 43,798 km^2 of water from Point Arena to Point Arguello, from the coastline to the 3,000 m isobath, overlapping with	High risk due to their vulnerability to entanglement in fishing gear.

Species	Listing Status[1]	Likelihood of Presence[2]	Seasonality	Habitat Association	Vulnerability Index[3]
		overlap with designated critical habitat)	found that they arrived in the CCS between April and July and departed in October and November when water temperatures decreased (Benson et al. 2011).	the Morro Bay WEA but not the Humboldt WEA. The essential habitat feature for leatherback turtles are their prey, which include a range of gelatinous organisms (NMFS 2012), primarily jellyfish, tunicates, and ctenophores (NMFS and USFWS 2020a). These prey are found in ocean frontal habitats and regions strongly influenced by upwelling. Habitat Associations: Leatherbacks use relatively cool waters between 14°C	

Species	Listing Status[1]	Likelihood of Presence[2]	Seasonality	Habitat Association	Vulnerability Index[3]
				and 16°C, over the continental shelf (i.e., < 200 m depth), and regions with high chlorophyll-a and eddy kinetic energy (Benson et al. 2011).	
Olive ridley sea turtle (*Lepidochelys olivacea*)—N/A	T	Humboldt WEA: Rare Morro Bay WEA: Rare	Presence in the Morro Bay WEA is possible in the summer/fall or during warming events, albeit rare given their preference for warmer waters.	They generally are found in the open ocean but can occur in coastal areas. Unlike the leatherback turtle, the olive ridley sea turtle requires warmer waters, although they have been reported as far north as Alaska (NMFS and USFWS 2014).	High risk due to their vulnerability to entanglement in fishing gear

Species	Listing Status[1]	Likelihood of Presence[2]	Seasonality	Habitat Association	Vulnerability Index[3]
Green sea turtle (*Chelonia mydas*)—Eastern Pacific DPS	T	Humboldt WEA: Rare Morro Bay WEA: Rare	Migratory as adults.	Normally found nearshore in warm tropical and subtropical coastal waters. Adults are rarely seen along the U.S. West Coast (including northern California), and there are no known nesting locations along the U.S. West Coast (Seminoff et al. 2015). They tend to occur in coastal waters south of San Diego, California, but may occasionally move northward during warming events.	High risk due to their vulnerability to entanglement in fishing gear.

Species	Listing Status[1]	Likelihood of Presence[2]	Seasonality	Habitat Association	Vulnerability Index[3]
Loggerhead sea turtle (*Caretta caretta*)—North Pacific DPS	E	Humboldt WEA: Rare Morro Bay WEA: Rare	Presence in the Morro Bay WEA is possible in the summer/fall or during warming events, albeit rare given their preference for warmer waters.	Loggerhead sea turtles in the eastern North Pacific occur primarily in waters south of San Diego, California, as some of the most productive neritic foraging hotspots are off Baja California, Mexico (USFWS 2011, NMFS and USFWS 2020b). Unlike the leatherback sea turtle, loggerheads require warmer waters than typical conditions in either WEA.	High risk due to their vulnerability to entanglement in fishing gear.

[1] Listing Status: Marine Mammal Protection Act (MMPA); Threatened (ESA–T) and Endangered (ESA–E) under the federal Endangered Species Act (ESA); Threatened under the CESA (CESA–T). California Fully Protected (CA–FP). [2] Likelihood of Presence: Present or Rare in each respective Wind Energy Area (WEA). Presence based on the most recent stock assessment reports (SAR), subject matter expert knowledge, and whether ESA critical habitat overlaps the WEA. Rare indicates that the species may potentially occur, but unlikely

given the current state of knowledge. [3] Vulnerability Index: Sources: Saez et al. (2021), Southall et al. (2023); National Marine Fisheries Service (NMFS) entanglement summary documents, NMFS (unpublished), NMFS 2023 (unpublished). Other Abbreviations: California, Oregon, Washington (COW); California Current System (CCS); Sea Surface Temperature (SST); Distinct Population Segment (DPS); Eastern North Pacific (ENP); Biologically Important Area (BIA); California sea lions (CSLs); U.S. Fish and Wildlife Service (USFWS).

Appendix B. Cetacean Specimen-level Force Dataset and Inputs

Table B1: Cetacean Specimen-level Force Dataset and Inputs

Common Name (Scientific Name)	Museum	Animal ID	TL (m)	Epaxial Muscle Cross-Sectional Area (CSA) (cm^2)	Minimum Muscle Stress Value (kPa)	Maximum Muscle Stress Value (kPa)	Min Force (N); CSA*1.5	Min Force (kN) at Size Measured	Max Force (N); CSA*6.1	Max Force (kN) at Size Measured	Juvenile Length (m)	Adult Max Length (m)
Atlantic spotted dolphin (*Stenella frontalis*)	UNCW	1497	2.11	206.5	1.5	6.1	309.8	0.3098	1260	1.260	1.2	2.305
Atlantic spotted dolphin (*Stenella frontalis*)	UNCW	LEB 003	2.12	194.7	1.5	6.1	292.1	0.2921	1188	1.188	1.2	2.305

Common Name (Scientific Name)	Museum	Animal ID	TL (m)	Epaxial Muscle Cross-Sectional Area (CSA) (cm^2)	Minimum Muscle Stress Value (kPa)	Maximum Muscle Stress Value (kPa)	Min Force (N); CSA*1.5	Min Force (kN) at Size Measured	Max Force (N); CSA*6.1	Max Force (kN) at Size Measured	Juvenile Length (m)	Adult Max Length (m)
Atlantic spotted dolphin (*Stenella frontalis*)	UNCW	3011	2.14	199.1	1.5	6.1	298.7	0.2987	1215	1.215	1.2	2.305
Atlantic spotted dolphin (*Stenella frontalis*)	USNM	550800	2.15	227.6	1.5	6.1	341.4	0.3414	1388	1.388	1.2	2.305
Atlantic spotted dolphin	NCSM	CAHA 117	2.18	207.47	1.5	6.1	311.2	0.3112	1266	1.266	1.2	2.305

Common Name (Scientific Name)	**Museum**	**Animal ID**	**TL (m)**	**Epaxial Muscle Cross-Sectional Area (CSA) (cm^2)**	**Minimum Muscle Stress Value (kPa)**	**Maximum Muscle Stress Value (kPa)**	**Min Force (N); CSA*1.5**	**Min Force (kN) at Size Measured**	**Max Force (N); CSA*6.1**	**Max Force (kN) at Size Measured**	**Juvenile Length (m)**	**Adult Max Length (m)**
(*Stenella frontalis*)												
Atlantic spotted dolphin (*Stenella frontalis*)	UNCW	WAM 655	2.2	222.7	1.5	6.1	334.1	0.3341	1358	1.358	1.2	2.305
Atlantic spotted dolphin (*Stenella frontalis*)	USNM	504762	2.21	217.2	1.5	6.1	325.9	0.3259	1325	1.325	1.2	2.305
Atlantic spotted	USNM	550431	2.23	245.3	1.5	6.1	367.9	0.3679	1496	1.496	1.2	2.305

Common Name (Scientific Name)	Museum	Animal ID	TL (m)	Epaxial Muscle Cross-Sectional Area (CSA) (cm^2)	Minimum Muscle Stress Value (kPa)	Maximum Muscle Stress Value (kPa)	Min Force (N); CSA*1.5	Min Force (kN) at Size Measured	Max Force (N); CSA*6.1	Max Force (kN) at Size Measured	Juvenile Length (m)	Adult Max Length (m)
dolphin (*Stenella frontalis*)												
Atlantic spotted dolphin (*Stenella frontalis*)	NCSM	CAHA 120	2.25	238.64	1.5	6.1	358.0	0.3580	1456	1.456	1.2	2.305
Atlantic spotted dolphin (*Stenella frontalis*)	UNCW	WAM 653	2.305	224.8	1.5	6.1	337.2	0.3372	1371	1.371	1.2	2.305

Common Name (Scientific Name)	Museum	Animal ID	TL (m)	Epaxial Muscle Cross-Sectional Area (CSA) (cm^2)	Minimum Muscle Stress Value (kPa)	Maximum Muscle Stress Value (kPa)	Min Force (N); CSA*1.5	Min Force (kN) at Size Measured	Max Force (N); CSA*6.1	Max Force (kN) at Size Measured	Juvenile Length (m)	Adult Max Length (m)
Baird's beaked whale (*Berardius bairdii*)	HSU	Cat. No. 2679	9.56	1350.25	1.5	6.1	2025.4	2.0254	8237	8.237	4.5	11
Blainville's beaked whale (*Mesoplodon densirostris*)	USNM	550754	4.2	760.3	1.5	6.1	1140.4	1.1404	4638	4.638	1.9	6.1
Blainville's beaked	USNM	WAM 593	4.23	798.3	1.5	6.1	1197.4	1.1974	4870	4.870	1.9	6.1

Common Name (Scientific Name)	Museum	Animal ID	TL (m)	Epaxial Muscle Cross-Sectional Area (CSA) (cm^2)	Minimum Muscle Stress Value (kPa)	Maximum Muscle Stress Value (kPa)	Min Force (N); CSA*1.5	Min Force (kN) at Size Measured	Max Force (N); CSA*6.1	Max Force (kN) at Size Measured	Juvenile Length (m)	Adult Max Length (m)
whale (*Mesoplodon densirostris*)												
Blue whale (Balaenoptera musculus)	NBWM	Kobo	20	6957	1.5	6.1	10435.5	10.4355	42438	42.438	7.0	33.5
Blue whale (Balaenoptera musculus)	NCSM	8381	22.4	9814.34	1.5	6.1	14721.5	14.7215	59867	59.867	7.0	33.5

Common Name (Scientific Name)	Museum	Animal ID	TL (m)	Epaxial Muscle Cross-Sectional Area (CSA) (cm^2)	Minimum Muscle Stress Value (kPa)	Maximum Muscle Stress Value (kPa)	Min Force (N); CSA*1.5	Min Force (kN) at Size Measured	Max Force (N); CSA*6.1	Max Force (kN) at Size Measured	Juvenile Length (m)	Adult Max Length (m)
Blue whale (Balaenoptera musculus)	USNM	124326	22.76	9197.2	1.5	6.1	13795.8	13.7958	56103	56.103	7.0	33.5
Blue whale (Balaenoptera musculus)	NOYO	NOYO2	22.25	5921.9	1.5	6.1	8882.9	8.8829	36124	36.124	7.0	33.5
Bryde's whale (Balaenoptera edeni)	USNM	WAM 587	11.05	2626.4	1.5	6.1	3939.7	3.9397	16021	16.021	3.5	14
Clymene dolphin	USNM	504408	1.86	179.6	1.5	6.1	269.4	0.2694	1096	1.096	0.76	2.0

Common Name (Scientific Name)	Museum	Animal ID	TL (m)	Epaxial Muscle Cross-Sectional Area (CSA) (cm^2)	Minimum Muscle Stress Value (kPa)	Maximum Muscle Stress Value (kPa)	Min Force (N); CSA*1.5	Min Force (kN) at Size Measured	Max Force (N); CSA*6.1	Max Force (kN) at Size Measured	Juvenile Length (m)	Adult Max Length (m)
(*Stenella clymene*)												
Common bottlenose dolphin (*Tursiops truncatus*)	Photo	UNCW x-section	1.709	127.1	1.5	6.1	190.7	0.1907	775	0.775	1.0	4.0
Common bottlenose dolphin (*Tursiops truncatus*)	UNCW	WAM 651	2.28	222.7	1.5	6.1	334.1	0.3341	1358	1.358	1.0	4.0
Common bottlenose	NCSM	WAM 573	2.415	238.67	1.5	6.1	358.0	0.3580	1456	1.456	1.0	4.0

Common Name (Scientific Name)	Museum	Animal ID	TL (m)	Epaxial Muscle Cross-Sectional Area (CSA) (cm^2)	Minimum Muscle Stress Value (kPa)	Maximum Muscle Stress Value (kPa)	Min Force (N); CSA*1.5	Min Force (kN) at Size Measured	Max Force (N); CSA*6.1	Max Force (kN) at Size Measured	Juvenile Length (m)	Adult Max Length (m)
dolphin (*Tursiops truncatus*)												
Common bottlenose dolphin (*Tursiops truncatus*)	NECRO	WAM 672	2.46	265.1	1.5	6.1	397.6	0.3976	1617	1.617	1.0	4.0
Common bottlenose dolphin (*Tursiops truncatus*)	UNCW	MDB 091	2.53	273.8	1.5	6.1	410.7	0.4107	1670	1.670	1.0	4.0

Common Name (Scientific Name)	Museum	Animal ID	TL (m)	Epaxial Muscle Cross-Sectional Area (CSA) (cm^2)	Minimum Muscle Stress Value (kPa)	Maximum Muscle Stress Value (kPa)	Min Force (N); CSA*1.5	Min Force (kN) at Size Measured	Max Force (N); CSA*6.1	Max Force (kN) at Size Measured	Juvenile Length (m)	Adult Max Length (m)
Common bottlenose dolphin (*Tursiops truncatus*)	NCSM	WAM 533	2.61	252.82	1.5	6.1	379.2	0.3792	1542	1.542	1.0	4.0
Common bottlenose dolphin (*Tursiops truncatus*)	NCSM	ASF 038	2.63	246.03	1.5	6.1	369.0	0.3690	1501	1.501	1.0	4.0
Common bottlenose dolphin	NCSM	WAM 535	2.64	301.4	1.5	6.1	452.1	0.4521	1839	1.839	1.0	4.0

Common Name (Scientific Name)	**Museum**	**Animal ID**	**TL (m)**	**Epaxial Muscle Cross-Sectional Area (CSA) (cm^2)**	**Minimum Muscle Stress Value (kPa)**	**Maximum Muscle Stress Value (kPa)**	**Min Force (N); CSA*1.5**	**Min Force (kN) at Size Measured**	**Max Force (N); CSA*6.1**	**Max Force (kN) at Size Measured**	**Juvenile Length (m)**	**Adult Max Length (m)**
(*Tursiops truncatus*)												
Common bottlenose dolphin (*Tursiops truncatus*)	UNCW	RJM 013b	2.64	315.5	1.5	6.1	473.3	0.4733	1925	1.925	1.0	4.0
Common bottlenose dolphin (*Tursiops truncatus*)	NCSM	WAM 530	2.68	299.47	1.5	6.1	449.2	0.4492	1827	1.827	1.0	4.0
Common bottlenose	NCSM	DAP 027	2.83	306.6	1.5	6.1	459.9	0.4599	1870	1.870	1.0	4.0

Common Name (Scientific Name)	Museum	Animal ID	TL (m)	Epaxial Muscle Cross-Sectional Area (CSA) (cm^2)	Minimum Muscle Stress Value (kPa)	Maximum Muscle Stress Value (kPa)	Min Force (N); CSA*1.5	Min Force (kN) at Size Measured	Max Force (N); CSA*6.1	Max Force (kN) at Size Measured	Juvenile Length (m)	Adult Max Length (m)
dolphin (*Tursiops truncatus*)												
Common bottlenose dolphin (*Tursiops truncatus*)	UNCW	WAM 656	2.91	297.3	1.5	6.1	446.0	0.4460	1814	1.814	1.0	4.0
Common bottlenose dolphin (*Tursiops truncatus*)	USNM	571687	3.01	462.6	1.5	6.1	693.9	0.6939	2822	2.822	1.0	4.0

Common Name (Scientific Name)	Museum	Animal ID	TL (m)	Epaxial Muscle Cross-Sectional Area (CSA) (cm^2)	Minimum Muscle Stress Value (kPa)	Maximum Muscle Stress Value (kPa)	Min Force (N); CSA*1.5	Min Force (kN) at Size Measured	Max Force (N); CSA*6.1	Max Force (kN) at Size Measured	Juvenile Length (m)	Adult Max Length (m)
Common bottlenose dolphin (*Tursiops truncatus*)	USNM	396165	3.03	341.0	1.5	6.1	511.5	0.5115	2080	2.080	1.0	4.0
Common bottlenose dolphin (*Tursiops truncatus*)	HSU	MMPL0413	2.37	229.48	1.5	6.1	344.2	0.3442	1400	1.400	1.0	4.0
Cuvier's beaked whale	NCSM	ASF 043	4.45	965.27	1.5	6.1	1447.9	1.4479	5888	5.888	2.0	7.0

Common Name (Scientific Name)	Museum	Animal ID	TL (m)	Epaxial Muscle Cross-Sectional Area (CSA) (cm^2)	Minimum Muscle Stress Value (kPa)	Maximum Muscle Stress Value (kPa)	Min Force (N); CSA*1.5	Min Force (kN) at Size Measured	Max Force (N); CSA*6.1	Max Force (kN) at Size Measured	Juvenile Length (m)	Adult Max Length (m)
(*Ziphius cavirostris*)												
Cuvier's beaked whale (*Ziphius cavirostris*)	HSU	HSU20180504-PT5	4.5	546.24	1.5	6.1	819.4	0.8194	3332	3.332	2.0	7.0
Dall's porpoise (*Phocoenoides dalli*)	HSU	Cat. No. 2696	1.78	206.76	1.5	6.1	310.1	0.3101	1261	1.261	1.0	2.4
Dall's porpoise	HSU	Cat No. 7031	1.61	182.75	1.5	6.1	274.1	0.2741	1115	1.115	1.0	2.4

Common Name (Scientific Name)	Museum	Animal ID	TL (m)	Epaxial Muscle Cross-Sectional Area (CSA) (cm^2)	Minimum Muscle Stress Value (kPa)	Maximum Muscle Stress Value (kPa)	Min Force (N); CSA*1.5	Min Force (kN) at Size Measured	Max Force (N); CSA*6.1	Max Force (kN) at Size Measured	Juvenile Length (m)	Adult Max Length (m)
(*Phocoenoices dalli*)												
Dwarf sperm whale (*Kogia sima*)	USNM	WAM 609	1.975	222.1	1.5	6.1	333.1	0.3331	1355	1.355	1.0	3.0
Dwarf sperm whale (*Kogia sima*)	USNM	550482	2.13	220.4	1.5	6.1	330.5	0.3305	1344	1.344	1.0	3.0
Dwarf sperm	USNM	550487	2.24	261.0	1.5	6.1	391.5	0.3915	1592	1.592	1.0	3.0

Common Name (Scientific Name)	Museum	Animal ID	TL (m)	Epaxial Muscle Cross-Sectional Area (CSA) (cm^2)	Minimum Muscle Stress Value (kPa)	Maximum Muscle Stress Value (kPa)	Min Force (N); CSA*1.5	Min Force (kN) at Size Measured	Max Force (N); CSA*6.1	Max Force (kN) at Size Measured	Juvenile Length (m)	Adult Max Length (m)
whale (*Kogia sima*)												
Gray whale (Eschrichtius robustus)	Becky	Homer	11.3	3184.8	1.5	6.1	4777.1	4.7771	19427	19.427	4.0	17
Gray whale (Eschrichtius robustus)	Becky	SBMNH 4932	11.5	3380.2	1.5	6.1	5070.3	5.0703	20619	20.619	4.0	17
Gray whale (Eschrichtius robustus)	HSU	Cat. No. 8398	8.55	996.67	1.5	6.1	1495.0	1.4950	6080	6.080	4.0	17

Common Name (Scientific Name)	Museum	Animal ID	TL (m)	Epaxial Muscle Cross-Sectional Area (CSA) (cm^2)	Minimum Muscle Stress Value (kPa)	Maximum Muscle Stress Value (kPa)	Min Force (N); CSA*1.5	Min Force (kN) at Size Measured	Max Force (N); CSA*6.1	Max Force (kN) at Size Measured	Juvenile Length (m)	Adult Max Length (m)
Harbor porpoise (*Phocoena phocoena*)	HSU	HSU20150412-TB23	1.6	99.65	1.5	6.1	149.5	0.1495	608	0.608	0.68	1.6
Hubb's beaked whale (*Mesoplodon carlhubbsi*)	HSU	Cat. No. 1999	5.1	964.86	1.5	6.1	1447.3	1.4473	5886	5.886	2.5	5.3
Hubb's beaked whale (*Mesoplodo*	HSU	Cat. No. 2680	4.955	1094.75	1.5	6.1	1642.1	1.6421	6678	6.678	2.5	5.3

Common Name (Scientific Name)	Museum	Animal ID	TL (m)	Epaxial Muscle Cross-Sectional Area (CSA) (cm^2)	Minimum Muscle Stress Value (kPa)	Maximum Muscle Stress Value (kPa)	Min Force (N); CSA*1.5	Min Force (kN) at Size Measured	Max Force (N); CSA*6.1	Max Force (kN) at Size Measured	Juvenile Length (m)	Adult Max Length (m)
n carlhubbsi)												
Hubb's beaked whale (*Mesoplodon carlhubbsi*)	HSU	1476	5.45	1046.54	1.5	6.1	1569.8	1.5698	6384	6.384	2.5	5.3
Humpback whale (Megaptera novaeangliae)	UNCW	MDB 068	8.53	1684.1	1.5	6.1	2526.2	2.5262	10273	10.273	4.5	18.6

Common Name (Scientific Name)	Museum	Animal ID	TL (m)	Epaxial Muscle Cross-Sectional Area (CSA) (cm^2)	Minimum Muscle Stress Value (kPa)	Maximum Muscle Stress Value (kPa)	Min Force (N); CSA*1.5	Min Force (kN) at Size Measured	Max Force (N); CSA*6.1	Max Force (kN) at Size Measured	Juvenile Length (m)	Adult Max Length (m)
Humpback whale (Megaptera novaeangliae)	NCSM	8201	8.98	1820.55	1.5	6.1	2730.8	2.7308	11105	11.105	4.5	18.6
Humpback whale (Megaptera novaeangliae)	NECRO	VAQS20131013	9.42	1899.7	1.5	6.1	2849.6	2.8496	11588	11.588	4.5	18.6
Humpback whale (Megaptera	NECRO	CAHA 173	9.76	2579.4	1.5	6.1	3869.1	3.8691	15734	15.734	4.5	18.6

Common Name (Scientific Name)	Museum	Animal ID	TL (m)	Epaxial Muscle Cross-Sectional Area (CSA) (cm^2)	Minimum Muscle Stress Value (kPa)	Maximum Muscle Stress Value (kPa)	Min Force (N); CSA*1.5	Min Force (kN) at Size Measured	Max Force (N); CSA*6.1	Max Force (kN) at Size Measured	Juvenile Length (m)	Adult Max Length (m)
novaeangliae)												
Humpback whale (Megaptera novaeangliae)	NECRO	VAQS20131335	10.55	2433.2	1.5	6.1	3649.8	3.6498	14843	14.843	4.5	18.6
Humpback whale (Megaptera novaeangliae)	NBWM	Quisimodo	11.2	2144	1.5	6.1	3216.0	3.2160	13078	13.078	4.5	18.6

Common Name (Scientific Name)	Museum	Animal ID	TL (m)	Epaxial Muscle Cross-Sectional Area (CSA) (cm^2)	Minimum Muscle Stress Value (kPa)	Maximum Muscle Stress Value (kPa)	Min Force (N); CSA*1.5	Min Force (kN) at Size Measured	Max Force (N); CSA*6.1	Max Force (kN) at Size Measured	Juvenile Length (m)	Adult Max Length (m)
Humpback whale (Megaptera novaeangliae)	Becky	Pitfall (01-975 Mn)	11.37	2447.4	1.5	6.1	3671.1	3.6711	14929	14.929	4.5	18.6
Killer whale (*Orcinus orca*)	MVZ	129686	6.858	1182.02	1.5	6.1	1773.0	1.7730	7210	7.210	2.5	9.8
Killer whale (*Orcinus orca*)	HSU	Cat. No. 8404	6.5	1175.15	1.5	6.1	1762.7	1.7627	7168	7.168	2.5	9.8
Killer whale (*Orcinus orca*)	NOYO	NOYO1	7.93	1715.31	1.5	6.1	2573.0	2.5730	10463	10.463	2.5	9.8

Common Name (Scientific Name)	Museum	Animal ID	TL (m)	Epaxial Muscle Cross-Sectional Area (CSA) (cm^2)	Minimum Muscle Stress Value (kPa)	Maximum Muscle Stress Value (kPa)	Min Force (N); CSA*1.5	Min Force (kN) at Size Measured	Max Force (N); CSA*6.1	Max Force (kN) at Size Measured	Juvenile Length (m)	Adult Max Length (m)
Melon-headed whale (*Peponocephala electra*)	UNCW	WAM 663	2.25	170.6	1.5	6.1	255.9	0.2559	1041	1.041	1	2.8
Minke whale (Balaenoptera acutorostrata)	UNCW	WAM 662	5.505	1051.5	1.5	6.1	1577.3	1.5773	6414	6.414	2.5	11
Minke whale	Becky	SBMNH 2213	8.2	2319.5	1.5	6.1	3479.3	3.4793	14149	14.149	2.5	11

Common Name (Scientific Name)	Museum	Animal ID	TL (m)	Epaxial Muscle Cross-Sectional Area (CSA) (cm^2)	Minimum Muscle Stress Value (kPa)	Maximum Muscle Stress Value (kPa)	Min Force (N); CSA*1.5	Min Force (kN) at Size Measured	Max Force (N); CSA*6.1	Max Force (kN) at Size Measured	Juvenile Length (m)	Adult Max Length (m)
(Balaenoptera acutorostrata)												
North Atlantic right whale[2] (*Eubalaena glacialis*)	NCSM	3286	13.72	4521.54	1.5	6.1	6782.3	6.7823	27581	27.581	4.26	16
North Atlantic right whale[2]	NCSM	WJW 101	14.6	4628.94	1.5	6.1	6943.4	6.9434	28237	28.237	4.26	16

Common Name (Scientific Name)	Museum	Animal ID	TL (m)	Epaxial Muscle Cross-Sectional Area (CSA) (cm^2)	Minimum Muscle Stress Value (kPa)	Maximum Muscle Stress Value (kPa)	Min Force (N); CSA*1.5	Min Force (kN) at Size Measured	Max Force (N); CSA*6.1	Max Force (kN) at Size Measured	Juvenile Length (m)	Adult Max Length (m)
(*Eubalaena glacialis*)												
North Atlantic right whale[2] (*Eubalaena glacialis*)	Becky	NEAq Eg 1909	14.9	5524.8	1.5	6.1	8287.2	8.2872	33701	33.701	4.26	16
North Atlantic right whale[2] (*Eubalaena glacialis*)	NCSM	NARW "Stumpy"	16	6296.2	1.5	6.1	9444.3	9.4443	38407	38.407	4.26	16

Common Name (Scientific Name)	Museum	Animal ID	TL (m)	Epaxial Muscle Cross-Sectional Area (CSA) (cm^2)	Minimum Muscle Stress Value (kPa)	Maximum Muscle Stress Value (kPa)	Min Force (N); CSA*1.5	Min Force (kN) at Size Measured	Max Force (N); CSA*6.1	Max Force (kN) at Size Measured	Juvenile Length (m)	Adult Max Length (m)
Northern right whale dolphin (*Lissodelphis borealis*)	HSU	Cat. No. 2001	2.59	160.42	1.5	6.1	240.6	0.2406	979	0.979	0.8	3.0
Pacific white-sided dolphin (*Lagenorynchus obliquidens*)	MVZ	208596	1.88	204.2	1.5	6.1	306.3	0.3063	1246	1.246	0.97	2.5
Pacific white-sided	HSU	HSU2345	1.79	179.07	1.5	6.1	268.6	0.2686	1092	1.092	0.97	2.5

Common Name (Scientific Name)	Museum	Animal ID	TL (m)	Epaxial Muscle Cross-Sectional Area (CSA) (cm^2)	Minimum Muscle Stress Value (kPa)	Maximum Muscle Stress Value (kPa)	Min Force (N); CSA*1.5	Min Force (kN) at Size Measured	Max Force (N); CSA*6.1	Max Force (kN) at Size Measured	Juvenile Length (m)	Adult Max Length (m)
dolphin (*Lagenorynchus obliquidens*)												
Pacific white-sided dolphin (*Lagenorynchus obliquidens*)	HSU	HSU2418	1.71	172.79	1.5	6.1	259.2	0.2592	1054	1.054	0.97	2.5
Pacific white-sided	HSU	HSU2689	1.885	171.61	1.5	6.1	257.4	0.2574	1047	1.047	0.97	2.5

Common Name (Scientific Name)	Museum	Animal ID	TL (m)	Epaxial Muscle Cross-Sectional Area (CSA) (cm^2)	Minimum Muscle Stress Value (kPa)	Maximum Muscle Stress Value (kPa)	Min Force (N); CSA*1.5	Min Force (kN) at Size Measured	Max Force (N); CSA*6.1	Max Force (kN) at Size Measured	Juvenile Length (m)	Adult Max Length (m)
dolphin (*Lagenorynchus obliquidens*)												
Pacific white-sided dolphin (*Lagenorynchus obliquidens*)	HSU	Cat. No. 4254	1.6	151.97	1.5	6.1	228.0	0.2280	927	0.927	0.97	2.5

Common Name (Scientific Name)	Museum	Animal ID	TL (m)	Epaxial Muscle Cross-Sectional Area (CSA) (cm^2)	Minimum Muscle Stress Value (kPa)	Maximum Muscle Stress Value (kPa)	Min Force (N); CSA*1.5	Min Force (kN) at Size Measured	Max Force (N); CSA*6.1	Max Force (kN) at Size Measured	Juvenile Length (m)	Adult Max Length (m)
Pacific white-sided dolphin (*Lagenorynchus obliquidens*)	HSU	HSU20150809-CC16	1.79	187.61	1.5	6.1	281.4	0.2814	1144	1.144	0.97	2.5
Pilot whale (Globiocephala sp?)	HSU	VM2671	4.4	485.08	1.5	6.1	727.6	0.7276	2959	2.959	1.4	7.3
Pygmy sperm whale	USNM	BRF 092	2.67	378.7	1.5	6.1	568.0	0.5680	2310	2.310	1.0	4.0

Common Name (Scientific Name)	Museum	Animal ID	TL (m)	Epaxial Muscle Cross-Sectional Area (CSA) (cm^2)	Minimum Muscle Stress Value (kPa)	Maximum Muscle Stress Value (kPa)	Min Force (N); CSA*1.5	Min Force (kN) at Size Measured	Max Force (N); CSA*6.1	Max Force (kN) at Size Measured	Juvenile Length (m)	Adult Max Length (m)
(*Kogia breviceps*)												
Pygmy sperm whale (*Kogia breviceps*)	USNM	KMS 429	2.83	403.5	1.5	6.1	605.2	0.6052	2461	2.461	1.0	4.0
Pygmy sperm whale (*Kogia breviceps*)	USNM	DAP 033	3.02	461.4	1.5	6.1	692.1	0.6921	2814	2.814	1.0	4.0
Risso's dolphin	NECRO	CAHA 171	2.52	262.2	1.5	6.1	393.3	0.3933	1599	1.599	1.1	3.8

Common Name (Scientific Name)	Museum	Animal ID	TL (m)	Epaxial Muscle Cross-Sectional Area (CSA) (cm^2)	Minimum Muscle Stress Value (kPa)	Maximum Muscle Stress Value (kPa)	Min Force (N); CSA*1.5	Min Force (kN) at Size Measured	Max Force (N); CSA*6.1	Max Force (kN) at Size Measured	Juvenile Length (m)	Adult Max Length (m)
(*Grampus griseus*)												
Risso's dolphin (*Grampus griseus*)	UNCW	WAM 659	2.71	353.7	1.5	6.1	530.6	0.5306	2158	2.158	1.1	3.8
Risso's dolphin (*Grampus griseus*)	USNM	550108	2.77	350.6	1.5	6.1	525.8	0.5258	2138	2.138	1.1	3.8
Risso's dolphin (*Grampus griseus*)	UNCW	MDB 057	2.79	333.2	1.5	6.1	499.8	0.4998	2033	2.033	1.1	3.8

Common Name (Scientific Name)	Museum	Animal ID	TL (m)	Epaxial Muscle Cross-Sectional Area (CSA) (cm^2)	Minimum Muscle Stress Value (kPa)	Maximum Muscle Stress Value (kPa)	Min Force (N); CSA*1.5	Min Force (kN) at Size Measured	Max Force (N); CSA*6.1	Max Force (kN) at Size Measured	Juvenile Length (m)	Adult Max Length (m)
Risso's dolphin (*Grampus griseus*)	USNM	550437	2.96	423.6	1.5	6.1	635.4	0.6354	2584	2.584	1.1	3.8
Risso's dolphin (*Grampus griseus*)	MVZ	153257	2.75	252.9	1.5	6.1	379.4	0.3794	1543	1.543	1.1	3.8
Risso's dolphin (*Grampus griseus*)	HSU	Cat. No. 4105	3.03	409.83	1.5	6.1	614.7	0.6147	2500	2.500	1.1	3.8
Risso's dolphin	HSU	VM2631	3.45	428.83	1.5	6.1	643.2	0.6432	2616	2.616	1.1	3.8

Common Name (Scientific Name)	Museum	Animal ID	TL (m)	Epaxial Muscle Cross-Sectional Area (CSA) (cm^2)	Minimum Muscle Stress Value (kPa)	Maximum Muscle Stress Value (kPa)	Min Force (N); CSA*1.5	Min Force (kN) at Size Measured	Max Force (N); CSA*6.1	Max Force (kN) at Size Measured	Juvenile Length (m)	Adult Max Length (m)
(*Grampus griseus*)												
Rough-toothed dolphin (*Steno bredanensis*)	MVZ	175112	2.175	192.42	1.5	6.1	288.6	0.2886	1174	1.174	1	2.8
Sei whale (Balaenoptera borealis)	USNM	236680	13.5	4820.7	1.5	6.1	7231.1	7.2311	29406	29.406	4.5	18
Short-beaked	UNCW	CAHA 010	2.02	183.4	1.5	6.1	275.1	0.2751	1119	1.119	0.8	2.43

Common Name (Scientific Name)	Museum	Animal ID	TL (m)	Epaxial Muscle Cross-Sectional Area (CSA) (cm^2)	Minimum Muscle Stress Value (kPa)	Maximum Muscle Stress Value (kPa)	Min Force (N); CSA*1.5	Min Force (kN) at Size Measured	Max Force (N); CSA*6.1	Max Force (kN) at Size Measured	Juvenile Length (m)	Adult Max Length (m)
common dolphin (*Delphinus delphis*)												
Short-beaked common dolphin (*Delphinus delphis*)	USNM	550450	2.04	194.8	1.5	6.1	292.2	0.2922	1188	1.188	0.8	2.43
Short-beaked common dolphin	USNM	572630	2.08	190.4	1.5	6.1	285.6	0.2856	1161	1.161	0.8	2.43

Common Name (Scientific Name)	Museum	Animal ID	TL (m)	Epaxial Muscle Cross-Sectional Area (CSA) (cm^2)	Minimum Muscle Stress Value (kPa)	Maximum Muscle Stress Value (kPa)	Min Force (N); CSA*1.5	Min Force (kN) at Size Measured	Max Force (N); CSA*6.1	Max Force (kN) at Size Measured	Juvenile Length (m)	Adult Max Length (m)
(*Delphinus delphis*)												
Short-beaked common dolphin (*Delphinus delphis*)	USNM	571991	2.25	212.8	1.5	6.1	319.1	0.3191	1298	1.298	0.8	2.43
Short-beaked common dolphin (*Delphinus delphis*)	USNM	571620	2.3	231.8	1.5	6.1	347.7	0.3477	1414	1.414	0.8	2.43

Common Name (Scientific Name)	Museum	Animal ID	TL (m)	Epaxial Muscle Cross-Sectional Area (CSA) (cm^2)	Minimum Muscle Stress Value (kPa)	Maximum Muscle Stress Value (kPa)	Min Force (N); CSA*1.5	Min Force (kN) at Size Measured	Max Force (N); CSA*6.1	Max Force (kN) at Size Measured	Juvenile Length (m)	Adult Max Length (m)
Short-beaked common dolphin (*Delphinus delphis*)	MVZ	208604	2.43	218.54	1.5	6.1	327.8	0.3278	1333	1.333	0.8	2.43
Short-beaked common dolphin (*Delphinus delphis*)	HSU	Cat. No. 2366	1.65	126.84	1.5	6.1	190.3	0.1903	774	0.774	0.8	2.43

Common Name (Scientific Name)	Museum	Animal ID	TL (m)	Epaxial Muscle Cross-Sectional Area (CSA) (cm^2)	Minimum Muscle Stress Value (kPa)	Maximum Muscle Stress Value (kPa)	Min Force (N); CSA*1.5	Min Force (kN) at Size Measured	Max Force (N); CSA*6.1	Max Force (kN) at Size Measured	Juvenile Length (m)	Adult Max Length (m)
Short-beaked common dolphin (*Delphinus delphis*)	HSU	HSU20220409-HB16	1.57	108.24	1.5	6.1	162.4	0.1624	660	0.660	0.8	2.43
Short-finned pilot whale (*Globicephala macrorhynchus*)	NCSM	WAM 555	3.67	410.5	1.5	6.1	615.8	0.6158	2504	2.504	1.4	7.3

Common Name (Scientific Name)	Museum	Animal ID	TL (m)	Epaxial Muscle Cross-Sectional Area (CSA) (cm^2)	Minimum Muscle Stress Value (kPa)	Maximum Muscle Stress Value (kPa)	Min Force (N); CSA*1.5	Min Force (kN) at Size Measured	Max Force (N); CSA*6.1	Max Force (kN) at Size Measured	Juvenile Length (m)	Adult Max Length (m)
Short-finned pilot whale (*Globicephala macrorhynchus*)	USNM	504395	3.81	450.9	1.5	6.1	676.3	0.6763	2750	2.750	1.4	7.3
Short-finned pilot whale (*Globicephala macrorhynchus*)	NCSM	DAP 035	5.01	598	1.5	6.1	897.0	0.8970	3648	3.648	1.4	7.3

Common Name (Scientific Name)	Museum	Animal ID	TL (m)	Epaxial Muscle Cross-Sectional Area (CSA) (cm^2)	Minimum Muscle Stress Value (kPa)	Maximum Muscle Stress Value (kPa)	Min Force (N); CSA*1.5	Min Force (kN) at Size Measured	Max Force (N); CSA*6.1	Max Force (kN) at Size Measured	Juvenile Length (m)	Adult Max Length (m)
Short-finned pilot whale (*Globicephala macrorhynchus*)	UNSM	504396	5.07	756.1	1.5	6.1	1134.2	1.1342	4613	4.613	1.4	7.3
Sowerby's beaked whale (*Mesoplodon bidens*)	USNM	NEFC-3070	4.62	827.5	1.5	6.1	1241.3	1.2413	5048	5.048	2.4	6.4
Sperm whale	NBWM	NBWM	14.65	3023	1.5	6.1	4534.5	4.5345	18440	18.440	4	17.68

Common Name (Scientific Name)	Museum	Animal ID	TL (m)	Epaxial Muscle Cross-Sectional Area (CSA) (cm^2)	Minimum Muscle Stress Value (kPa)	Maximum Muscle Stress Value (kPa)	Min Force (N); CSA*1.5	Min Force (kN) at Size Measured	Max Force (N); CSA*6.1	Max Force (kN) at Size Measured	Juvenile Length (m)	Adult Max Length (m)
(Physeter macrocephalus)												
Sperm whale (Physeter macrocephalus)	NCSM	3281	17	3357.58	1.5	6.1	5036.4	5.0364	20481	20.481	4	17.68
Sperm whale (Physeter macrocephalus)	USNM	301634	17.68	4220.0	1.5	6.1	6330.0	6.3300	25742	25.742	4	17.68

Common Name (Scientific Name)	Museum	Animal ID	TL (m)	Epaxial Muscle Cross-Sectional Area (CSA) (cm^2)	Minimum Muscle Stress Value (kPa)	Maximum Muscle Stress Value (kPa)	Min Force (N); CSA*1.5	Min Force (kN) at Size Measured	Max Force (N); CSA*6.1	Max Force (kN) at Size Measured	Juvenile Length (m)	Adult Max Length (m)
Striped dolphin (Stenella coeruleoalba)	USNM	SGB 126	1.725	134.1	1.5	6.1	201.1	0.2011	818	0.818	1	2.7
Striped dolphin (Stenella coeruleoalba)	USNM	VMSM 20031005	1.844	166.3	1.5	6.1	249.4	0.2494	1014	1.014	1	2.7
Striped dolphin (Stenella	UNCW	NCARI 007	1.96	200.0	1.5	6.1	300.0	0.3000	1220	1.220	1	2.7

Common Name (Scientific Name)	Museum	Animal ID	TL (m)	Epaxial Muscle Cross-Sectional Area (CSA) (cm^2)	Minimum Muscle Stress Value (kPa)	Maximum Muscle Stress Value (kPa)	Min Force (N); CSA*1.5	Min Force (kN) at Size Measured	Max Force (N); CSA*6.1	Max Force (kN) at Size Measured	Juvenile Length (m)	Adult Max Length (m)
coeruleoalba)												
Striped dolphin (Stenella coeruleoalba)	UNCW	EWC 002	1.965	167.8	1.5	6.1	251.7	0.2517	1024	1.024	1	2.7
Striped dolphin (Stenella coeruleoalba)	UNCW	RJM 013	2.12	247.3	1.5	6.1	371.0	0.3710	1509	1.509	1	2.7
Striped dolphin	USNM	571260	2.24	230.9	1.5	6.1	346.3	0.3463	1408	1.408	1	2.7

Common Name (Scientific Name)	Museum	Animal ID	TL (m)	Epaxial Muscle Cross-Sectional Area (CSA) (cm^2)	Minimum Muscle Stress Value (kPa)	Maximum Muscle Stress Value (kPa)	Min Force (N); CSA*1.5	Min Force (kN) at Size Measured	Max Force (N); CSA*6.1	Max Force (kN) at Size Measured	Juvenile Length (m)	Adult Max Length (m)
(Stenella coeruleoalba)												
Striped dolphin (Stenella coeruleoalba)	USNM	504350	2.25	258.9	1.5	6.1	388.3	0.3883	1579	1.579	1	2.7
Striped dolphin (Stenella coeruleoalba)	USNM	572695	2.33	244.2	1.5	6.1	366.3	0.3663	1489	1.489	1	2.7

Common Name (Scientific Name)	Museum	Animal ID	TL (m)	Epaxial Muscle Cross-Sectional Area (CSA) (cm^2)	Minimum Muscle Stress Value (kPa)	Maximum Muscle Stress Value (kPa)	Min Force (N); CSA*1.5	Min Force (kN) at Size Measured	Max Force (N); CSA*6.1	Max Force (kN) at Size Measured	Juvenile Length (m)	Adult Max Length (m)
Striped dolphin (Stenella coeruleoalba)	HSU	HSU20180904-KG3	2.05	232.28	1.5	6.1	348.4	0.3484	1417	1.417	1	2.7
True's beaked whale (*Mesoplodon mirus*)	USNM	504724	4.56	991.8	1.5	6.1	1487.7	1.4877	6050	6.050	2.0	5.3
True's beaked whale	NCSM	KLC 131	5	900.07	1.5	6.1	1350.1	1.3501	5490	5.490	2.0	5.3

Common Name (Scientific Name)	Museum	Animal ID	TL (m)	Epaxial Muscle Cross-Sectional Area (CSA) (cm^2)	Minimum Muscle Stress Value (kPa)	Maximum Muscle Stress Value (kPa)	Min Force (N); CSA*1.5	Min Force (kN) at Size Measured	Max Force (N); CSA*6.1	Max Force (kN) at Size Measured	Juvenile Length (m)	Adult Max Length (m)
(*Mesoplodon mirus*)												

Notes: Yellow highlighted cells represent data provided by Arthur et al. (2015). Blue highlighted cells represent data collected and calculations performed by Schatz Energy Research Center staff. Acronyms: HSU = Cal Poly Humboldt Vertebrate Museum; MVZ = UC Berkeley Museum of Vertebrate Zoology; NBWM = New Bedford Whaling Museum; NCMNS = North Carolina Museum of Natural Sciences; NECRO = Necropsied animal; NOYO = NOYO Center for Marine Science; PM = Pratt Museum; SBMNH = Santa Barbara Museum of Natural History; UMaine = University of Maine Natural History collection; UNCW = University of North Carolina Wilmington Natural History collection; USNM = Smithsonian Institution's Museum of Natural History. N = Newtons, kN = kilonewtons, kPa = kilopascal, m = meters, cm = centimeters.

Appendix C. Cetacean Force Calculation Methods and Complete Results

Initial Plotting

Plotting grouped data scatterplots prior to modeling. Based on visual inspection, the relationship between cetacean total length and epaxial muscle cross-sectional area appears to follow a linear or power curve. Note that the "Misc" group is composed exclusively of species of the genus *Kogia*. Species were organized into size classes based on a qualitative assessment of body shape, relatedness/taxonomic group, and length.

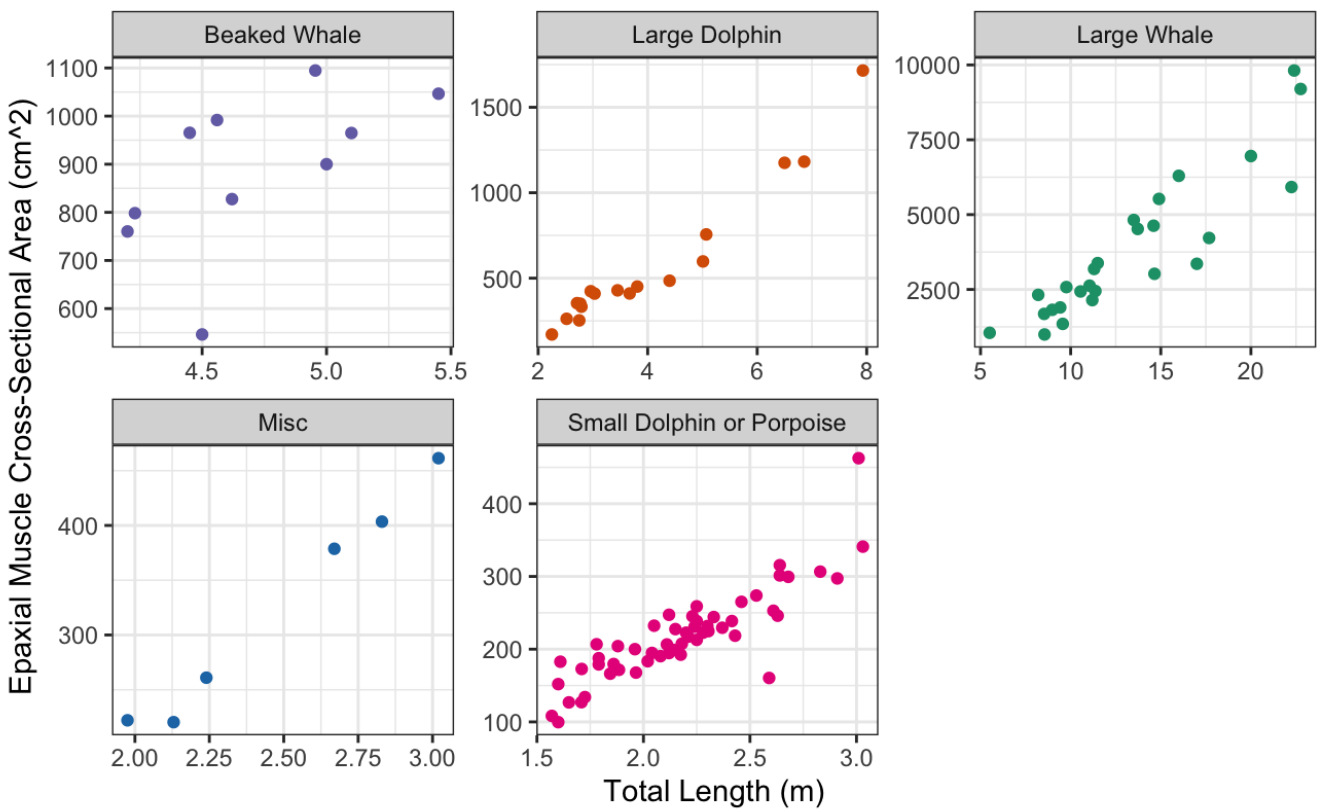

Figure C1: Epaxial Cross-Sectional Area by Total Length within each cetacean size class

Source: Schatz Energy Research Center

Notes: Cross-sectional area is shown in square-centimeters (cm^2). Total length is shown in meters (m)

The following plots show the observed data with a power regression (using log-transformed data) and a linear regression (without log-transformation).

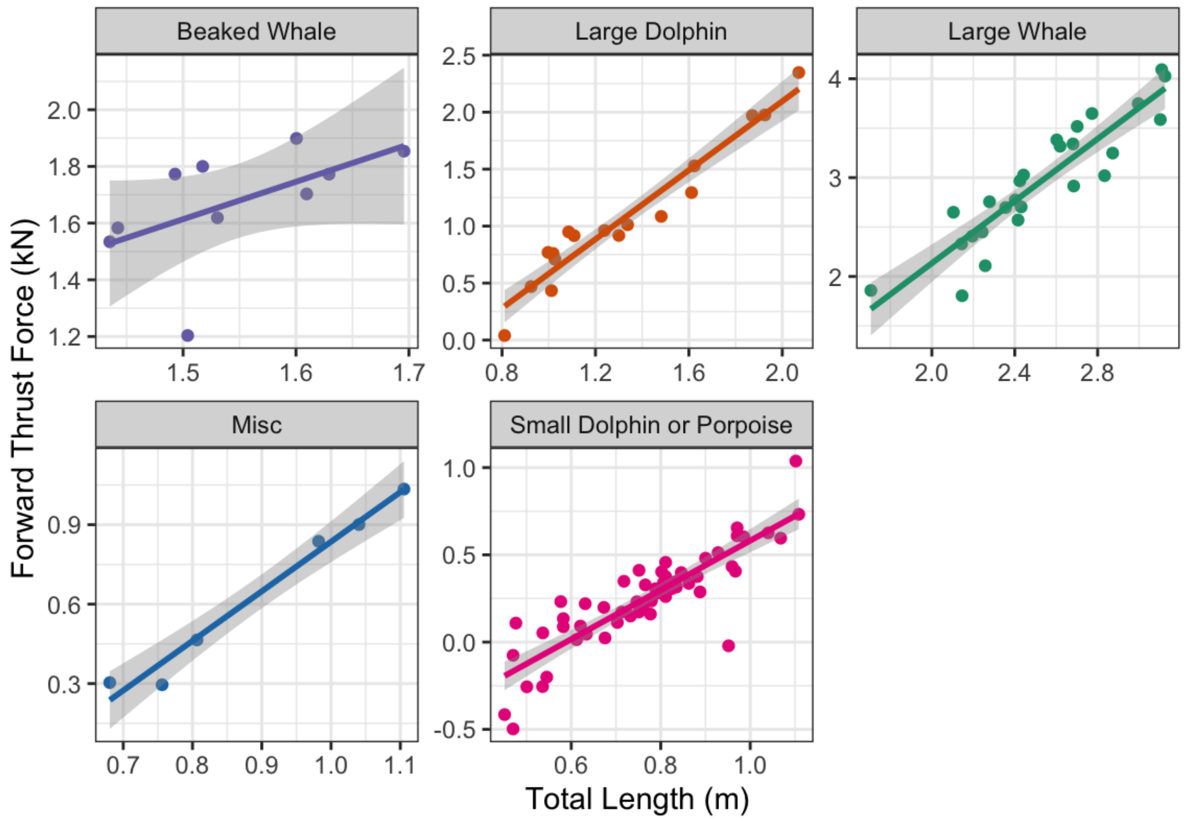

Figure C2: Maximum force vs. total length trend using a power regression (log-log)

Source: Schatz Energy Research Center

Notes: Shaded areas show the 95% Confidence Interval. Forward thrust force is in kilonewtons (kN). Total length is in meters (m). Axes are log-transformed.

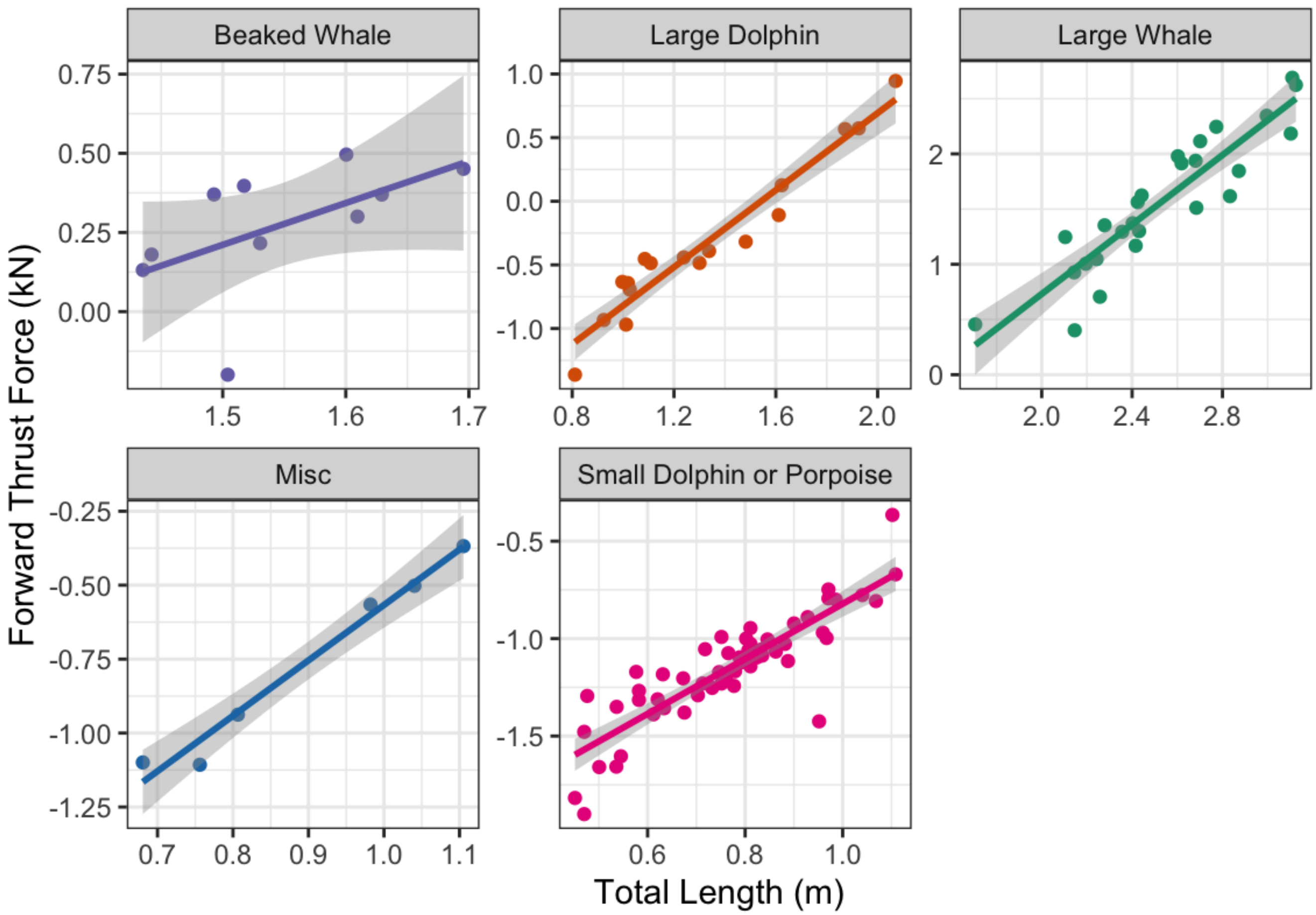

Figure C3: Sub-maximum force vs. total length trend using a power regression (log-log)

Source: Schatz Energy Research Center

Notes: Shaded areas show the 95% Confidence Interval. Forward thrust force is in kilonewtons (kN). Total length is in meters (m). Axes are log-transformed.

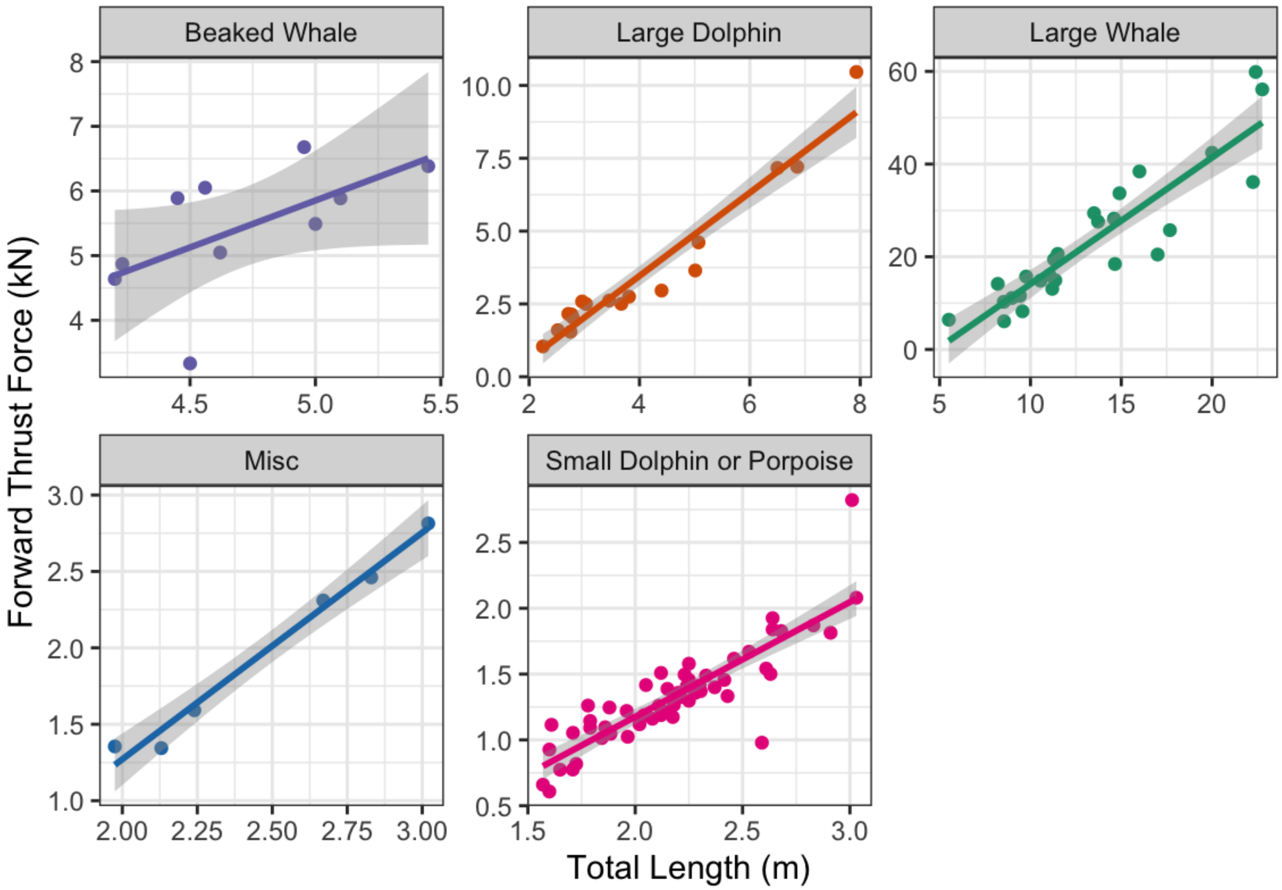

Figure C4: Maximum force vs. total length trend using a linear regression

Source: Schatz Energy Research Center

Notes: Shaded areas show the 95% Confidence Interval. Forward thrust force is in kilonewtons (kN). Total length is in meters (m).

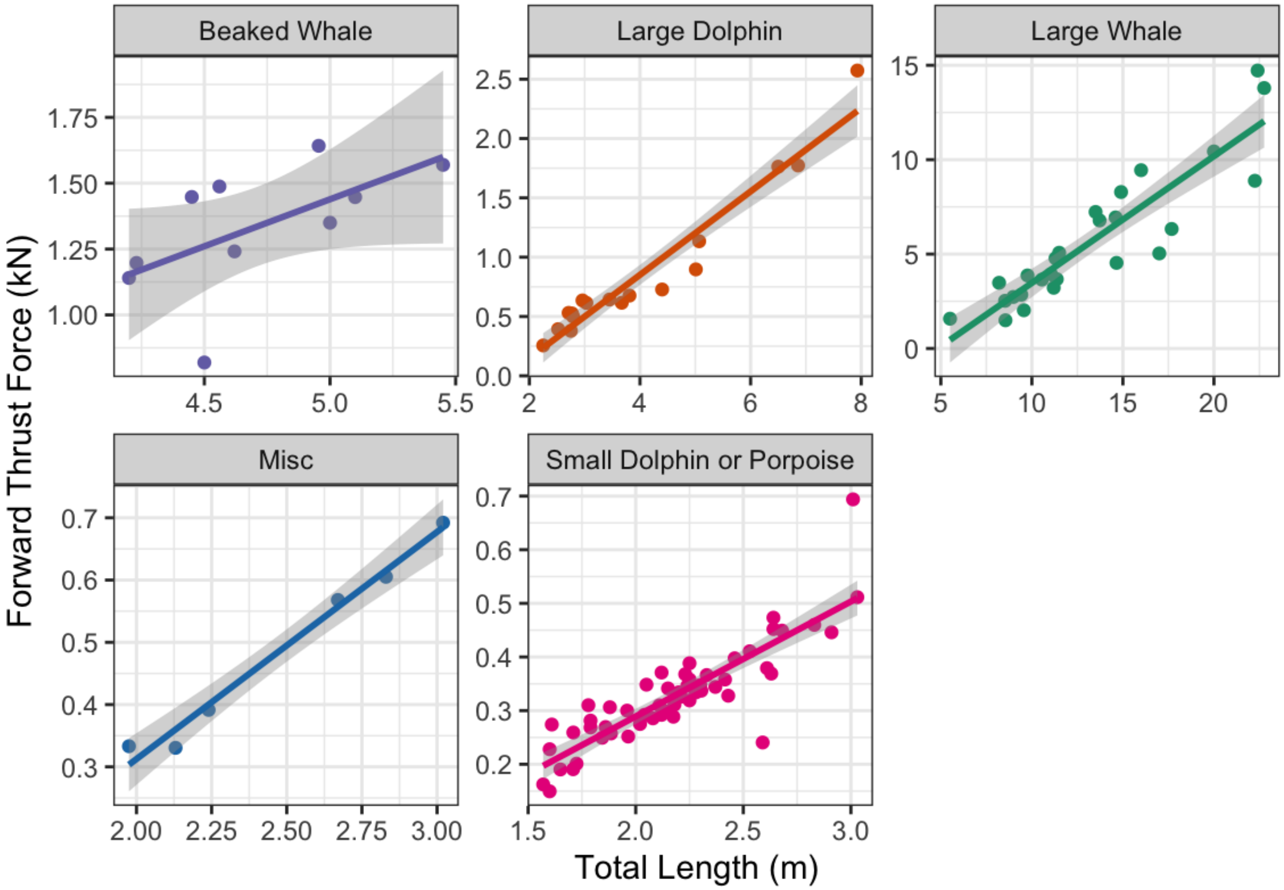

Figure C5: Sub-maximum force vs. total length trend using a linear regression

Source: Schatz Energy Research Center

Notes: Shaded areas show the 95% Confidence Interval. Forward thrust force is in kilonewtons (kN). Total length is in meters (m).

Model Fit

We generate AIC and R-squared values for both models. However, comparison of adjusted R-squared values when one model is log-transformed is not useful. Based on AIC only, the power regression fits better than linear regression. According to the Adjusted R-squared, both appear to explain the variance well.

```
Power Regression: Maximum Force

lm(formula = log(max force) ~ log(total length) * size class)


Residuals:
     Min       1Q   Median       3Q      Max
-0.55853 -0.06597  0.00164  0.12376  0.35185


Coefficients:
                                     Estimate Std. Error t value Pr(>|t|)
(Intercept)                          -0.36609    1.09125  -0.335    0.738
log(Total Length)                     1.31994    0.70505   1.872    0.064 .
Large Dolphin                        -0.56491    1.10310  -0.512    0.610
Large Whale                          -0.64552    1.12120  -0.576    0.566
Misc                                 -0.67069    1.17200  -0.572    0.568
Small Dolphin or Porpoise            -0.46440    1.09711  -0.423    0.673
log(Total Length):Large Dolphin       0.19352    0.71479   0.271    0.787
log(Total Length):Large Whale         0.25287    0.71225   0.355    0.723
log(Total Length):Misc                0.55270    0.84762   0.652    0.516
log(Total Length):Small Dolphin       0.09188    0.71971   0.128    0.899
Signif. codes:  0 '***' 0.001 '**' 0.01 '*' 0.05 '.' 0.1 ' ' 1


Residual standard error: 0.1798 on 103 degrees of freedom
```

```
Multiple R-squared:  0.9783, Adjusted R-squared:  0.9764
F-statistic: 516.4 on 9 and 103 DF,  p-value: < 2.2e-16
```

<u>Power Regression: Minimum Force</u>

```
lm(formula = log(min force) ~ log(total length) * size class)

Residuals:
     Min       1Q   Median       3Q      Max
-0.55859 -0.06595  0.00187  0.12376  0.35185

Coefficients:
                                     Estimate Std. Error t value Pr(>|t|)
(Intercept)                           -1.7692     1.0913  -1.621    0.108
log(Total Length)                      1.3201     0.7051   1.872    0.064 .
Large Dolphin                         -0.5647     1.1032  -0.512    0.610
Large Whale                           -0.6452     1.1213  -0.575    0.566
Misc                                  -0.6710     1.1721  -0.572    0.568
Small Dolphin or Porpoise             -0.4639     1.0972  -0.423    0.673
log(Total Length):Large Dolphin        0.1934     0.7148   0.271    0.787
log(Total Length):Large Whale          0.2526     0.7123   0.355    0.724
log(Total Length):Misc                0.5532     0.8477   0.653    0.515
log(Total Length):Small Dolphin       0.0914     0.7198   0.127    0.899
---
Signif. codes:  0 '***' 0.001 '**' 0.01 '*' 0.05 '.' 0.1 ' ' 1

Residual standard error: 0.1798 on 103 degrees of freedom
Multiple R-squared:  0.9783, Adjusted R-squared:  0.9764
F-statistic: 516.3 on 9 and 103 DF,  p-value: < 2.2e-16
```

Linear Regression: Maximum Force

```
Call:
lm(formula = max force ~ total length * size class)

Residuals:
     Min       1Q   Median       3Q      Max
-12.7495  -0.1475  -0.0229   0.1914  11.8956

Coefficients:
                                       Estimate Std. Error t value Pr(>|t|)
(Intercept)                            -1.40282   11.69916  -0.120    0.905
Total Length                            1.45102    2.47750   0.586    0.559
Large Dolphin                          -0.85238   11.85720  -0.072    0.943
Large Whale                           -11.77340   11.83414  -0.995    0.322
Misc                                   -0.29159   14.18507  -0.021    0.984
Small Dolphin or Porpoise               0.83643   11.95328   0.070    0.944
Total Length:Large Dolphin             -0.02187    2.51686  -0.009    0.993
Total Length:Large Whale                1.27879    2.48074   0.515    0.607
Total Length:Misc                       0.03183    4.04662   0.008    0.994
Total Length:Small Dolphin or Porpoise -0.57979    2.71425  -0.214    0.831

Residual standard error: 3.01 on 103 degrees of freedom
Multiple R-squared:  0.9336, Adjusted R-squared:  0.9277
F-statistic: 160.8 on 9 and 103 DF,  p-value: < 2.2e-16
```

Linear Regression: Minimum Force

```
lm(formula = min force ~ total length * size class)


Residuals:
     Min       1Q   Median       3Q      Max
-3.13505 -0.03617 -0.00557  0.04701  2.92524


Coefficients:
                                       Estimate Std. Error t value Pr(>|t|)
(Intercept)                           -0.345170   2.876865  -0.120    0.905
TL..m.                                 0.356849   0.609226   0.586    0.559
groupLarge Dolphin                    -0.209470   2.915727  -0.072    0.943
groupLarge Whale                      -2.894830   2.910057  -0.995    0.322
groupMisc                             -0.071810   3.488160  -0.021    0.984
groupSmall Dolphin or Porpoise         0.205959   2.939354   0.070    0.944
TL..m.:groupLarge Dolphin             -0.005399   0.618906  -0.009    0.993
TL..m.:groupLarge Whale                0.314413   0.610023   0.515    0.607
TL..m.:groupMisc                       0.007919   0.995078   0.008    0.994
TL..m.:groupSmall Dolphin or Porpoise -0.142644   0.667445  -0.214    0.831


Residual standard error: 0.7403 on 103 degrees of freedom
Multiple R-squared:  0.9336, Adjusted R-squared:  0.9277
F-statistic: 160.8 on 9 and 103 DF,  p-value: < 2.2e-16
```

AIC

	df	AIC
Power Regression, Max Force	11	-55.61930
Power Regression, Min Force	11	-55.60371
Linear Regression, Max Force	11	581.28166
Linear Regression, Min Force	11	264.24532

Testing Full Models for Normality

QQ plots show that the power regression roughly fits the QQ line (demonstrates normality) within one standard deviation, but has less extreme tails than the linear regression. The linear regression follows the QQ line within one standard deviation from the mean, but has tails that diverge more outside of that range.

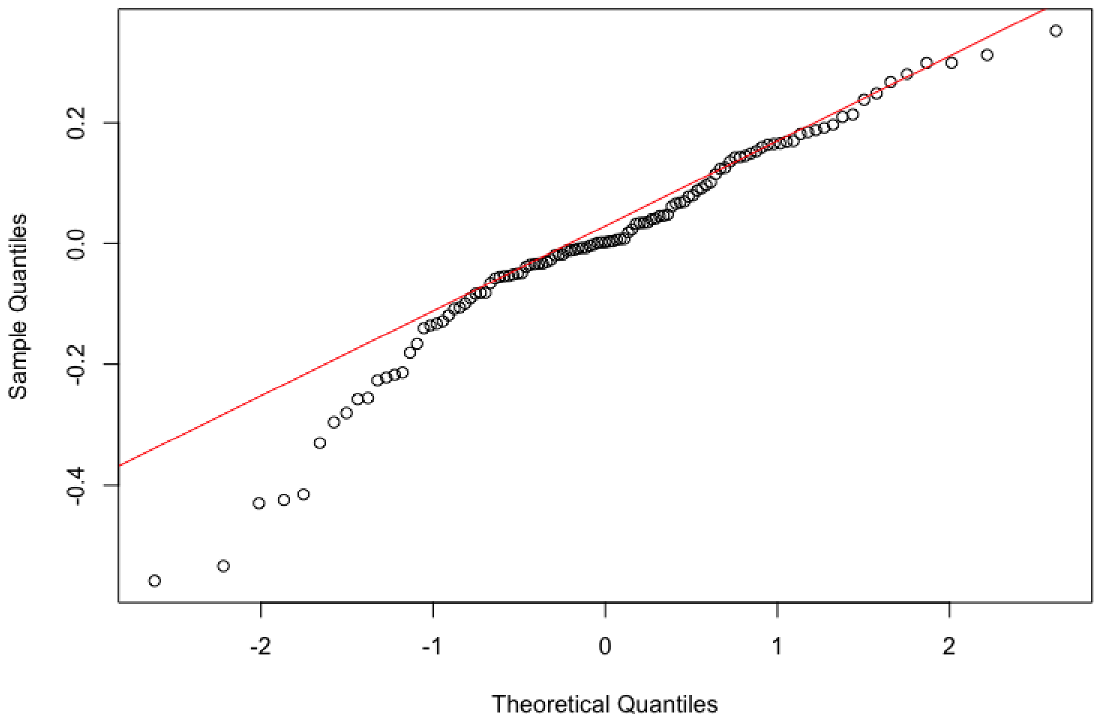

Figure C6: Normal Q-Q Plot for Maximum Force Residuals Using a Power Regression

Source: Schatz Energy Research Center

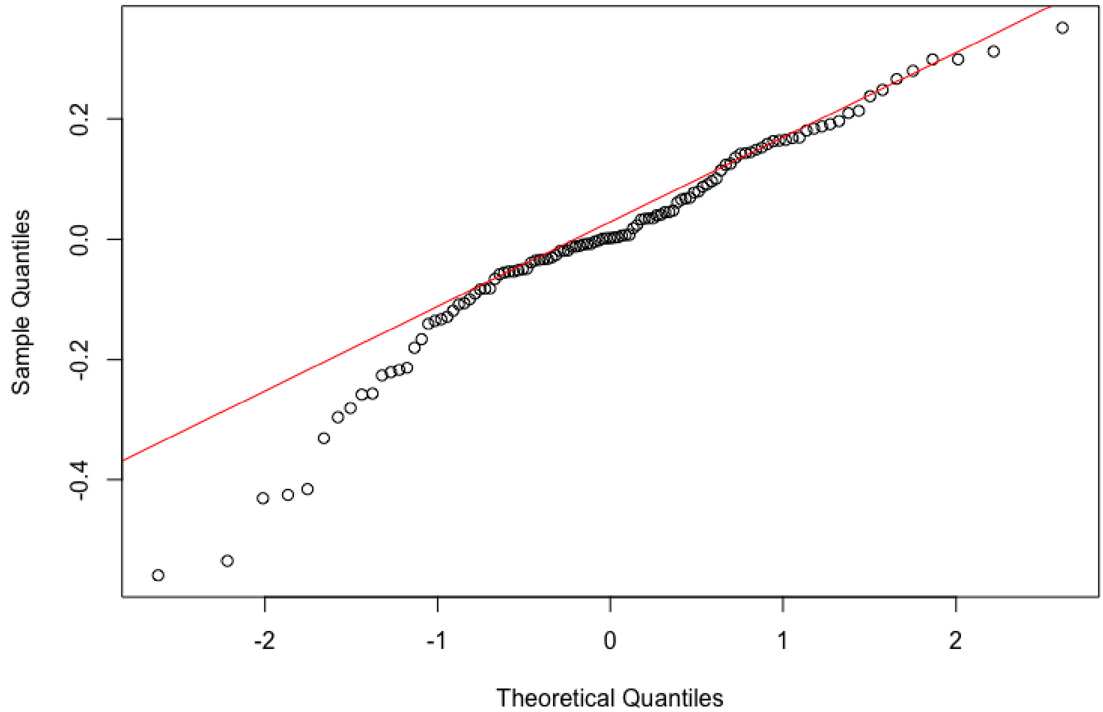

Figure C7: Normal Q-Q Plot for Sub-Maximum Force Residuals Using a Power Regression

Source: Schatz Energy Research Center

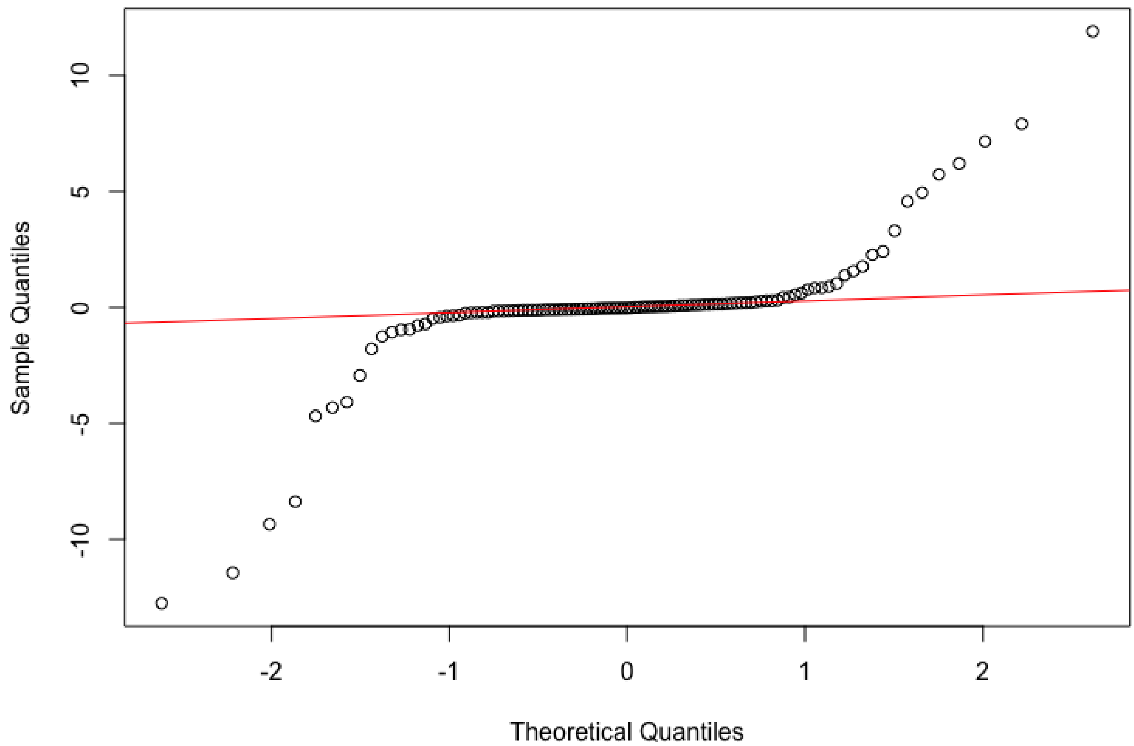

Figure C8: Normal Q-Q Plot for Maximum Force Residuals Using a Linear Regression

Source: Schatz Energy Research Center

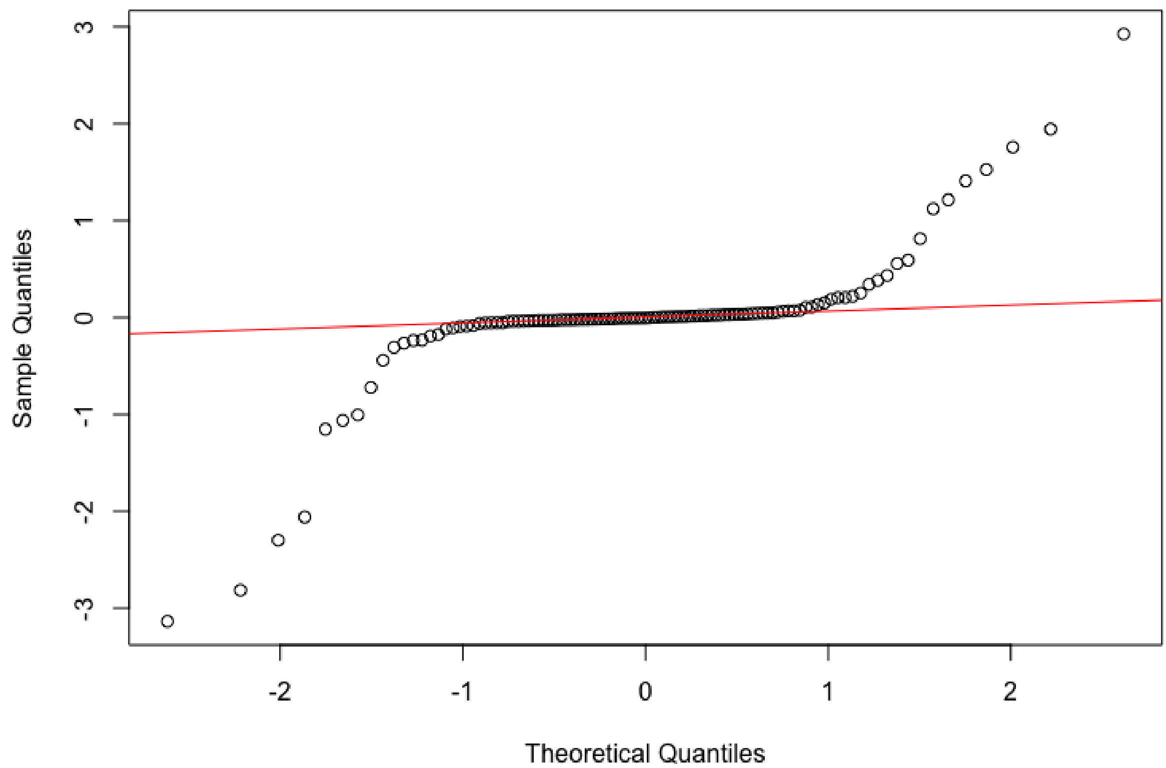

Figure C9: Normal Q-Q Plot for Sub-Maximum Force Residuals Using a Linear Regression

Source: Schatz Energy Research Center

Fitting Submodels by Group (Size Class)

According to the Shapiro-Wilk test, the residuals of three of the five submodels of the power regression are normally distributed (both for minimum and maximum force). We expect the same behavior of the residuals between the minimum and maximum force models because the data are generated using the same measurements, but using different coefficients (1.5 kPa muscle stress factor for minimum force, 6.1 kPa for maximum force).

```
Shapiro-Wilk normality test

data:  resid(Power Regression, Max Force, Large Whale)
W = 0.93362, p-value = 0.09456


Shapiro-Wilk normality test

data:  resid(Power Regression, Max Force, Large Dolphin)
W = 0.94812, p-value = 0.4275


Shapiro-Wilk normality test

data:  resid(Power Regression, Max Force, Beaked Whale)
W = 0.80537, p-value = 0.01685


Shapiro-Wilk normality test

data:  resid(Power Regression, Max Force, Small Dolphin or Porpoise)
W = 0.94193, p-value = 0.01122
Shapiro-Wilk normality test
```

```
data:  resid(Power Regression, Max Force, Kogia [Misc])
W = 0.94713, p-value = 0.717


Shapiro-Wilk normality test


data:  resid(Power Regression, Min Force, Large Whale)
W = 0.93363, p-value = 0.09458

Shapiro-Wilk normality test


data:  resid(Power Regression, Min Force, Large Dolphin)
W = 0.94816, p-value = 0.4281

Shapiro-Wilk normality test


data:  resid(Power Regression, Min Force, Beaked Whale)
W = 0.80541, p-value = 0.01687


Shapiro-Wilk normality test


data:  resid(Power Regression, Min Force, Small Dolphin or Porpoise)
W = 0.94178, p-value = 0.01107

Shapiro-Wilk normality test


data:  resid(Power Regression, Min Force, Kogia [Misc])
W = 0.94713, p-value = 0.717
```

Meanwhile, according to the Shapiro-Wilk test, the residuals of four of the five submodels of the power regression are normally distributed (both for minimum and maximum). This is the first example of the linear regression demonstrating greater residual normality than the power regression.

```
Shapiro-Wilk normality test


data:  resid(Linear Regression, Max Force, Large Whale)
W = 0.97532, p-value = 0.7626


Shapiro-Wilk normality test


data:  resid(Linear Regression, Max Force, Large Dolphin)
W = 0.97117, p-value = 0.8387


Shapiro-Wilk normality test


data:  resid(Linear Regression, Max Force, Beaked Whale)
W = 0.85764, p-value = 0.07156

Shapiro-Wilk normality test


data:  resid(Linear Regression, Max Force, Small Dolphin or Porpoise)
W = 0.8733, p-value = 3.843e-05

Shapiro-Wilk normality test


data:  resid(Linear Regression, Max Force, Kogia [Misc])
W = 0.97947, p-value = 0.9489

Shapiro-Wilk normality test


data:  resid(Linear Regression, Min Force, Large Whale)
W = 0.97532, p-value = 0.7626
```

```
Shapiro-Wilk normality test

data:  resid(Linear Regression, Min Force, Large Dolphin)
W = 0.97115, p-value = 0.8383


Shapiro-Wilk normality test

data:  resid(Linear Regression, Min Force, Beaked Whale)
W = 0.85754, p-value = 0.07138


Shapiro-Wilk normality test

data:  resid(Linear Regression, Min Force, Small Dolphin or Porpoise)
W = 0.87327, p-value = 3.837e-05


Shapiro-Wilk normality test

data:  resid(Linear Regression, Min Force, Kogia [Misc])
W = 0.97943, p-value = 0.9487
```

Testing for Homoscedasticity

All submodels (groups) in the power regression appear to meet the assumption of homoscedasticity, indicated by non-significant results from the Breusch-Pagan test.

```
Non-constant Variance Score Test
Variance formula: ~ fitted.values
Chisquare = 0.08463856, Df = 1, p = 0.77111
```

```
Non-constant Variance Score Test
Variance formula: ~ fitted.values
Chisquare = 0.7338336, Df = 1, p = 0.39164

Non-constant Variance Score Test
Variance formula: ~ fitted.values
Chisquare = 0.7672018, Df = 1, p = 0.38108

Non-constant Variance Score Test
Variance formula: ~ fitted.values
Chisquare = 0.1434163, Df = 1, p = 0.70491

Non-constant Variance Score Test
Variance formula: ~ fitted.values
Chisquare = 2.428678, Df = 1, p = 0.11913

Non-constant Variance Score Test
Variance formula: ~ fitted.values
Chisquare = 0.08482271, Df = 1, p = 0.77087

Non-constant Variance Score Test
Variance formula: ~ fitted.values
Chisquare = 0.7353312, Df = 1, p = 0.39116

Non-constant Variance Score Test
Variance formula: ~ fitted.values
Chisquare = 0.7671614, Df = 1, p = 0.3811

Non-constant Variance Score Test
Variance formula: ~ fitted.values
Chisquare = 0.1383619, Df = 1, p = 0.70991
```

```
Non-constant Variance Score Test
Variance formula: ~ fitted.values
Chisquare = 2.429313, Df = 1, p = 0.11909
```

Meanwhile, for the linear regression submodels, all groups but the beaked whale and Kogia groups fail to meet the assumption of homoscedasticity, indicated by significant results.

```
Non-constant Variance Score Test
Variance formula: ~ fitted.values
Chisquare = 10.00686, Df = 1, p = 0.0015596

Non-constant Variance Score Test
Variance formula: ~ fitted.values
Chisquare = 5.136302, Df = 1, p = 0.023431

Non-constant Variance Score Test
Variance formula: ~ fitted.values
Chisquare = 0.5341693, Df = 1, p = 0.46486

Non-constant Variance Score Test
Variance formula: ~ fitted.values
Chisquare = 19.41829, Df = 1, p = 1.05e-05

Non-constant Variance Score Test
Variance formula: ~ fitted.values
Chisquare = 2.07797, Df = 1, p = 0.14944

Non-constant Variance Score Test
Variance formula: ~ fitted.values
Chisquare = 10.00676, Df = 1, p = 0.0015597

Non-constant Variance Score Test
Variance formula: ~ fitted.values
Chisquare = 5.138282, Df = 1, p = 0.023404
```

```
Non-constant Variance Score Test
Variance formula: ~ fitted.values
Chisquare = 0.5342377, Df = 1, p = 0.46483

Non-constant Variance Score Test
Variance formula: ~ fitted.values
Chisquare = 19.43266, Df = 1, p = 1.0421e-05

Non-constant Variance Score Test
Variance formula: ~ fitted.values
Chisquare = 2.074318, Df = 1, p = 0.1498
```

Generating Predictions to the Full Spectrum of Whale Lengths

Predictions – Power Regression

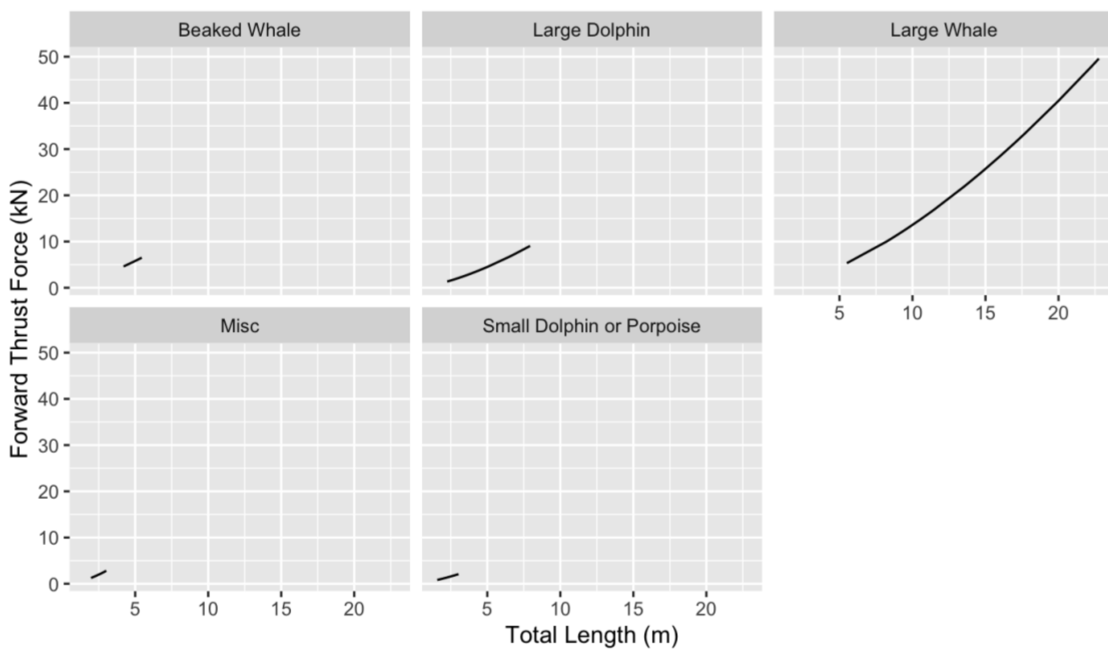

Figure C10: Predicted Maximum Force based on Power Regression

Notes: Forward thrust force is in kilonewtons (kN). Total length is in meters (m).

Source: Schatz Energy Research Center

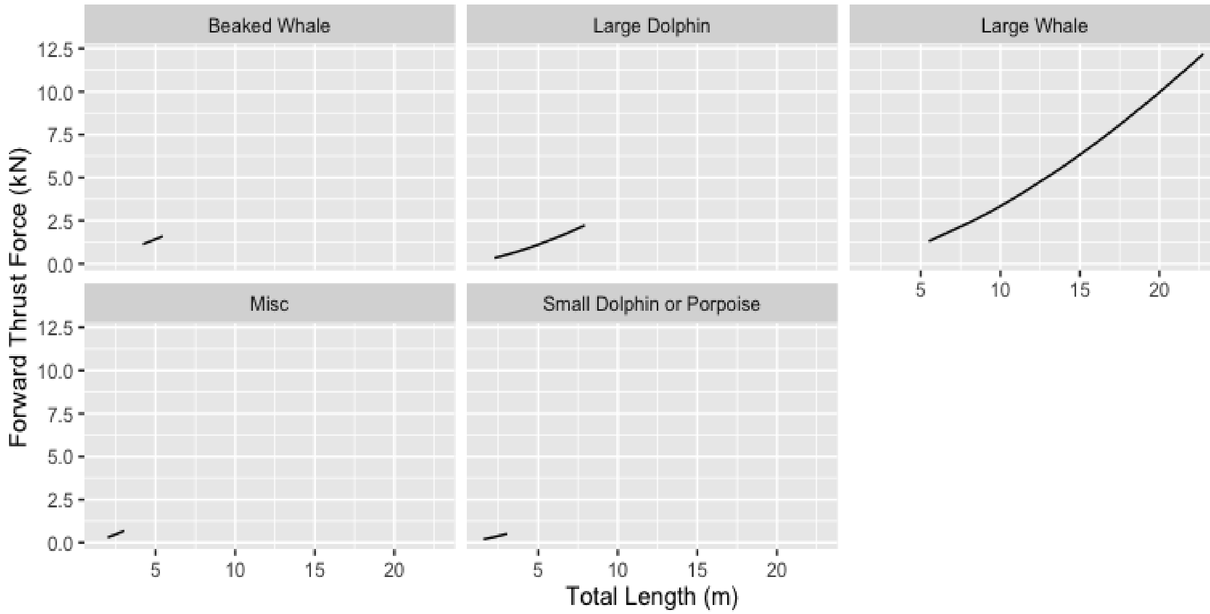

Figure C11: Predicted Sub-Maximum Force based on Power Regression

Notes: Forward thrust force is in kilonewtons (kN). Total length is in meters (m).

Source: Schatz Energy Research Center

Predictions – Linear Regression

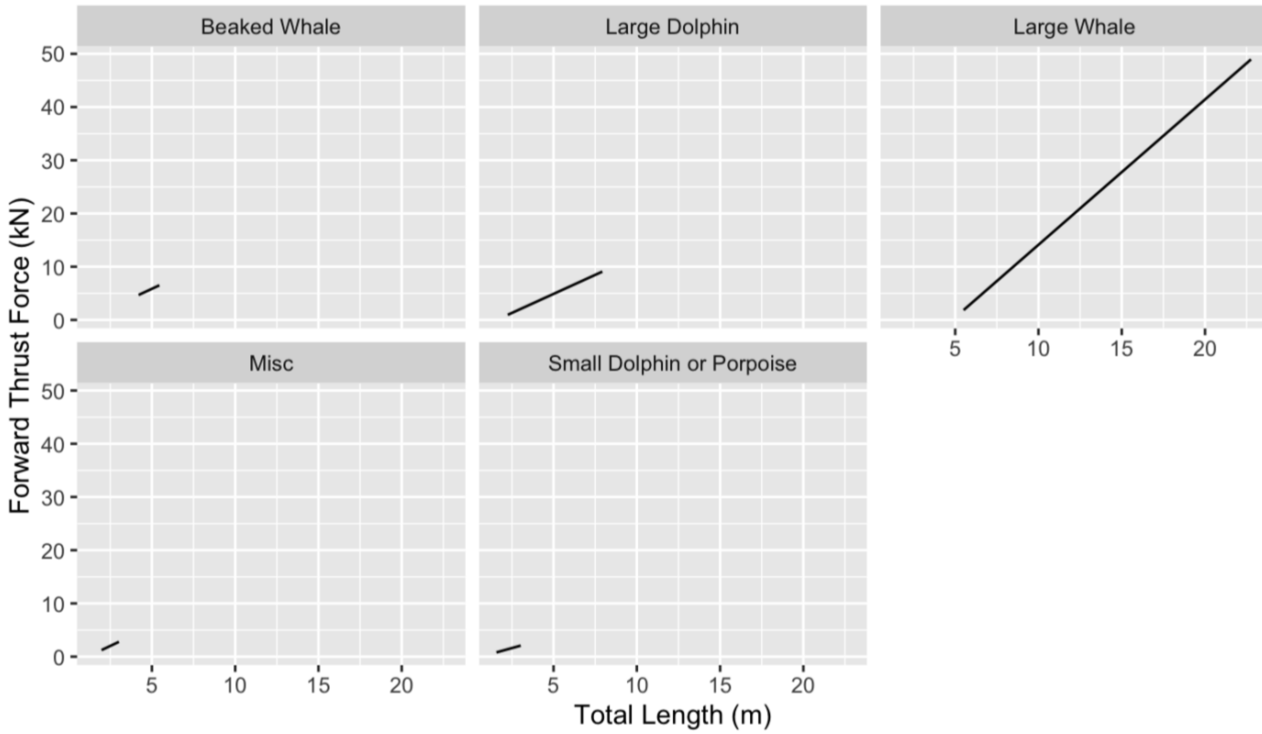

Figure C12: Predicted Maximum Force based on Linear Regression

<u>Notes</u>: Forward thrust force is in kilonewtons (kN). Total length is in meters (m).

<u>Source</u>: Schatz Energy Research Center

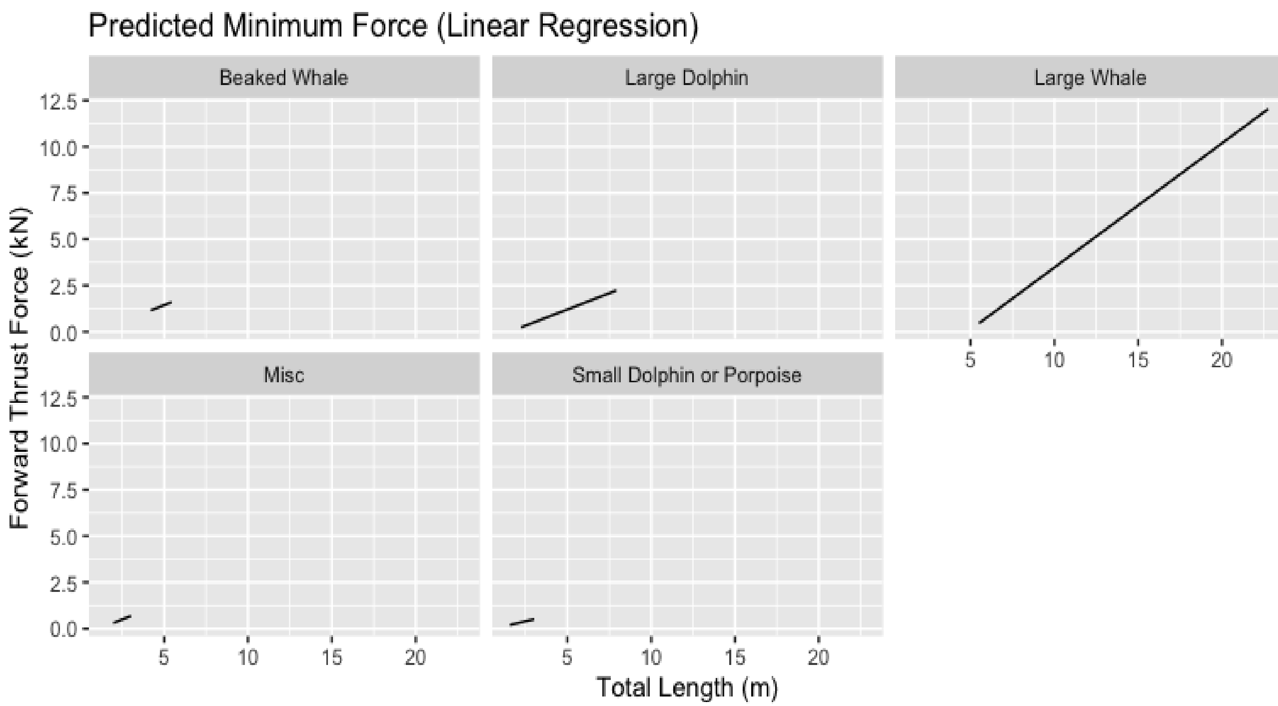

Figure C13: Predicted Sub-Maximum Force based on Linear Regression

<u>Notes</u>: Forward thrust force is in kilonewtons (kN). Total length is in meters (m).

<u>Source</u>: Schatz Energy Research Center

Modeled Minimum and Maximum Force Plots

Power Regression Extrapolated Plots – Maximum and Minimum Force plots are displayed in the Environmental Data Memo (Figure 2 and Figure 3, respectively).

Linear Regression Extrapolated Plots – Maximum Force

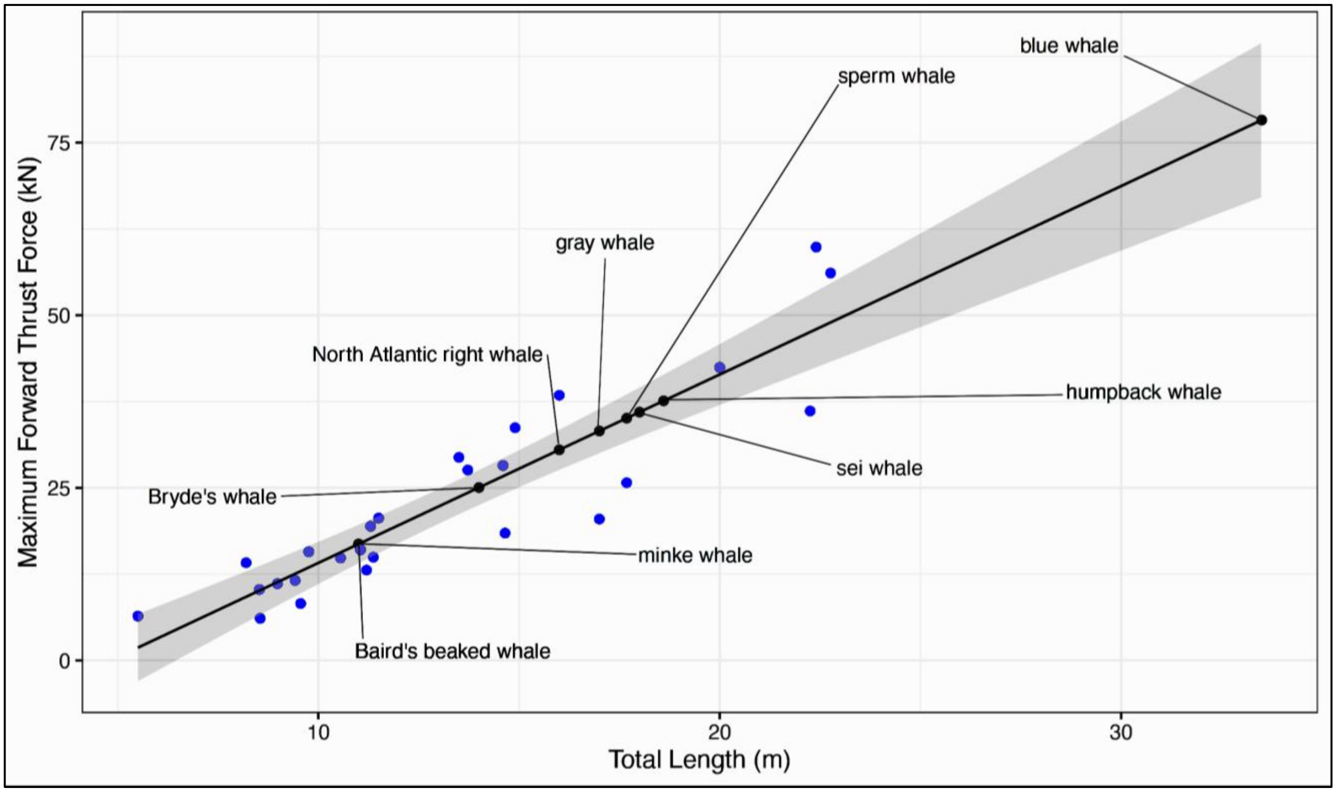

Figure C14. Predicted Maximum Force of Large Whale Species based on Linear Regression

Notes: Blue points = observed data; black points = modeled species forces. Shaded areas show the 95% Confidence Interval. Forward thrust force is in kilonewtons (kN). Total length is in meters (m).

Source: Schatz Energy Research Center

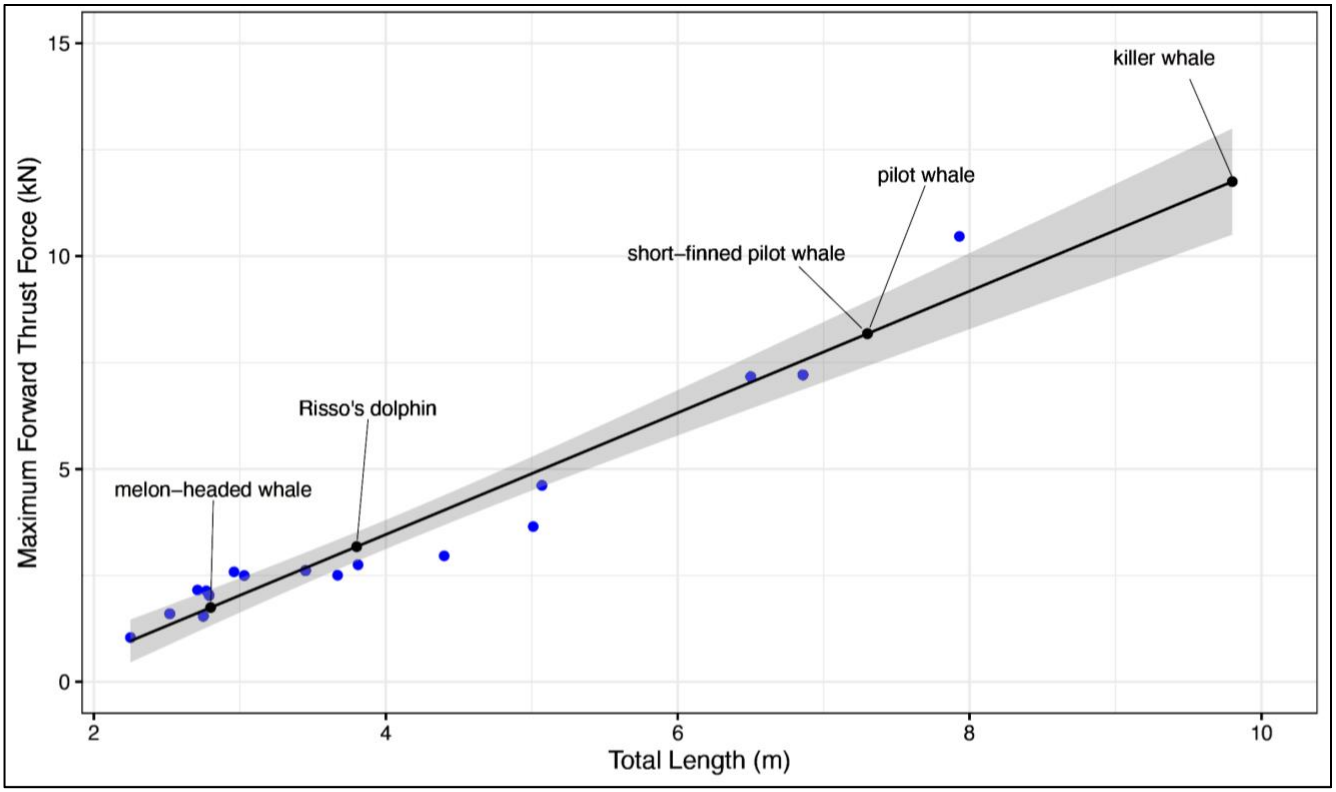

Figure C15. Predicted Maximum Force of Large Dolphin Species based on Linear Regression

Notes: Blue points = observed data; black points = modeled species forces. Shaded areas show the 95% Confidence Interval. Forward thrust force is in kilonewtons (kN). Total length is in meters (m).

Source: Schatz Energy Research Center

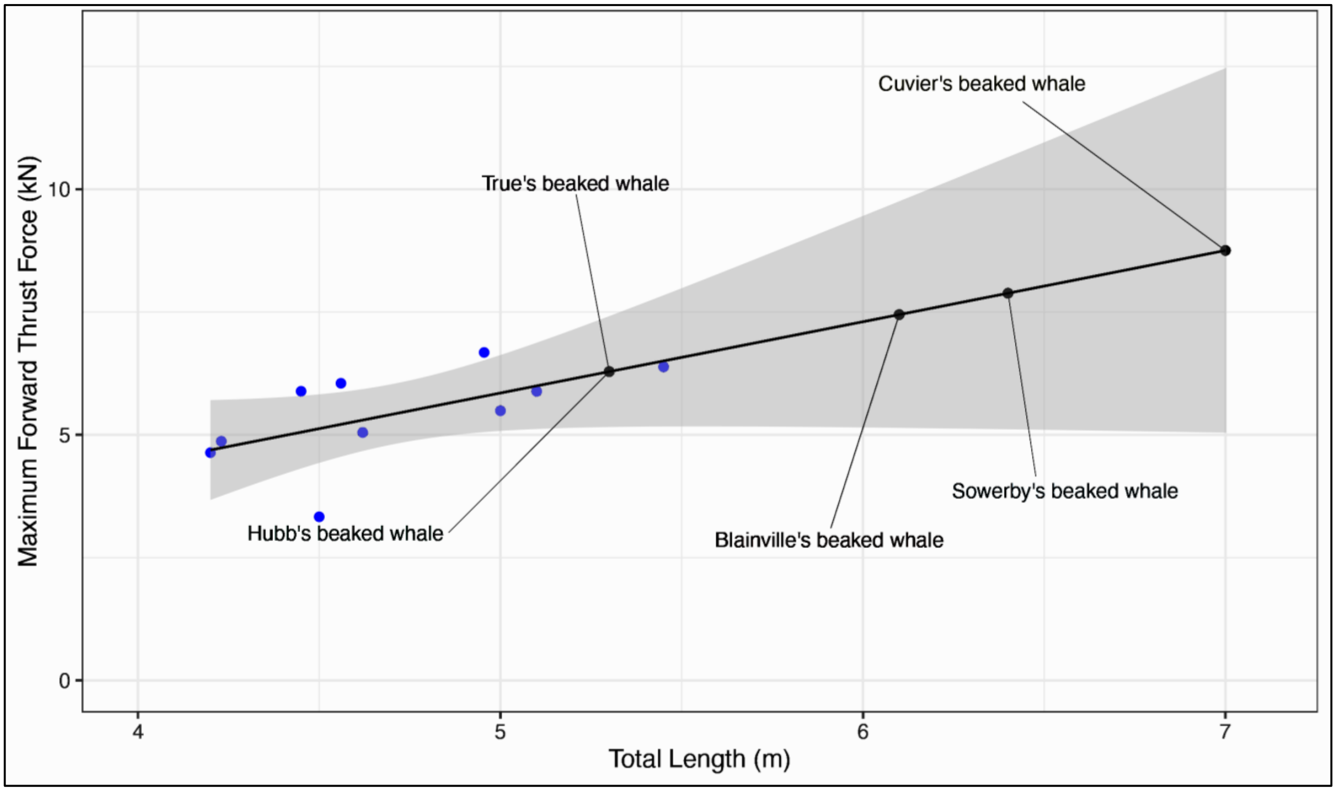

Figure C16. Predicted Maximum Force of Beaked Whale Species based on Linear Regression

Notes: Baird's beaked whales are in the Large Whale group due to their considerably larger size than other beaked whales. Blue points = observed data; black points = modeled species forces. Shaded areas show the 95% Confidence Interval. Forward thrust force is in kilonewtons (kN). Total length is in meters (m).

Source: Schatz Energy Research Center

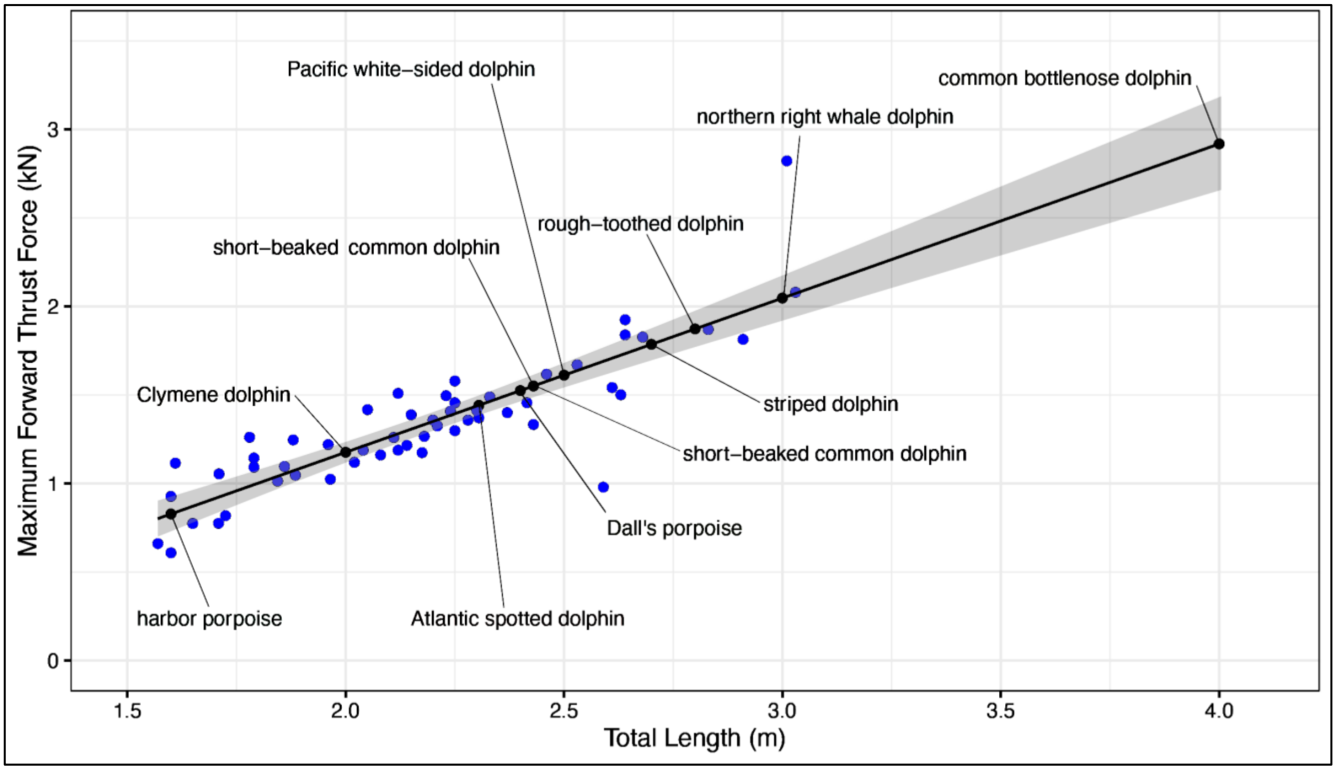

Figure C17. Predicted Maximum Force of Small Dolphin and Porpoise Species based on Linear Regression

Notes: Blue points = observed data; black points = modeled species forces. Shaded areas show the 95% Confidence Interval. Forward thrust force is in kilonewtons (kN). Total length is in meters (m).

Source: Schatz Energy Research Center

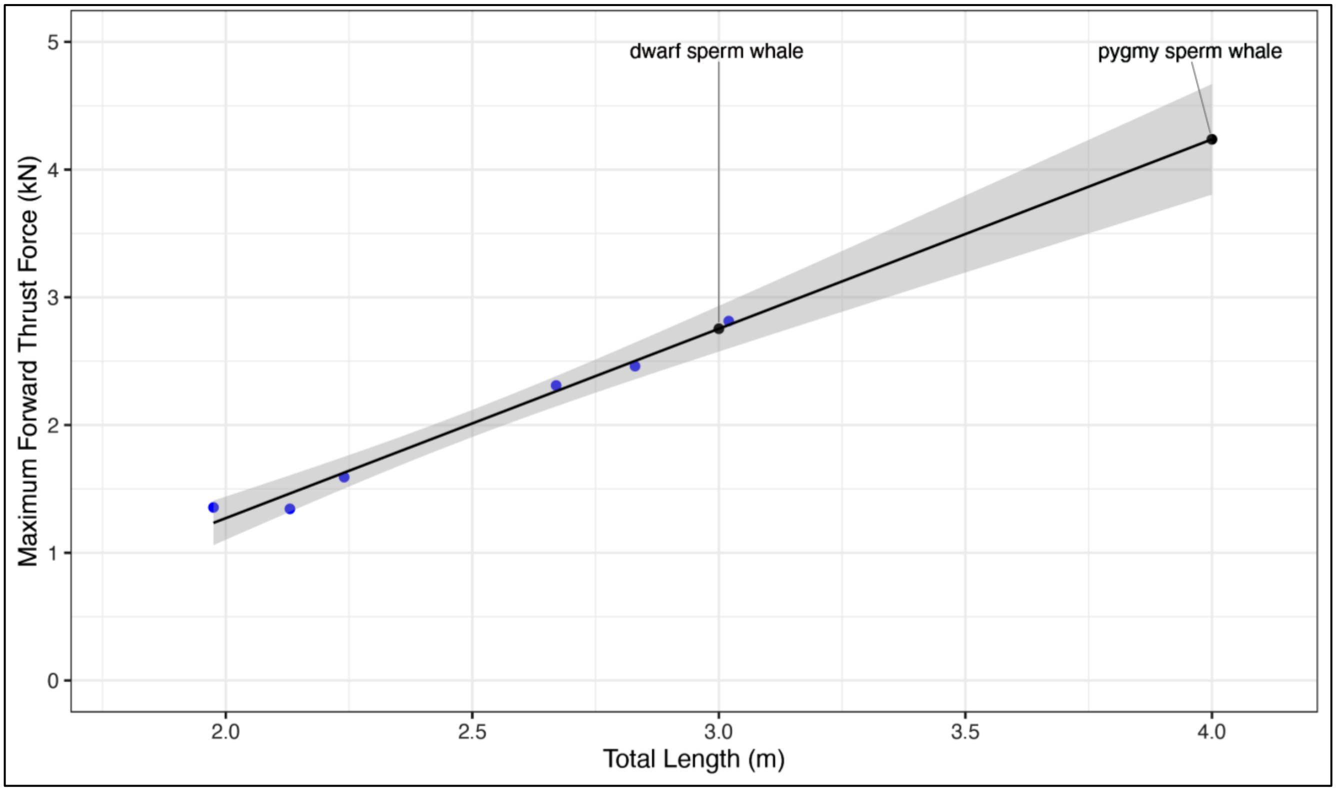

Figure C18. Predicted Maximum Force of *Kogia* Species based on Linear Regression

Notes: Blue points = observed data; black points = modeled species forces. Shaded areas show the 95% Confidence Interval. Forward thrust force is in kilonewtons (kN). Total length is in meters (m).

Source: Schatz Energy Research Center

Linear Regression Extrapolated Plots – Minimum Force

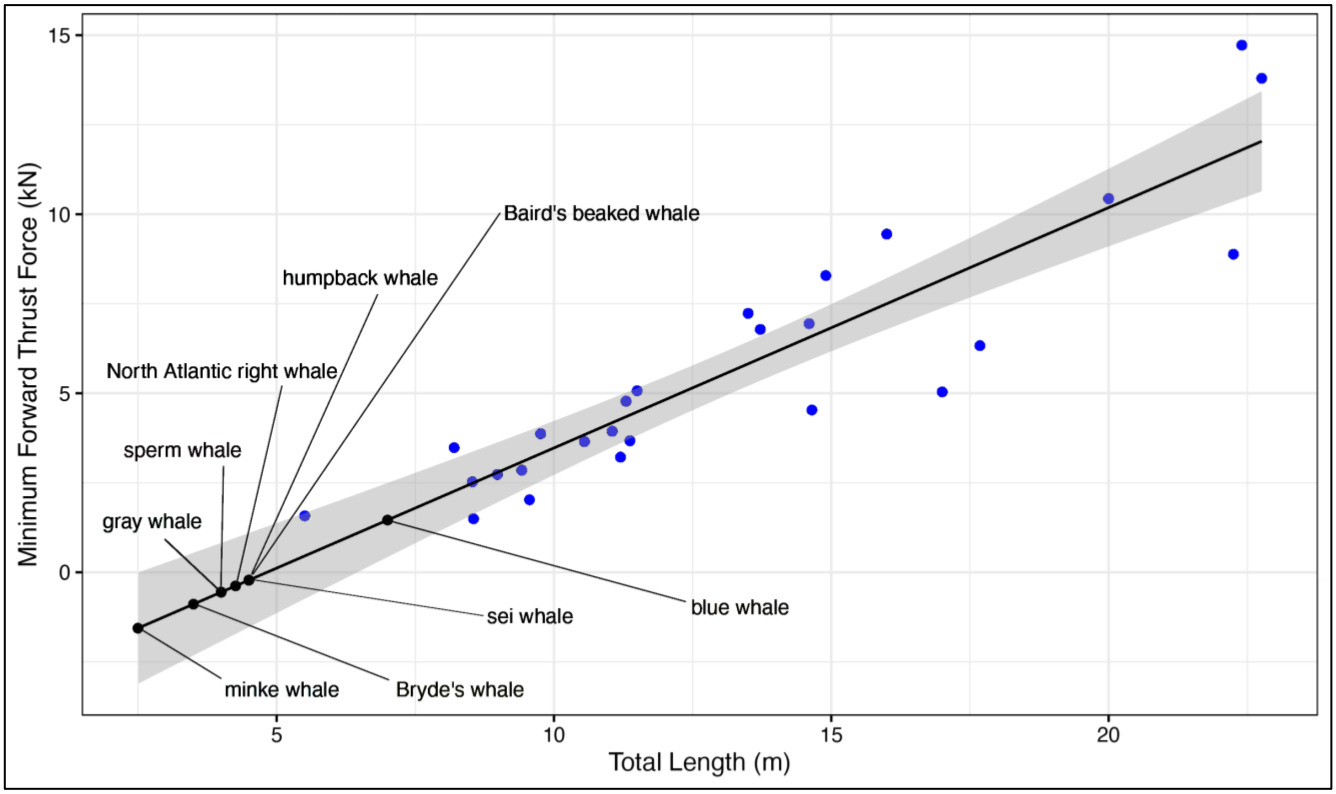

Figure C19. Predicted Sub-maximum Force of Juvenile Large Whales based on Linear Regression

Notes: Blue points = observed data; black points = modeled species forces. Shaded areas show the 95% Confidence Interval. Forward thrust force is in kilonewtons (kN). Total length is in meters (m).

Source: Schatz Energy Research Center

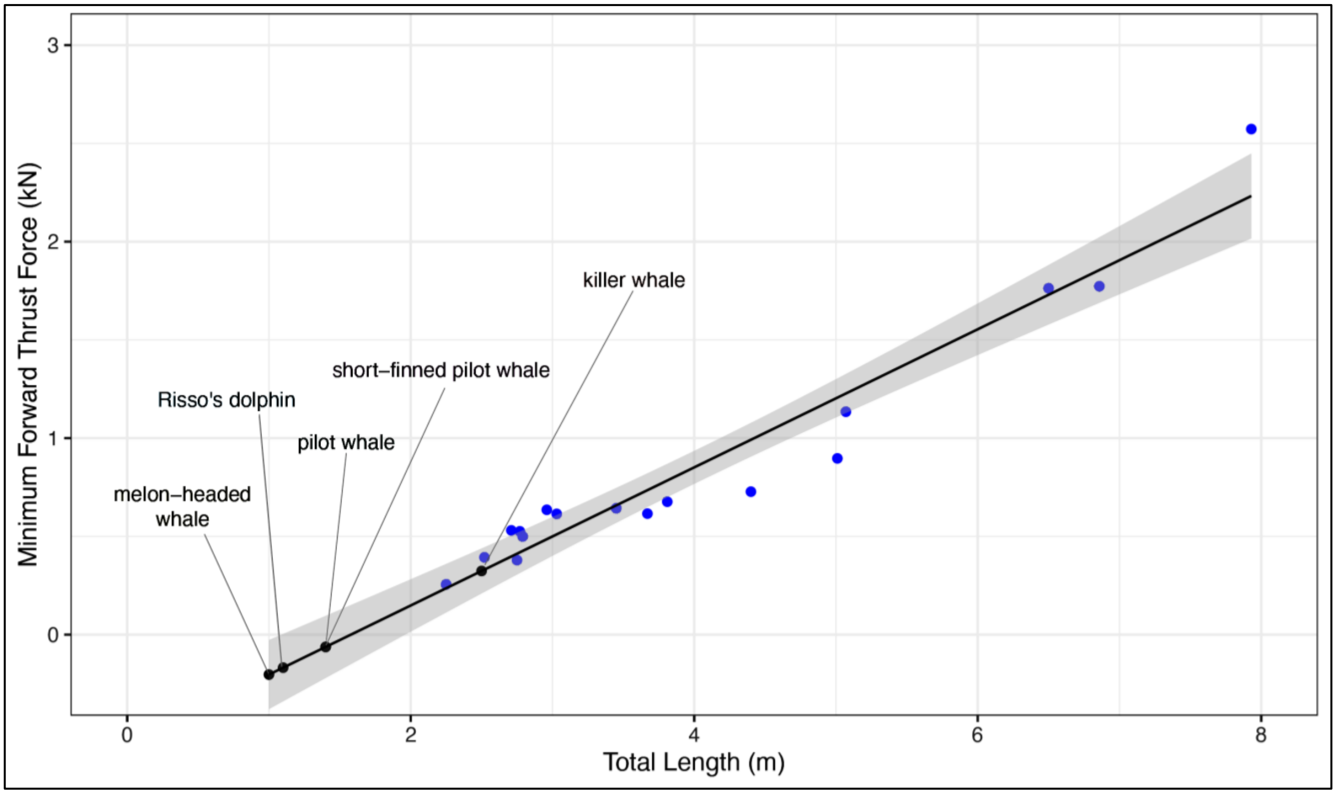

Figure C20. Predicted Sub-maximum Force of Juvenile Large Dolphins based on Linear Regression

Notes: Blue points = observed data; black points = modeled species forces. Shaded areas show the 95% Confidence Interval. Forward thrust force is in kilonewtons (kN). Total length is in meters (m).

Source: Schatz Energy Research Center

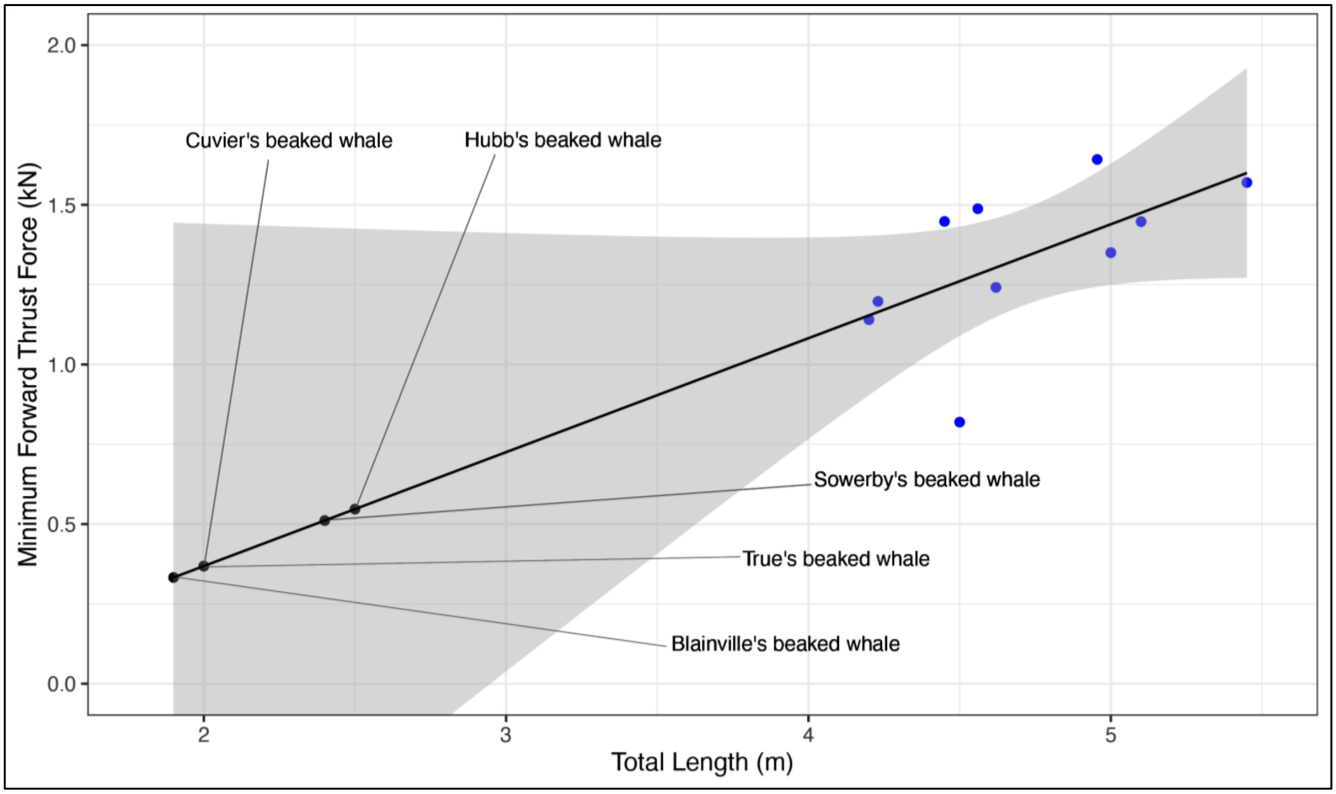

Figure C21. Predicted Sub-maximum Force of Juvenile Beaked Whales based on Linear Regression

Notes: Baird's beaked whale are in the Large Whale group due to their considerably larger size than other beaked whales. Baird's beaked whales reach over 10 m in length, overlapping in size more with smaller members of the large whale size class than with other beaked whales. Blue points = observed data; black points = modeled species forces. Shaded areas show the 95% Confidence Interval. Forward thrust force is in kilonewtons (kN). Total length is in meters (m).

Source: Schatz Energy Research Center

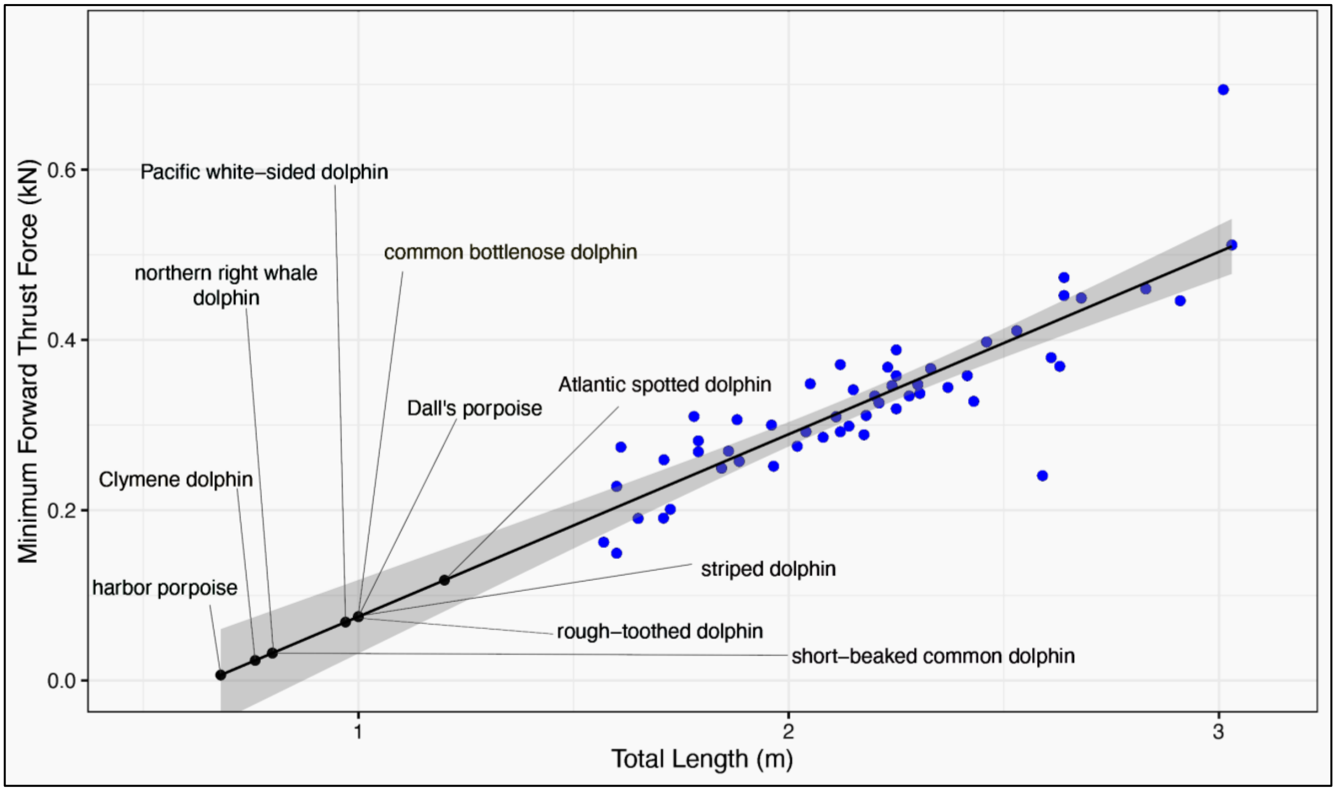

Figure C22. Predicted Sub-maximum Force of Juvenile Small Dolphins and Porpoises based on Linear Regression

Notes: Blue points = observed data; black points = modeled species forces. Shaded areas show the 95% Confidence Interval. Forward thrust force is in kilonewtons (kN). Total length is in meters (m).

Source: Schatz Energy Research Center

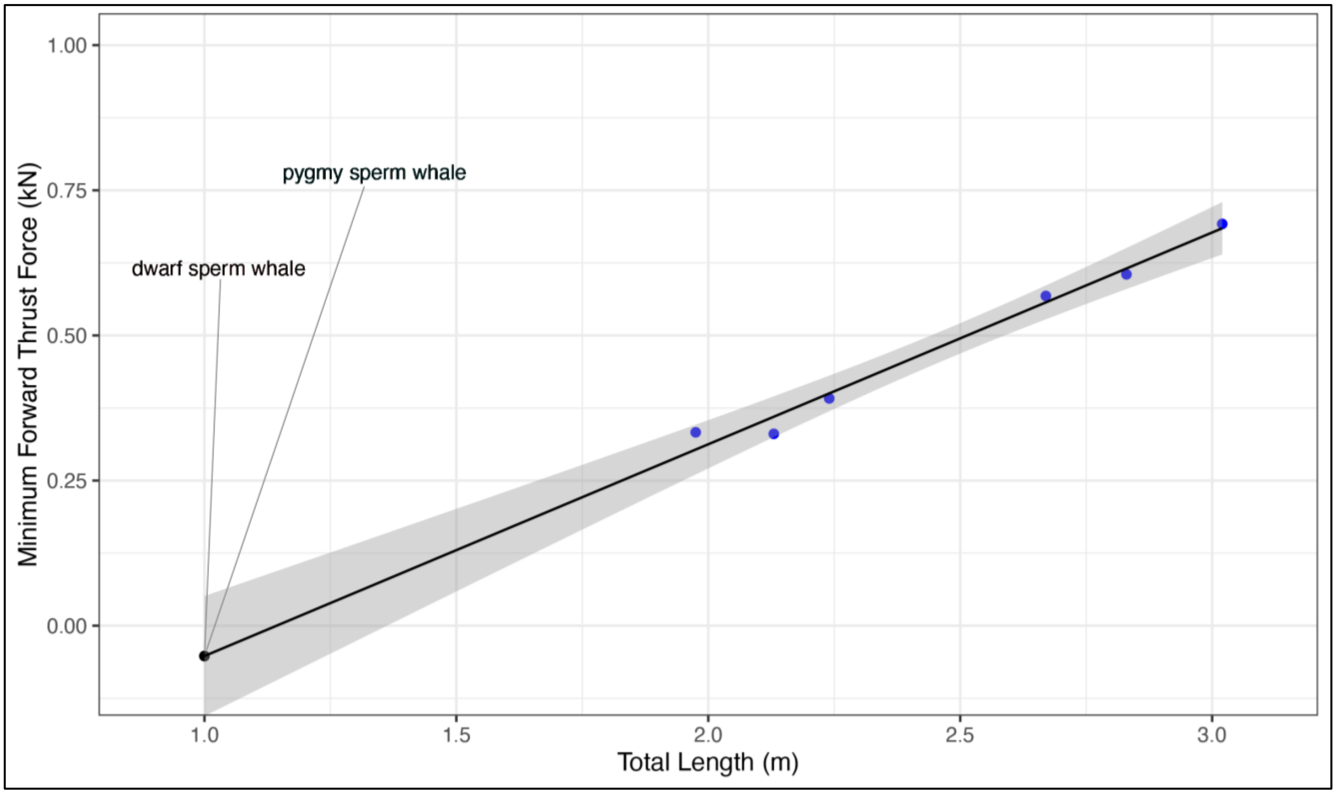

Figure C23. Predicted Sub-maximum Force of Juvenile *Kogia* Species based on Linear Regression

Notes: Blue points = observed data; black points = modeled species forces. Shaded areas show the 95% Confidence Interval. Forward thrust force is in kilonewtons (kN). Total length is in meters (m).

Source: Schatz Energy Research Center

Confidence Intervals

Power Regression Models (log-transformed)

Maximum Force

Table C1. 95% Confidence Intervals for Parameters of Maximum Force Power Regression Model

Term	2.5% (kN)	97.5% (kN)
(Intercept)	-2.530	1.798
log_x	-0.078	2.718
groupLarge Dolphin	-2.753	1.623
groupLarge Whale	-2.869	1.578
groupMisc	-2.995	1.654
groupSmall Dolphin or Porpoise	-2.640	1.711
log_x:groupLarge Dolphin	-1.224	1.611
log_x:groupLarge Whale	-1.160	1.665
log_x:groupMisc	-1.128	2.234
log_x:groupSmall Dolphin or Porpoise	-1.335	1.519

Minimum Force

Table C2. 95% Confidence Intervals for Parameters of Minimum Force Power Regression Model

Term	2.5% (kN)	97.5% (kN)
(Intercept)	-3.934	0.395
log_x	-0.078	2.719
groupLarge Dolphin	-2.753	1.623
groupLarge Whale	-2.869	1.579
groupMisc	-2.996	1.654
groupSmall Dolphin or Porpoise	-2.640	1.712
log_x:groupLarge Dolphin	-1.224	1.611
log_x:groupLarge Whale	-1.160	1.665
log_x:groupMisc	-1.128	2.234
log_x:groupSmall Dolphin or Porpoise	-1.336	1.519

Linear Regression Models

Maximum Force

Table C3. 95% Confidence Intervals for Parameters of Maximum Force Linear Regression Model

Term	2.5% (kN)	97.5% (kN)
(Intercept)	-24.605	21.800
TL..m	-3.463	6.365
groupLarge Dolphin	-24.368	22.664
groupLarge Whale	-35.244	11.697
groupMisc	-28.424	27.841
groupSmall Dolphin or Porpoise	-22.870	24.543
TL..m.:groupLarge Dolphin	-5.013	4.970
TL..m.:groupLarge Whale	-3.641	6.199
TL..m.:groupMisc	-7.994	8.057
TL..m.:groupSmall Dolphin or Porpoise	-5.963	4.803

Minimum Force

Table C4. 95% Confidence Intervals for Parameters of Minimum Force Linear Regression Model

Term	2.5% (kN)	97.5% (kN)
(Intercept)	-6.051	5.360
TL..m	-0.851	1.565
groupLarge Dolphin	-5.992	5.573
groupLarge Whale	-8.666	2.877
groupMisc	-6.990	6.846
groupSmall Dolphin or Porpoise	-5.624	6.035
TL..m.:groupLarge Dolphin	-1.233	1.222
TL..m.:groupLarge Whale	-0.895	1.524
TL..m.:groupMisc	-1.966	1.981
TL..m.:groupSmall Dolphin or Porpoise	-1.466	1.181

Species Force Results

Table C5. Maximum Species Forces, Power Regression

Common Name	Species Maximum Force, Power Regression (kN)
Baird's beaked whale	15.80
Blainville's beaked whale	7.54
Cuvier's beaked whale	9.05
Hubb's beaked whale	6.27
Sowerby's beaked whale	8.04
True's beaked whale	6.27
Blue whale	91.05
Bryde's whale	23.08
Gray whale	31.33
Humpback whale	36.09
Minke whale	15.80
North Atlantic right whale	28.48
Sei whale	34.27
Sperm whale	33.32
Killer whale	12.47
Melon-headed whale	1.87
Pilot whale (unidentified)	7.99
Risso's dolphin	2.97
Short-finned pilot whale	7.99
Northern right whale dolphin	2.06
Dwarf sperm whale	2.77
Pygmy sperm whale	4.76
Dall's porpoise	1.50
Atlantic spotted dolphin	1.42

Common Name	Species Maximum Force, Power Regression (kN)
Clymene dolphin	1.16
Common bottlenose dolphin	3.09
Harbor porpoise	0.85
Pacific white-sided dolphin	1.59
Rough-toothed dolphin	1.86
Short-beaked common dolphin	1.53
Striped dolphin	1.77

Table C6. Minimum Species Forces, Power Regression

Common Name	Species Minimum Force, Power Regression (kN)
Baird's beaked whale	0.95
Blainville's beaked whale	0.40
Cuvier's beaked whale	0.43
Hubb's beaked whale	0.57
Sowerby's beaked whale	0.54
True's beaked whale	0.43
Blue whale	1.91
Bryde's whale	0.64
Gray whale	0.79
Humpback whale	0.95
Minke whale	0.38
North Atlantic right whale	0.87
Sei whale	0.95
Sperm whale	0.79
Killer whale	0.39
Melon-headed whale	0.10
Pilot whale (unidentified)	0.16
Risso's dolphin	0.11
Short-finned pilot whale	0.16
Northern right whale dolphin	0.08
Dwarf sperm whale	0.09
Pygmy sperm whale	0.09
Dall's porpoise	0.11
Atlantic spotted dolphin	0.14
Clymene dolphin	0.07
Common bottlenose dolphin	0.11

Common Name	Species Minimum Force, Power Regression (kN)
Harbor porpoise	0.06
Pacific white-sided dolphin	0.10
Rough-toothed dolphin	0.11
Short-beaked common dolphin	0.08
Striped dolphin	0.11

Table C7. Maximum Species Forces, Linear Regression

Common Name	Species Maximum Force, Linear Regression (kN)
Baird's beaked whale	16.85
Blainville's beaked whale	7.45
Cuvier's beaked whale	8.75
Hubb's beaked whale	6.29
Sowerby's beaked whale	7.88
True's beaked whale	6.29
Blue whale	78.27
Bryde's whale	25.04
Gray whale	33.23
Humpback whale	37.60
Minke whale	16.85
North Atlantic right whale	30.50
Sei whale	35.96
Sperm whale	35.09
Killer whale	11.75
Melon-headed whale	1.75
Pilot whale (unidentified)	8.18
Risso's dolphin	3.18
Short-finned pilot whale	8.18
Northern right whale dolphin	2.05
Dwarf sperm whale	2.75
Pygmy sperm whale	4.24
Dall's porpoise	1.52
Atlantic spotted dolphin	1.44
Clymene dolphin	1.18
Common bottlenose dolphin	2.92

Common Name	Species Maximum Force, Linear Regression (kN)
Harbor porpoise	0.83
Pacific white-sided dolphin	1.61
Rough-toothed dolphin	1.87
Short-beaked common dolphin	1.55
Striped dolphin	1.79

Table C8. Minimum Species Forces, Linear Regression

Common Name	Species Minimum Force, Linear Regression (kN)
Baird's beaked whale	-0.22
Blainville's beaked whale	0.33
Cuvier's beaked whale	0.37
Hubb's beaked whale	0.55
Sowerby's beaked whale	0.51
True's beaked whale	0.37
Blue whale	1.46
Bryde's whale	-0.89
Gray whale	-0.55
Humpback whale	-0.22
Minke whale	-1.56
North Atlantic right whale	-0.38
Sei whale	-0.22
Sperm whale	-0.55
Killer whale	0.32
Melon-headed whale	-0.20
Pilot whale (unidentified)	-0.06
Risso's dolphin	-0.17
Short-finned pilot whale	-0.06
Northern right whale dolphin	0.03
Dwarf sperm whale	-0.05
Pygmy sperm whale	-0.05
Dall's porpoise	0.07
Atlantic spotted dolphin	0.12
Clymene dolphin	0.02
Common bottlenose dolphin	0.07

Common Name	Species Minimum Force, Linear Regression (kN)
Harbor porpoise	0.01
Pacific white-sided dolphin	0.07
Rough-toothed dolphin	0.07
Short-beaked common dolphin	0.03
Striped dolphin	0.07